School of Engineering

University of West Attica

Thesis

«Experimental set – up for the study of thermo-fluid mechanical quantities in a car radiator»

«Πειραματική διάταξη μελέτης θερμορευστομηχανικών μεγεθών σε ψυγείο αυτοκινήτου»

March 2024

Author: *Theofanis Kleitou*

Supervisor: *Konstantinos – Stefanos Nikas*

SID: *18392162*

Η Διπλωματική Εργασία έγινε αποδεκτή και βαθμολογήθηκε από την εξής τριμελή επιτροπή:

Κωνσταντίνος-Στέφανος Νίκας Καθηγητής Πα.Δ.Α. (επιβλέπων)	**Αντώνης Νάζος** Επίκουρος Καθηγητής Πα.Δ.Α.	**Ιωάννης Σιγάλας** Εργαστηριακό Διδακτικό Προσωπικό Πα.Δ.Α.
KSNikas Digitally signed by Konstantinos-Stefanos Nikas Date: 2024.04.20 16:40:28 +03'00' (Υπογραφή)	Antonios Nazos Digitally signed by Antonios Nazos Date: 2024.04.21 10:38:15 +03'00' (Υπογραφή)	Digitally signed by Ioannis Sigalas Date: 2024.04.30 10:47:33 +03'00' (Υπογραφή)

ΔΗΛΩΣΗ ΣΥΓΓΡΑΦΕΑ ΔΙΠΛΩΜΑΤΙΚΗΣ ΕΡΓΑΣΙΑΣ

Ο κάτωθι υπογεγραμμένος Κλείτου Θεοφάνης του Πανίκου, με αριθμό μητρώου 18392162 φοιτητής του Πανεπιστημίου Δυτικής Αττικής της Σχολής Μηχανικών του Τμήματος Μηχανολόγων Μηχανικών, δηλώνω υπεύθυνα ότι:

«Είμαι συγγραφέας αυτής της διπλωματικής εργασίας και ότι κάθε βοήθεια την οποία είχα για την προετοιμασία της είναι πλήρως αναγνωρισμένη και αναφέρεται στην εργασία. Επίσης, οι όποιες πηγές από τις οποίες έκανα χρήση δεδομένων, ιδεών ή λέξεων, είτε ακριβώς είτε παραφρασμένες, αναφέρονται στο σύνολό τους, με πλήρη αναφορά στους συγγραφείς, τον εκδοτικό οίκο ή το περιοδικό, συμπεριλαμβανομένων και των πηγών που ενδεχομένως χρησιμοποιήθηκαν από το διαδίκτυο. Επίσης, βεβαιώνω ότι αυτή η εργασία έχει συγγραφεί από μένα αποκλειστικά και αποτελεί προϊόν πνευματικής ιδιοκτησίας τόσο δικής μου, όσο και του Ιδρύματος.

Παράβαση της ανωτέρω ακαδημαϊκής μου ευθύνης αποτελεί ουσιώδη λόγο για την ανάκληση του πτυχίου μου».

Ο Δηλών

Κλείτου Θεοφάνης

Abstract

In this thesis, the construction of an experimental set – up for the study of thermo–fluid mechanical parameters in a car radiator was carried out. The experimental set – up offers the possibility for users to study any type of heat exchanger with the necessary modifications for its application in the system. An automated system controls some of the components of the experimental set – up, providing data on the fluid supply to the system and the temperatures at the inlet and outlet of the heat exchanger, as well as the air flow from the cooling fan to the radiator core and then to the environment. By utilizing the data retrieved from the experimental set – up automated system, the efficiency of the heat exchanger under study is determined by using the ε – NTU method.

Περίληψη

Στην παρούσα διπλωματική εργασία πραγματοποιήθηκε η κατασκευή πειραματικής διάταξης για την μελέτη θερμορευστομηχανικών μεγεθών σε ψυγείο αυτοκινήτου. Η πειραματική διάταξη προσφέρει την δυνατότητα στον χρήστη να μπορεί να μελετήσει οποιοδήποτε τύπο εναλλάκτη θερμότητας με τις απαραίτητες μετατροπές που πρέπει να γίνουν για την εφαρμογή του στο σύστημα. Υπάρχει αυτοματοποιημένο σύστημα για τον έλεγχο των εξαρτημάτων της πειραματικής διάταξης, όπου μας παρέχει δεδομένα σχετικά με την παροχή ρευστού στο σύστημα και τις θερμοκρασίες που έχουμε σε είσοδο-έξοδο του εναλλάκτη θερμότητας και του αέρα που απάγεται από τον ανεμιστήρα προς τον εναλλάκτη θερμότητας και έπειτα προς το περιβάλλον. Με τα δεδομένα που καταγράφουμε από την πειραματική διάταξη χρησιμοποιούμε την μέθοδο ε – NTU για τον προσδιορισμό της αποδοτικότητας του υπό μελέτη εναλλάκτη θερμότητας.

Key – Words

Radiator, Heat Exchanger, Heat Transfer, Water Pump, Experimental Setup, Boiler, Cooling System, Cooling Efficiency, Cooling Fan.

Λέξεις – Κλειδιά

Ψυγείο, Εναλλάκτης Θερμότητας, Μεταφορά Θερμότητας, Αντλία νερού, Πειραματική Διάταξη, Λέβητας, Σύστημα Ψύξης, Αποδοτικότητα Ψύξης, Ανεμιστήρας Ψύξης.

Table of Contents

Table of Figures

Contents of Tables

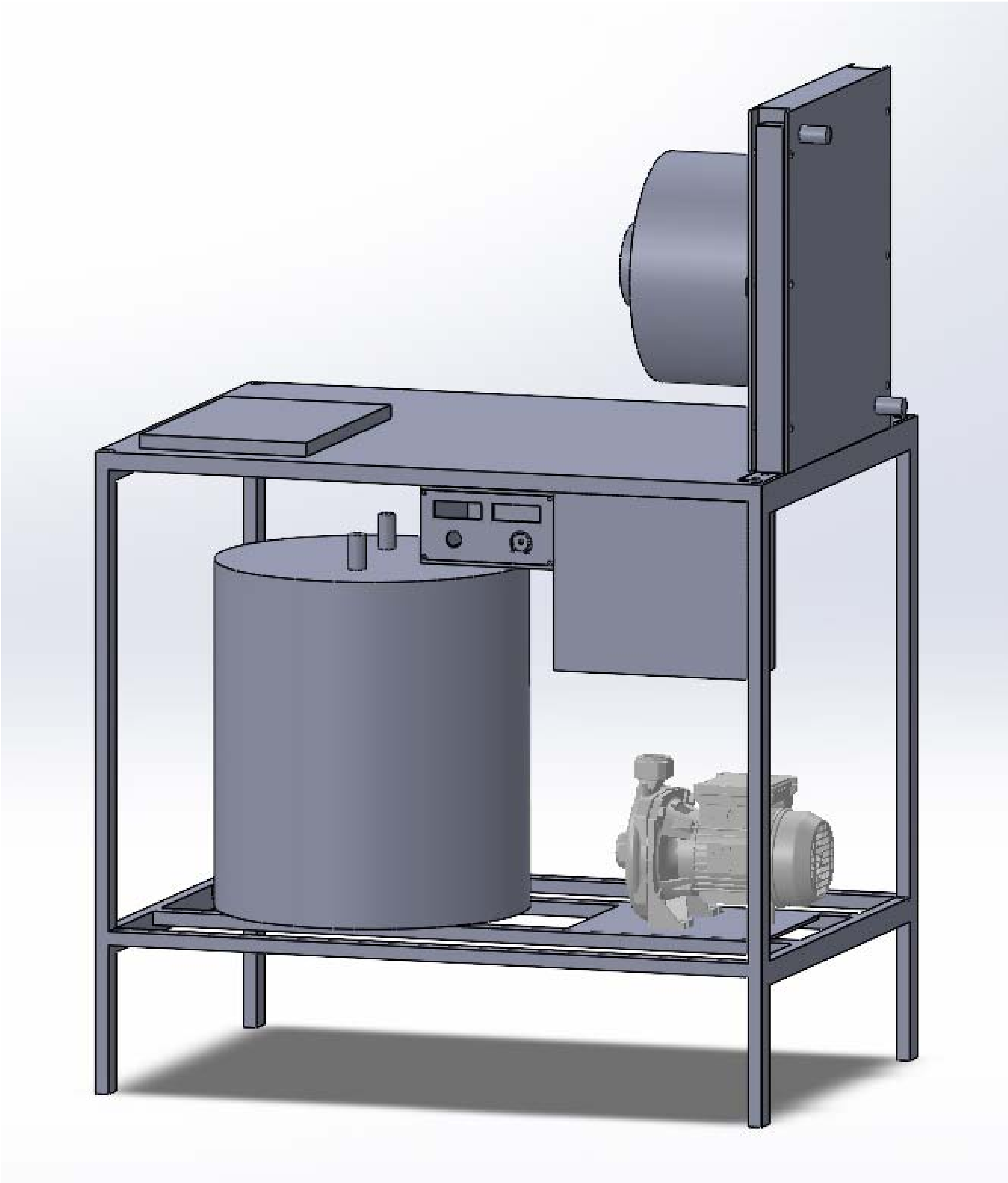

Figure 1: Experimental Set – Up (SolidWorks 2023)

Chapter 1: Introduction

The present thesis was initiated with the primary objective of analyzing the heat transfer methods within heat exchangers in a closed circuit simulating an automotive cooling system. This inquiry was facilitated through the utilization of an experimental set – up designed for comprehensive examination and investigation. Before delving into the topic and literature review, the author would like to explain the factors that lead to the creation of an experimental set – up, aside from a bibliography review. The initial concept of the experimental set – up is to adapt its functionality to suit the user's specific requirements, which means that the adaptability of the closed circuit will be demonstrated by its ability to accommodate different types and sizes of heat exchangers for testing purposes. In addition, the main objective is the determination of the heat dissipation capacity of a heat exchanger in a closed circuit, achieved through the cooperative function of other components integrated in the experimental set – up.

Furthermore, Chapter 2 provides a comprehensive analysis of heat exchangers, including a detailed examination of the different types, circuits and how they are used in automotive cooling systems. In Chapter 3, the analysis of two different methods for calculating the heat transfer of the heat exchanger in question is presented. Chapter 4 provides an in – depth analysis of the experimental set – up explaining the methodology used to construct the test bench. Each component will be examined in detail, accompanied by a presentation of the calculations carried out and a comprehensive presentation of the experimental data. Chapter 5 endorses all the findings from the research process and presents the relevant data in the form of graphs and tables with comprehensive discussions of the overarching aspects of the entire research. Chapter 6 will formulate the concluding remarks of the dissertation, providing insights from the extensive research and experimentation and also provide recommendations for future plans, based on the findings and experimental designs and conclude with a compiled list of references.

Chapter 2: Heat Exchangers & Cooling System

2.1 Heat Exchanger

2.1.1 Introduction

The interpretation of heat exchangers is related to the heat exchange between two fluids at different temperatures. Heat exchangers are widely used in a variety of industries for their versatile thermal management capabilities. The use of heat exchangers is particularly in several key sectors such as the following.

2.1.2 Automotive Industry

In the automotive sector, heat exchangers, particularly in the form of radiators, play an important role in the thermal regulation of engines. This is achieved by efficiently transferring heat from the engine coolant to the ambient air. *Figure 2* represents an automotive engine test bench involving the entire cooling system package to ensure that the engine remains within optimum temperature ranges and does not overheat.

Figure 2: Automotive Engine Test Bench

2.1.3 HVAC (Heating, Ventilation, Air Conditioning) Systems

Heating, Ventilation and Air Conditioning systems rely extensively on heat exchangers to modulate the temperature of the indoor air in order to ensure optimal thermal comfort.

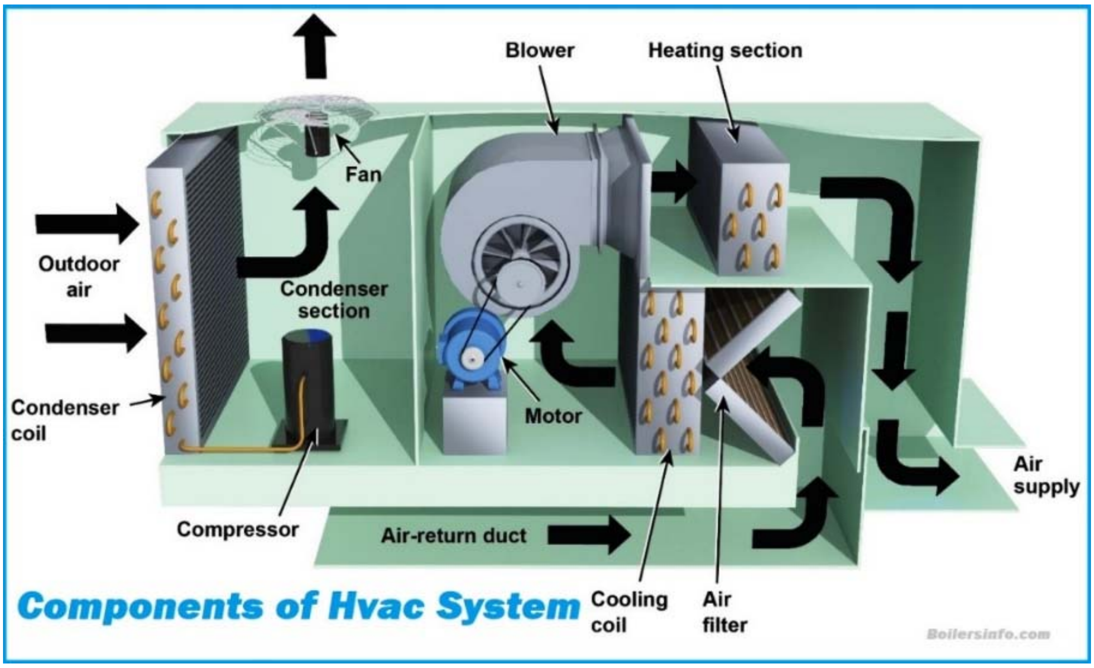

Figure 3: Heating, Ventilation and AC System

2.1.4 Power Generation

In power generation, heat exchangers are a major component in facilitating the transfer of heat between different fluids. This is particularly critical in processes such as steam generation.

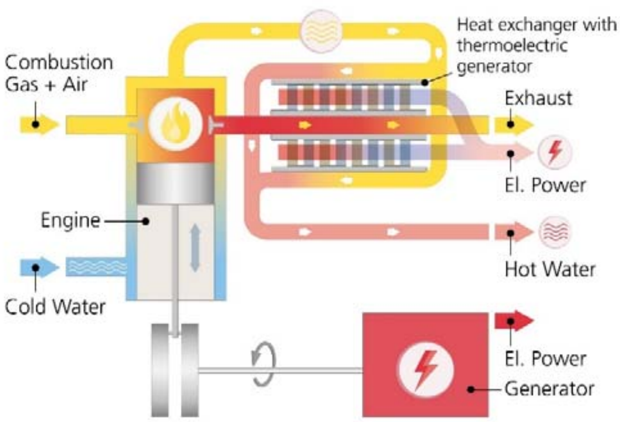

Figure 4: Power Generation System

2.1.5 Chemical Processing

Various chemical processes within the chemical industry utilize the functionality of heat exchangers, using them to heat or cool substances according to specific manufacturing requirements.

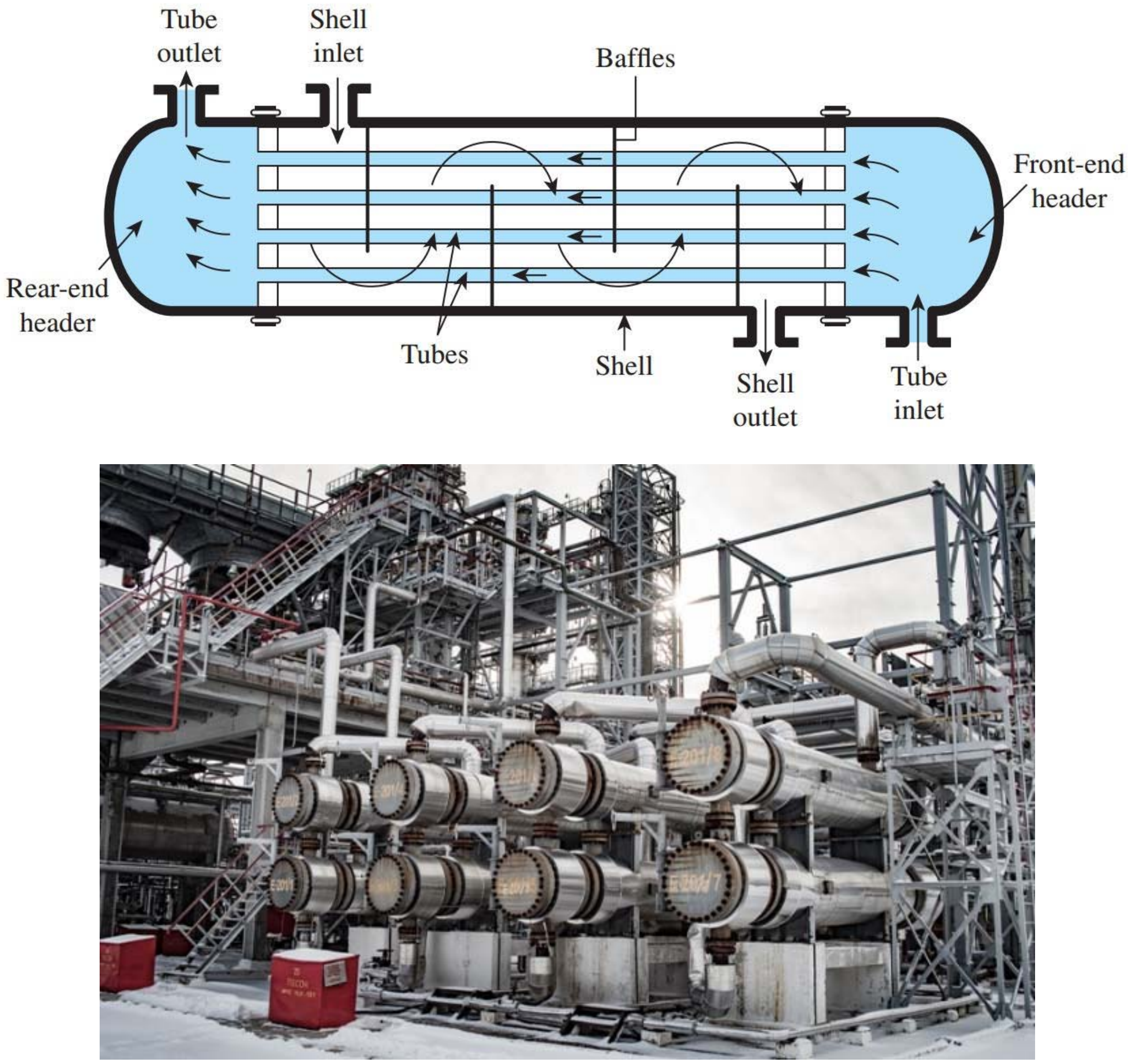

Figure 5: Chemical Cleaning of Oil Refinery & Heat Exchanger Diagram

2.2 Different Heat Exchanger Types

2.2.1 Introduction

In the industrial environment there are many different types of heat exchangers for various types of applications. *Chapter 2.1* describes where they are used and for which applications, with examples shown in the illustrations. In the following chapter, different types of heat exchangers are introduced, the general function is described and figures are provided for a better understanding of their operation.

2.2.2 Parallel – flow

In this particular configuration of heat exchanger, the flow of the two fluids is not only parallel, but also in the same direction. In addition, the working fluids enter on one side of the heat exchanger and exit on the opposite side.

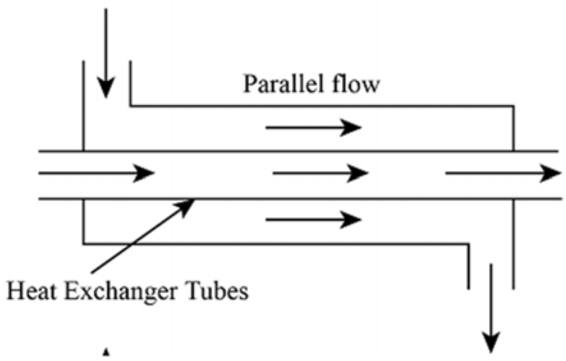

Figure 6: Parallel Flow Heat Exchanger

2.2.3 Counter – flow

In these heat exchangers the flow of the two fluids is likewise parallel, but in opposite directions. The fluids enter on the opposite sides and exit on the opposite side of the heat exchanger.

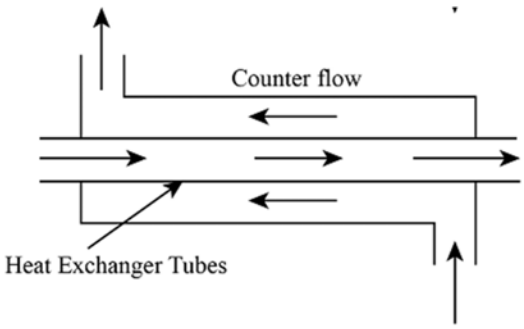

Figure 7: Counter Flow Heat Exchanger

2.2.4 Cross – flow

The cross – flow radiator is a type of heat exchanger in which the flow directions of the two working fluids are crossed and mainly vertical, and are distinguished by the mixing of the fluid moving around the tubes in the direction y. Moreover, cross – flow radiators are divided into unmixed fluid and mixed fluid heat exchangers.

Unmixed fluid:

In this category of heat exchanger, the presence of vanes impedes the fluid from traversing in the y – direction, channeling its movement solely through the openings they generate, specifically in the primary direction x, as depicted in the *figure 8(a)*. In such instances, temperature variation occurs in both vertical directions, x and y.

Mixed fluid:

In heat exchangers lacking fins, the fluid is mixed in the y direction. Consequently, temperature variation predominantly transpires along the primary flow direction x, as shown in the *figure 8(b)*. The presence and characteristics of fluid mixing are key factors with a significant influence on thermal characteristics. In particular, the efficiency of a heat exchanger is affected as the heat transfer mechanism depends on the temperature difference between the hot and cold flows.

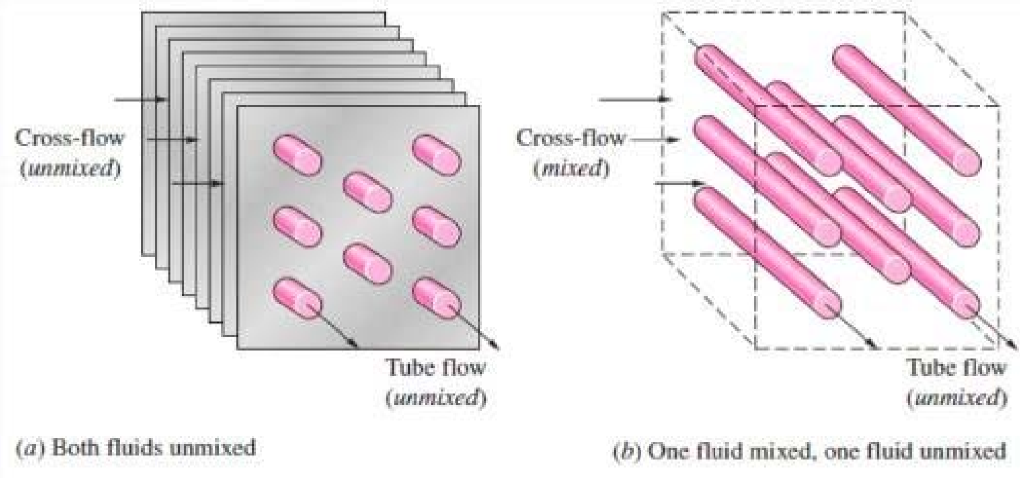

Figure 8: Cross – flow (unmixed) (a), Cross – flow (mixed) (b)

2.2.5 Down – flow

Down-flow radiators have the tanks located at the top and bottom of the radiator core. Coolant enters through the top tank and flows down through the core under the force of gravity, easing the work load of the water pump as the coolant returns to the engine. This design is well suited to early cars and trucks with a high but narrow radiator grille and support. Down-flow radiators also have the advantage of inlet and outlet placement. The inlets and outlets can be positioned center, left, right or anywhere in between.

Figure 9: Down – flow Radiator

2.2.6 Single – Pass

A single – pass radiator is a type of heat exchanger that allows the coolant to flow through the radiator once. The coolant enters the radiator at one end and flows through a series of tubes before exiting at the opposite end. They are generally simpler and more compact than a double – pass radiator, but may not be as efficient at dissipating heat. They can be used in street applications, as well as some racing applications.

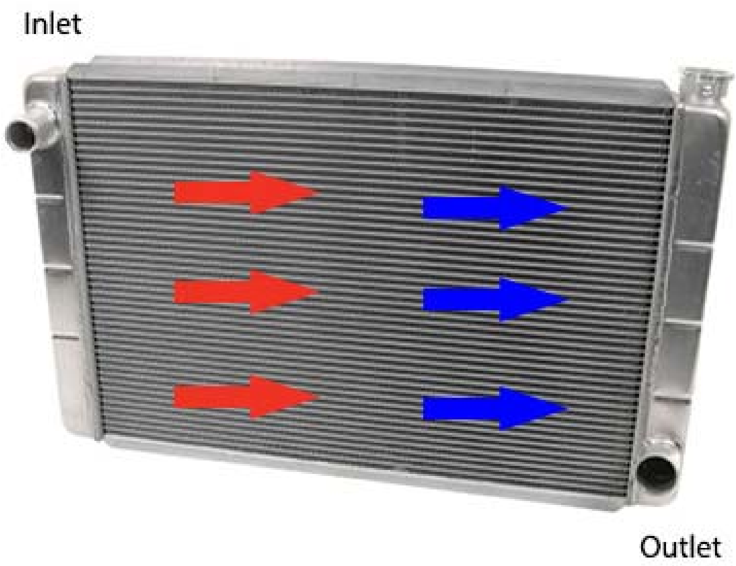

Figure 10: Single – Pass Radiator

2.2.7 Double – Pass

Double – pass radiator is a type of heat exchanger that allows the coolant to flow through the radiator twice before exiting. The coolant enters the radiator at one end and flows through a series of tubes before turning around and flowing back through the tubes at the same side. This type of radiator is generally larger and more complex than a single – pass radiator, but can be more efficient at dissipating heat. These radiators work well in both street and race applications.

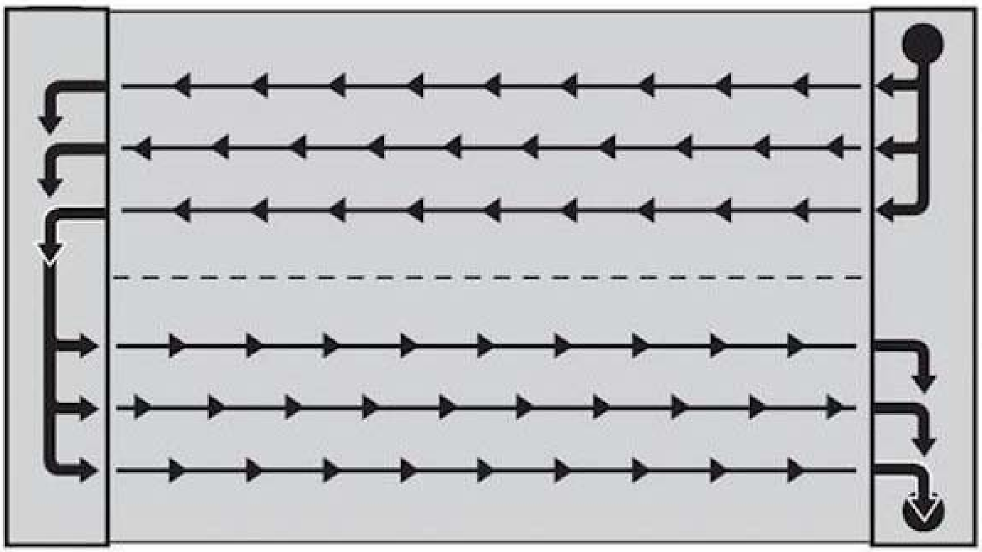

Figure 11: Double – Pass Radiator

2.2.8 Triple – Pass

Triple – pass radiator is more suitable for racing applications. The inlets and outlets are usually on opposite sides and the flow passes through the radiator three times. This type of radiator can withstand more heat dissipation because the coolant flows through the core three times and with the fan working, can dissipate more heat to the environment.

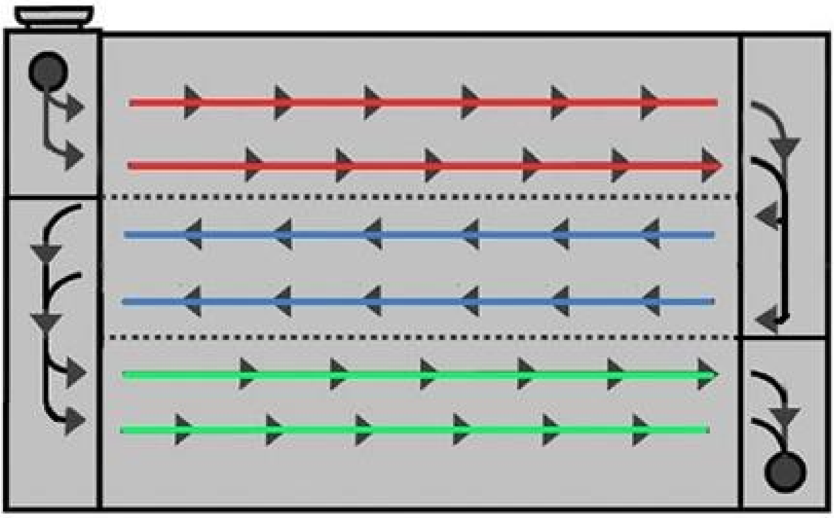

Figure 12: Triple – Pass Radiator

2.3 Automotive Cooling System

2.3.1 Introduction

Explanation of I.C.E (Internal Combustion Engine) & Cooling System:

The efficient operation of an internal combustion engine relies on maintaining an appropriate level of heat. While heat is essential for proper functioning and to prevent premature wear, excessive heat can have detrimental effects, potentially causing severe damage or even destruction of the engine. The central responsibility for regulating engine heat to the optimum level lies with the vehicle's cooling system and its integral components. Essentially, the cooling system works by transferring heat from the engine to the coolant. This coolant then travels to the radiator, where it dissipates the excess heat to the environment, with that leading to the coolant returning to the engine while the cycle begins again. Each component of the cooling system must function properly to keep the engine temperature at an optimum level, regardless of the ambient temperature conditions.

I.C.E cooling system main components:

- Radiator
- Radiator Fan
- Water Pump
- Thermostat
- Hoses
- Coolant

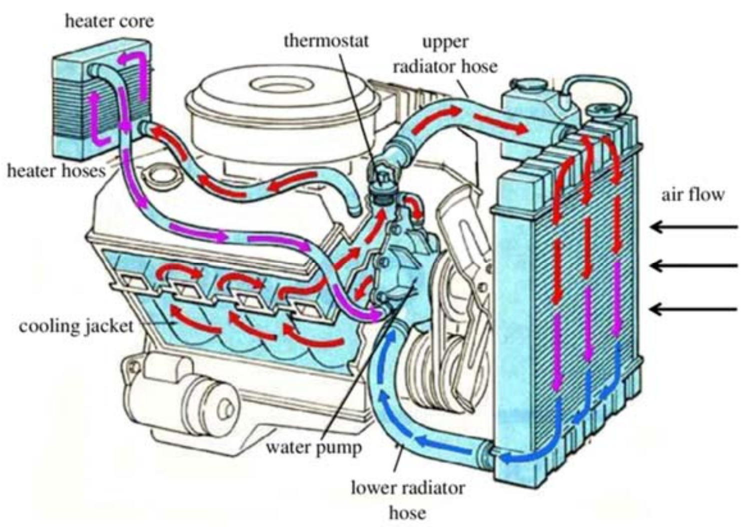

Figure 13: I.C.E (Internal Combustion Engine) & Car Cooling System

2.3.2 Radiator

The role of the radiator is to transfer heat from the coolant which flows through it, to the environment. Refer to *figure 9 & 10* for visual reference.

2.3.3 Radiator Fan

The radiator fan stands as a crucial component with the responsibility of dissipating heat from the radiator core, channeling it through the fins and releasing it into the environment. It helps maintain a consistent temperature, preventing overheating and ensuring that the engine operates optimally. For illustration, see *figure 14*.

Figure 14: Radiator Cooling Fan

2.3.4 Mechanical Water Pump

The water pump is a critical component within an Internal Combustion Engine's (I.C.E) cooling system. Its primary function is to facilitate the continuous circulation of coolant throughout the engine, ensuring efficient heat transfer and temperature regulation. The flow rate of the water pump changes according to the engine's RPM's. See *figure 15* for an illustration.

Figure 15: Cooling System Water Pump

2.3.5 Thermostat

A thermostat acts as a control valve, regulating the flow of coolant to the radiator by opening and closing as required. When the engine is cold, the closed thermostat restricts the flow of coolant to the radiator. The deliberate restriction helps the engine to warm up quickly, allowing it to reach its optimum operating temperature as fast as possible. As the engine warms up, the thermostat gradually opens, allowing coolant to circulate to the radiator for effective cooling once the optimum temperature is reached. Refer to *figure 16*.

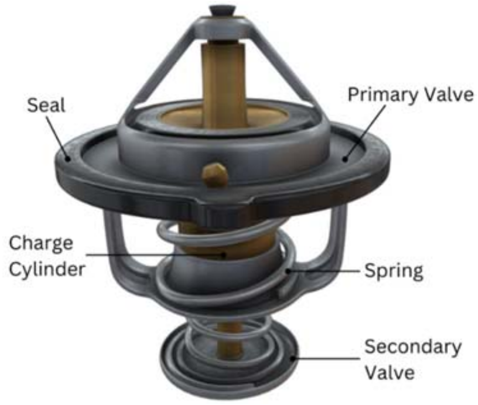

Figure 16: Cooling System Thermostat

2.3.6 Hoses

Rubber hoses is a path for the coolant to travel from the engine to the radiator and then circulate back again. The illustration depicted in *figure 17* provides visual representation.

Figure 17: Silicone Hoses

2.3.7 Coolant

Coolant, commonly known as antifreeze, is the fluid responsible for regulating the engine's temperature. The designation "antifreeze" refers to the low freezing point of the fluid, ensuring that the fluid remains in a liquid state even in extremely cold conditions. This characteristic prevents potential engine damage that could result from freezing.

2.4 Cooling System Circuits

2.4.1 Introduction

The optimal performance of an internal combustion engine relies heavily on the effectiveness of its cooling system. In the automotive sector, the configuration of the coolant circuits plays a key role in regulating engine temperature and preventing overheating. Moreover, the most common configurations within cooling systems include both parallel and series circuits, both of which will be thoroughly analyzed below.

2.4.2 Example of Series and Parallel Circuits

Series

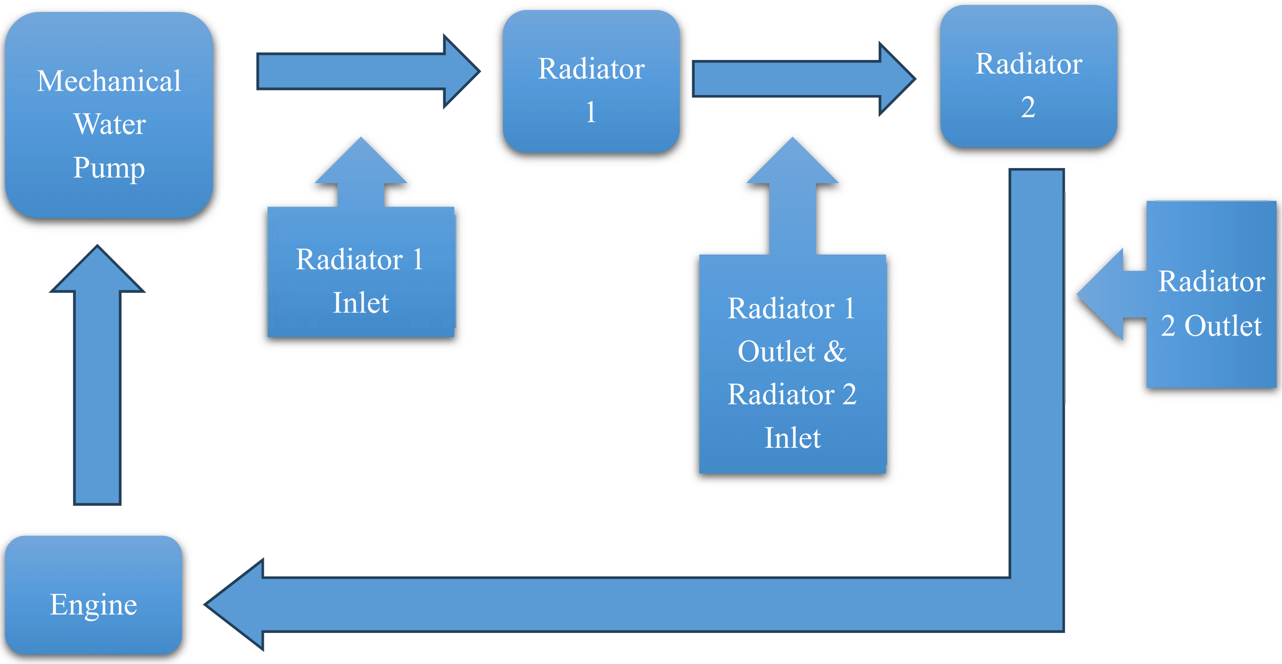

Figure 18: Example of Racing Car Series Circuit Cooling System

Series Example

40°C → Radiator 1 → 34°C → Radiator 2 → 30°C

Based on the aforementioned example, it can be seen that in a series circuit, Radiator 1 will dissipate more heat than Radiator 2.

Parallel

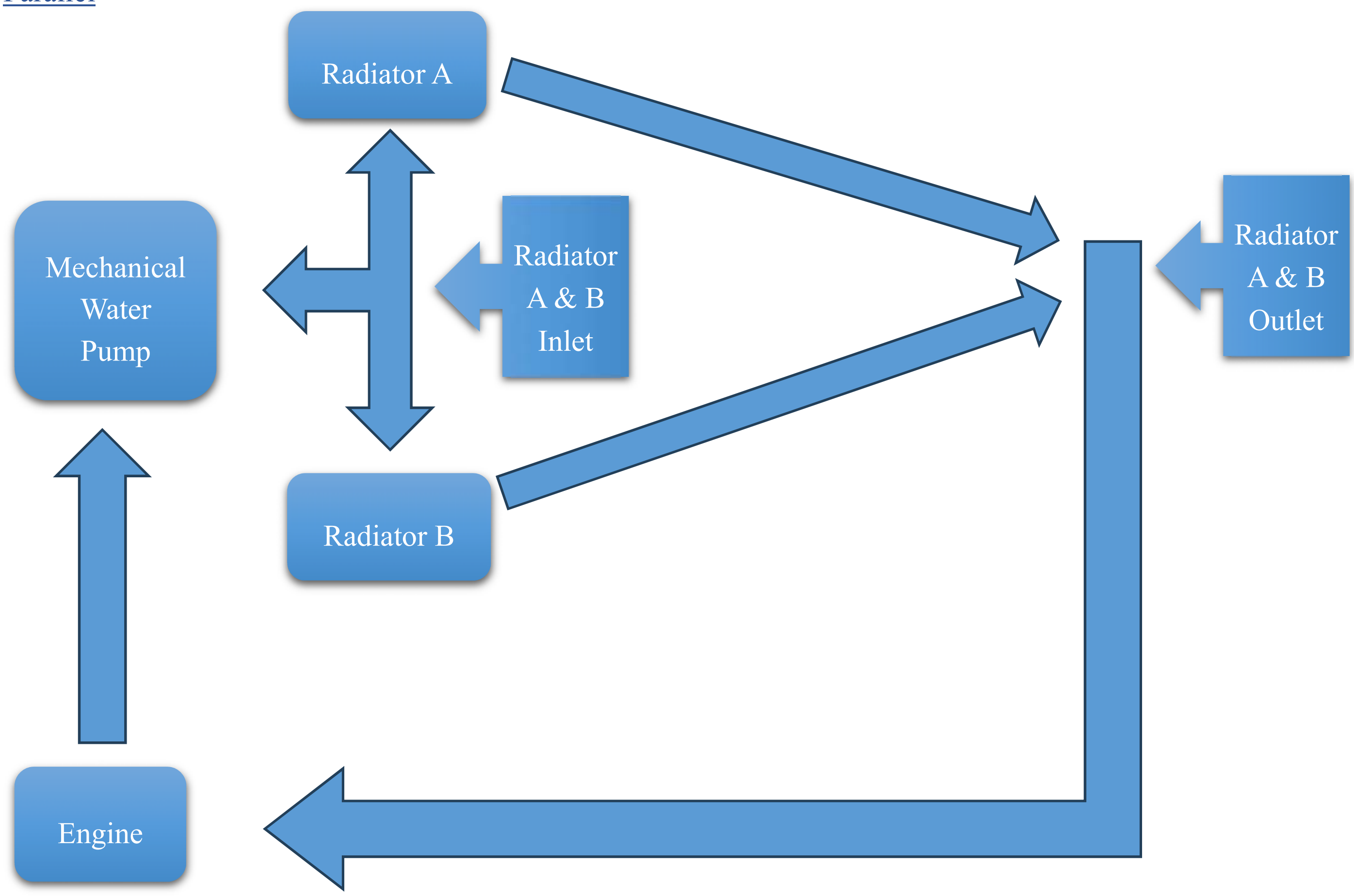

Figure 19: Example of Racing Car Parallel Circuit Cooling System

Parallel Example

40°C → Radiator A → 30°C

40°C → Radiator B → 30°C

From the example above we can see that the parallel circuit Radiator A and Radiator B are exhausting the same heat. Actually, both will dissipate less heat than Radiator 1 but more than Radiator 2 so, the net of both systems will remain the same.

As a result, we can see that Radiator A gives the same temperature drop as Radiator 1 & 2 combined because it has half the flow and half the cooling surface area.

Furthermore, the temperature gradient efficiency difference is that is made obvious by the less efficient by Radiator 2 and more efficient by Radiator 1 presented both in radiators A & B. Overall, by sampling the temperatures of A & B, will lead us in finding out that the temperatures will become the same as in 1 & 2 radiators.

2.4.3 Advantages and Disadvantages of Series and Parallel Circuits

Series Circuit Advantages:

- You can guarantee that the flow through each radiator is equal. This is necessary for optimum efficiency.
- Increased flow velocity increases turbulence inside the radiator.
- It takes less fittings to plumb radiators in series. This means less installation labor and less potential leak locations.

Series Circuit Disadvantages:

- If one component fails or becomes clogged, it can cause the entire cooling system to fail, resulting in overheating and potential engine damage.

Parallel Circuit Advantages:

- It has the ability to isolate a radiator for service during operation.
- It's easier to compare radiator efficiencies. For example, when one radiator has fouled from internal or external contamination it is easy to see that it has less of a differential than the other without doing any math.
- We can see below from the examples that is more efficient of the series system cause the job of 2 radiator in series circuit it can be done by 1 radiator in parallel circuit. But if you only make it work perfectly and share evenly the coolant to both of radiators.

Parallel Circuit Disadvantages:

- It may result in uneven distribution of coolant flow and temperature across the components in the cooling system, which can result in inefficient cooling.
- It requires the use of additional components such as an electric water pump, Y – Patterns and pipe adaptors which increases the complexity of the system and the likelihood of potential failures.

2.5 Heat Exchanger Analysis Methods

2.5.1 Introduction

The analysis in this chapter includes two main methods, the Logarithmic Mean Temperature Difference (LMTD) and the Effectiveness - Number of Transfer Units (e – NTU) method. These methods are used to investigate and evaluate the thermal performance of heat exchangers.

2.5.2 Thermal Analysis of Heat Exchangers

Heat exchangers can be analyzed as steady – state devices where the mass flow and the properties of the working fluids, such as temperature and density, remain constant at the inlet and outlet of the heat exchanger. The reason they can be analyzed as steady – state appliances is that they operate for long periods of time without changing their operating conditions. The thermal analysis of heat exchangers is often simplified through the use of certain approaches and idealizations. These methods do not compromise the accuracy of the corresponding calculations. According to the first law of thermodynamics, the rate of heat transfer from the hot stream is equal to the rate of heat transfer to the cold stream.

$$\dot{Q}_h = \dot{m}_h(h_{h,in} - h_{h,out}) \tag{1}$$

$$\dot{Q}_c = \dot{m}_c(h_{c,out} - h_{c,in}) \tag{2}$$

Where:

- $\dot{Q}_h$: Heat transfer flow of hot fluid
- $\dot{Q}_c$: Heat transfer flow of cold fluid
- h: Hot fluid
- c: Cold fluid
- in: Inlet
- out: Outlet
- $\dot{m}$: Mass flow rate
- h: Enthalpy of fluid

Furthermore, if the two fluids do not change phase and the specific heat capacities C_p, are assumed to be constant, *equations (1 and 2)* are transformed as follows:

$$\dot{Q}_h = \dot{m}_h C_{p_h}(T_{h,in} - T_{h,out}) \tag{3}$$

$$\dot{Q}_c = \dot{m}_c C_{p_c}(T_{c,out} - T_{c,in}) \tag{4}$$

where:

- $\dot{Q} = \dot{Q}_h = \dot{Q}_c$

According to the second law of thermodynamics, heat flow rate $\dot{Q}$ is considered positive while it is transferred from the hot fluid to the cold fluid. Moreover, the thermal analysis of heat exchangers is greatly facilitated by using the concept of the heat capacity rate C for each working fluid, which is defined as the product of the mass flow rate and its specific heat capacity, i.e.:

$$C_h = \dot{m}_h C_{p_h} \tag{5}$$

$$C_c = \dot{m}_c C_{p_c} \tag{6}$$

Where denotes the transfer rate required to change the temperature of a fluid passing through the heat exchanger by 1 degree Celsius. Considering the definition of heat capacity rate, we can summarize *equations (3 and 4)* in the following expression.

$$\dot{Q} = C_h\left(T_{h,in} - T_{h,out}\right) = C_c(T_{c,out} - T_{c,in}) \tag{7}$$

The rate of heat change in a heat exchanger is determined by the heat capacity rate of each fluid, multiplied by its temperature difference. A better analysis of heat exchangers requires an additional important relationship which relates the heat flow and the temperature difference between the hot and cold fluids, $(\Delta T \equiv T_h - T_c)$. This is a general expression of Newton's law, where the total heat transfer coefficient U, replaces the coefficient of thermal conductivity, h. However, in the case of a heat exchanger, the rate of heat change is transformed as the temperature difference ΔT, between the two streams changes at each position.

$$\dot{Q} = UA\Delta T_m \tag{8}$$

The appropriate average temperature difference for the thermal analysis of a heat exchanger is represented by ΔT_m, and its form is determined accordingly.

3.1.3 The LMTD Method (Log Mean Temperature Difference)

The Logarithmic Mean Temperature Difference (LMTD) is applied to select the most appropriate type or size of heat exchanger. The primary objective is to effectively handle specific heat transfer requirements. Moreover, this method is used in a straightforward manner to the thermal analysis of heat exchangers. This is achieved when the inlet and outlet temperatures of both the hot and cold flows are either known or can be determined by applying the energy conservation *equations (3 and 4)*. Once ΔT_{lm} (Logarithmic Mean Temperature Difference), the mass flows of the respective streams and the total heat transfer coefficient are known, the heat exchange surface area can be determined directly from *equation (9)*. The LMTD methodology is analyzed below for various types of heat exchangers.

$$\dot{Q} = UA\Delta T_{lm} \tag{9}$$

where:

$$\Delta T_{lm} = \frac{\Delta T_i - \Delta T_O}{\ln \frac{\Delta T_i}{\Delta T_O}} \tag{10}$$

This is defined as the Logarithmic Mean Temperature Difference and represents the exact average temperature difference between the two streams of the heat exchanger. Furthermore, the variables ΔT_i and ΔT_O represent the temperature difference between the two fluids at the inlet and the outlet of the heat exchanger, respectively.

Parallel Flow Heat Exchangers applies to:

$$\begin{gathered} \Delta T_i = T_{h,in} - T_{c,in} \\ \Delta T_o = T_{h,out} - T_{c,out} \end{gathered} \tag{11}$$

Counter Flow Heat Exchangers applies to:

$$\begin{gathered} \Delta T_i = T_{h,in} - T_{c,out} \\ \Delta T_o = T_{h,out} - T_{c,in} \end{gathered} \tag{12}$$

Cross Flow and Shell – and – Tube Heat Exchangers – Correction Factor:

The majority of practical applications involve heat exchangers other than the shell – and – tube type. Although, flow conditions can be complex in cross – flow and shell – and – tube heat exchangers, the basic *equations (3, 4 and 10)* presented in the previous sections are valid and can be applied by introducing the correction factor F, into the LMTD analysis of *equation (9),* in the following form:

$$\dot{Q} = FUA \frac{\Delta T_i - \Delta T_O}{\ln \frac{\Delta T_i}{\Delta T_O}} = FUA\Delta T_{lm} \tag{13}$$

In order to calculate the temperature differences ΔT_i and ΔT_O, consider the case of a counterflow heat exchanger, *equation (12)*.

Pertaining to cross – flow and shell – and – tube heat exchangers, it is noted that the correction factor invariably registers a value below one. This factor is integral to the operational efficiency of these heat exchangers and is derived through distinct graphical representations for each exchanger variant. These graphs are the visual culmination of resolves algebraic formulations specific to each type. Illustrative examples, as presented in *figures (20 – 24)* of this study, demonstrate the dependency of the coefficient F on two critical non-dimensional parameters, denoted as R and P. These parameters are essential in quantifying the proportional differences in temperature within the system and are defined in a detailed manner subsequently.

$$R = \frac{T_1 - T_2}{t_2 - t_1} \qquad P = \frac{t_2 - t_1}{T_1 - t_1} \tag{14}$$

In the shell – and – tube heat exchangers, "t" represents the temperature of the fluid flowing through the channels and "T" represents the temperature of the fluid flowing inside the shell, while the subscripts "1" and "2" represent the inlet and outlet of each flow from the heat exchanger, respectively. To calculate the correction factor, the temperatures of the two flows at the inlet and outlet of the heat exchanger to be studied must be known. It should be noted that when the parameters R and P approach zero, the correction factor tends to unity, so that *equation (13)* takes its original form as *equation (9)*. In particular, the values P range between 0 and 1. If it tends to 0, then the fluid moving inside the channels is undergoing an isothermal process, since $t_1 = t_2$, which indicates a phase change, i.e. condensation or evaporation processes, which is why heat exchangers are called condensers, evaporators or boilers. In addition, the values of R range from 0 to infinity. If R tends to 0, the isothermal process occurs on the side of the fluid moving in the shell. On the other hand, if R tends to infinity, the fluid undergoes a phase change in the flutes, and the processes are characterized as condensation and evaporation. In both cases the correction factor F for a boiler or condenser is equal to 1, regardless of the heat exchangers arrangement.

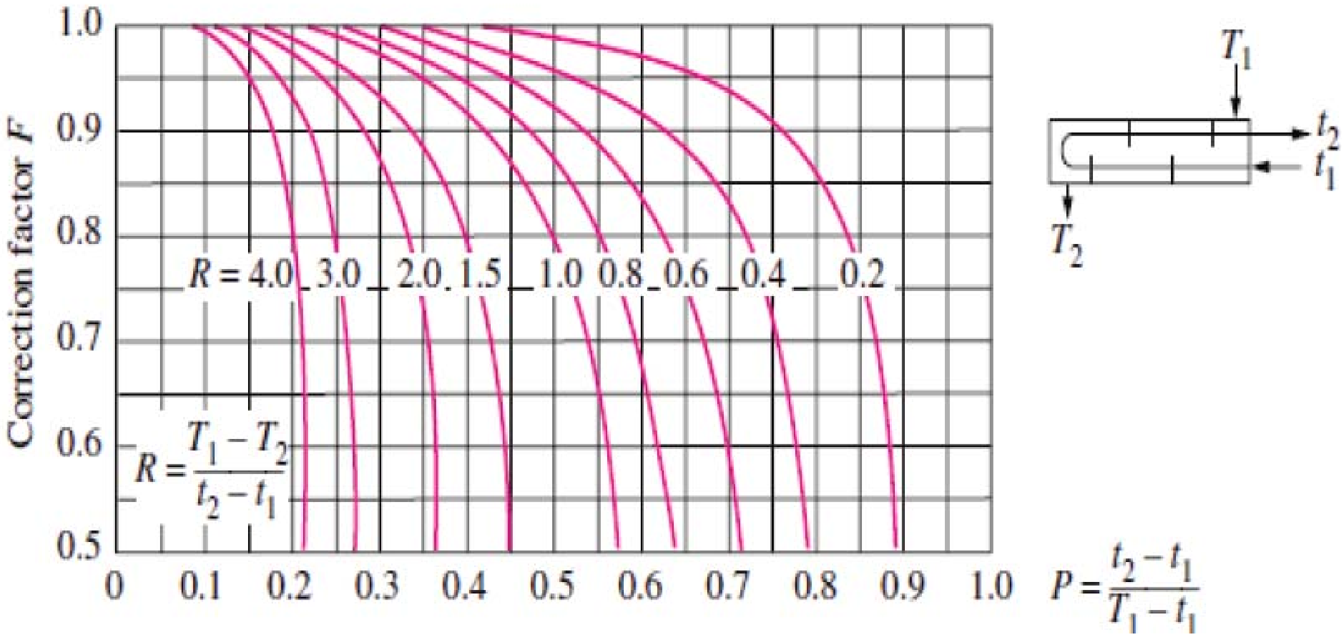

Figure 20: One – Shell Pass and 2,4,6, etc. (any multiple of 2), tube passes Heat Exchanger

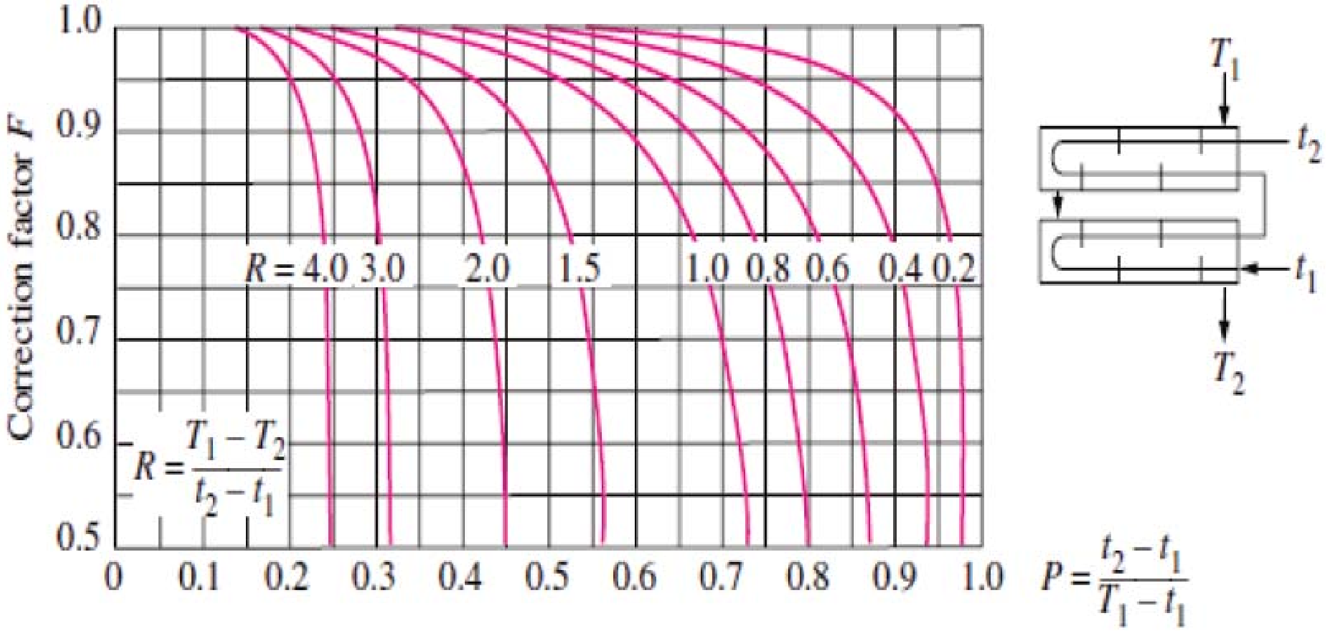

Figure 21: Two – Shell Passes and 4,8,12, etc. (any multiple of 4), tube passes Heat Exchanger

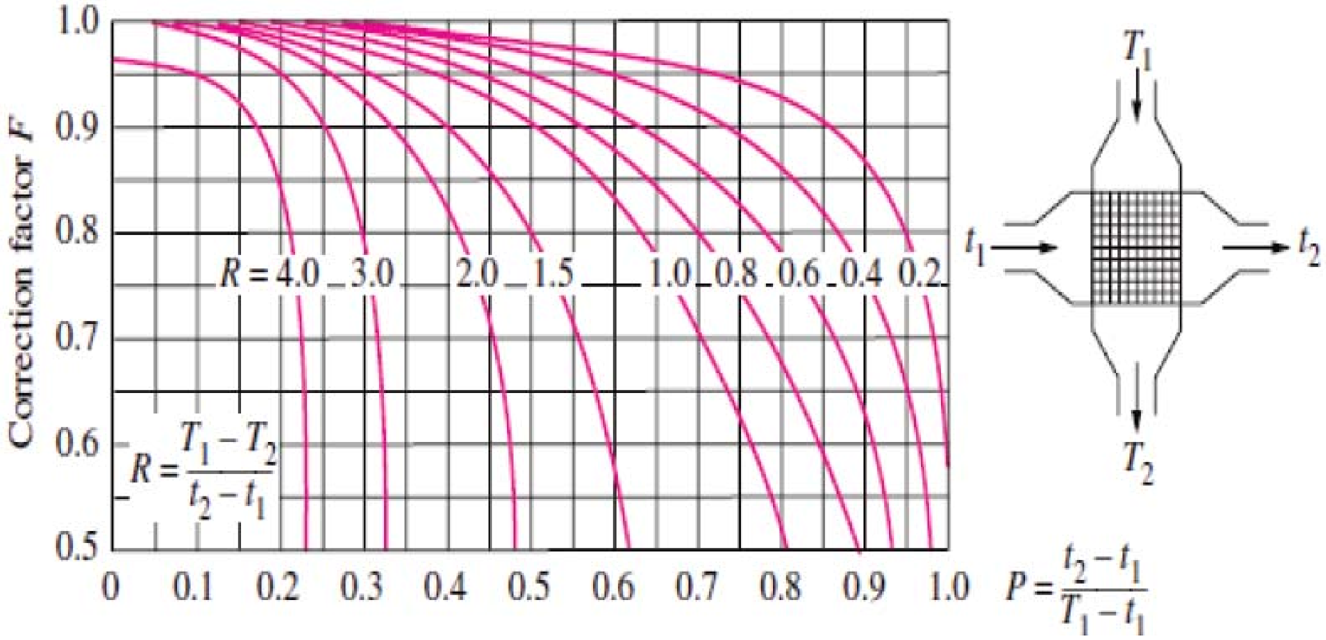

Figure 22: Single – Pass Cross – Flow Heat Exchanger with both fluids unmixed

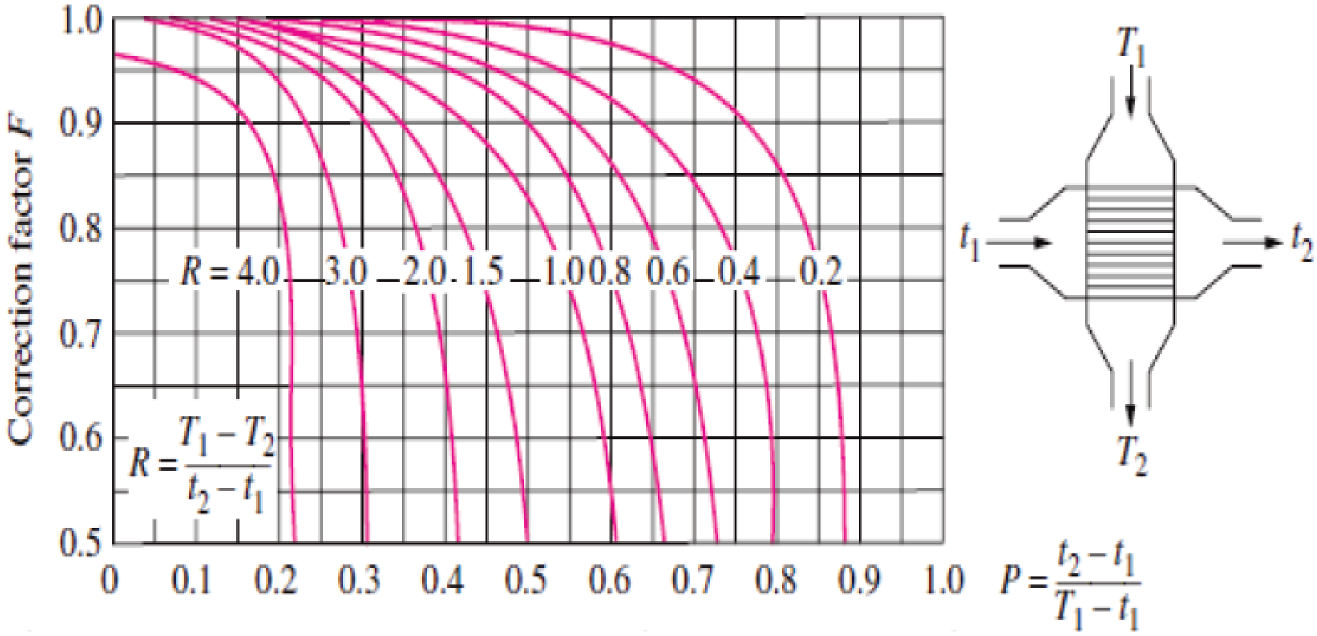

Figure 23: Single – Pass Cross – Flow Heat Exchanger with one fluid mixed and the other unmixed

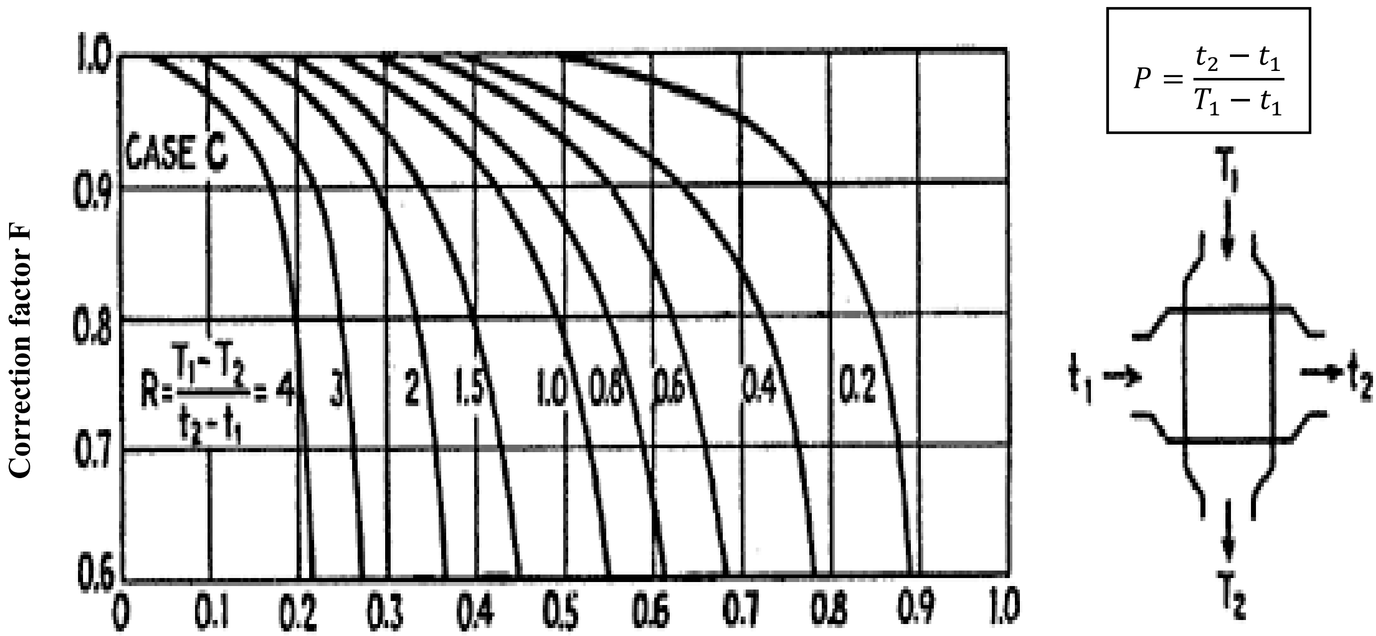

Figure 24: Single – Pass Cross – Flow Heat Exchanger with both fluids mixed

The LMTD method concludes by applying the following resolving procedure:

1. Select the appropriate heat exchanger type for the application.
2. Determine any unknown inlet or outlet temperature of fluid and heat transfer rate $\dot{Q}$ by heat balance.
3. Calculate the mean logarithmic temperature difference, ΔT_{lm} and apply the appropriate correction factor F if necessary.
4. Calculate or select the value of the total heat transfer coefficient U.
5. Calculate the heat exchange surface area, A.

To complete the process, select a heat exchanger with a heat exchange surface area equal to or larger than the one calculated in the previous step. However, if the inlet and outlet temperatures of a heat exchanger are unknown, determining its thermal behavior and efficiency can be challenging. In such cases, the LMTD methodology can still be applied, but it requires an iterative trial and error method, which is often impractical. Therefore, it is preferable to use an alternative methodology known as the Effectiveness - Number Transfer of Units (ε – NTU).

2.5.4 The ε – NTU Method (Effectiveness - Number Transfer of Units)

The ε – NTU methodology was first reported by Kays and London in 1955. However, it is commonly used in the thermal analysis of heat exchangers, where the type and size of heat exchanger is specified and it is necessary to determine the heat transfer rate and the outlet temperature of the fluids from the device. For a specific application, the mass flows and inlet temperatures of the two streams in the heat exchanger can be used as data. This method offers several benefits for problem analysis, allowing for a comparison between different types of heat exchangers to select the most suitable one for the desired application.

Effectiveness – ε

To define efficiency, it is necessary to first establish the concept of the maximum rate of thermal energy transfer in the case of a heat exchanger. The heat transfer amount $\dot{Q}$ is determined by calculating either the energy loss of the hot fluid or the heat gain of the cold fluid using *equation (7)*. To calculate the maximum heat transfer rate in a heat exchanger, it must first be clarified that the maximum temperature difference that exists is that between the inlet of the hot stream and that of the cold stream, i.e.:

$$\Delta T_{max} = (T_{h,in} - T_{c,in}) \quad (15)$$

The fluid with the lowest heat capacity rate experiences the largest temperature change and will therefore reach the maximum transferred heat value faster. This is because the rate of temperature change is inversely proportional to the heat capacity of the fluid.

$$\dot{Q}_{max} = C_{min}\Delta T_{max} = C_{min}(T_{h,in} - T_{c,in}) \tag{16}$$

Therefore, the efficiency of a heat exchanger is defined as the ratio of the actual heat flow to the maximum possible output, expressed as follows:

$$\varepsilon = \frac{\dot{Q}}{\dot{Q}_{max}} \tag{17}$$

The expression includes a dimensionless number that ranges from 0 to 1. It depends on the flow temperatures and is defined as follows:

$$\varepsilon = \frac{C_h(T_{h,in} - T_{h,out})}{C_{min}(T_{h,in} - T_{c,in})} \tag{18}$$

$$\varepsilon = \frac{C_c(T_{c,out} - T_{c,in})}{C_{min}(T_{h,in} - T_{c,in})} \tag{19}$$

If the parameters of the efficiency and the inlet temperatures of both fluids of a heat exchanger, then it is possible to calculate the actual amount of heat transferred using the equation:

$$\dot{Q} = \varepsilon\dot{Q}_{max} = \varepsilon C_{min}(T_{h,in} - T_{c,in}) \tag{20}$$

Number Transfer of Units (NTU)

In each heat exchanger case, the effectiveness, ε, is directly correlated as a function such as:

$$\varepsilon = f\left(NTU, \frac{C_{min}}{C_{max}}\right) \tag{21}$$

where the ratio C_{min}/C_{max} is called the heat capacity ratio and is equal to C_c/C_h or C_h/C_c depending on the magnitude of the values of the heat capacity rates of the hot and cold flows.

The quantity Number Transfer of Units (NTU) is defined and is a dimensionless parameter specified as follows:

$$NTU = \frac{UA}{C_{min}} = \frac{UA}{(\dot{m}C_p)_{min}} \tag{22}$$

where U is the total heat transfer coefficient and A is the heat exchange area of the heat exchanger. It should be noted that Number Transfer of Units (NTU) is a measure of surface area comparison of the heat exchangers because if given values of U and C_{min}, a higher Number Transfer of Units (NTU) value is associated with a larger heat exchanger.

The ε-NTU method concludes by applying the following resolving procedure:

1. Calculate the heat capacity ratio, C_{min}/C_{max}.
2. Calculate the $NTU = UA/C_{min}$.
3. Determine the efficiency ε either from graphs or from appropriate correlations, preferably with Number Transfer of Units (NTU) for the type of heat exchanger specified.
4. Calculate the heat transfer rate $\dot{Q}$ using the calculated value of $\dot{Q}_{max}$.
5. Calculate the outlet temperatures of the two streams using the thermal balance.

The above method can also be applied to calculate the surface area of the heat exchanger, as well as the LMTD method, as long as the inlet and outlet temperatures of the two fluids are known and once the effectiveness, ε, and the Number Transfer of Units, NTU, is calculated.

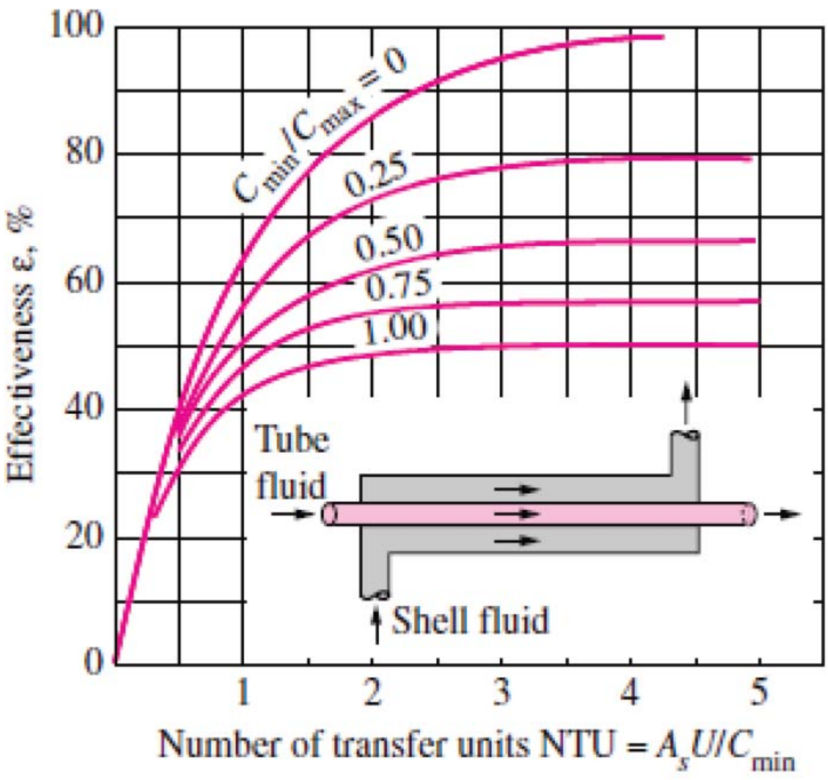

Figure 25: Parallel – Flow Heat Exchanger

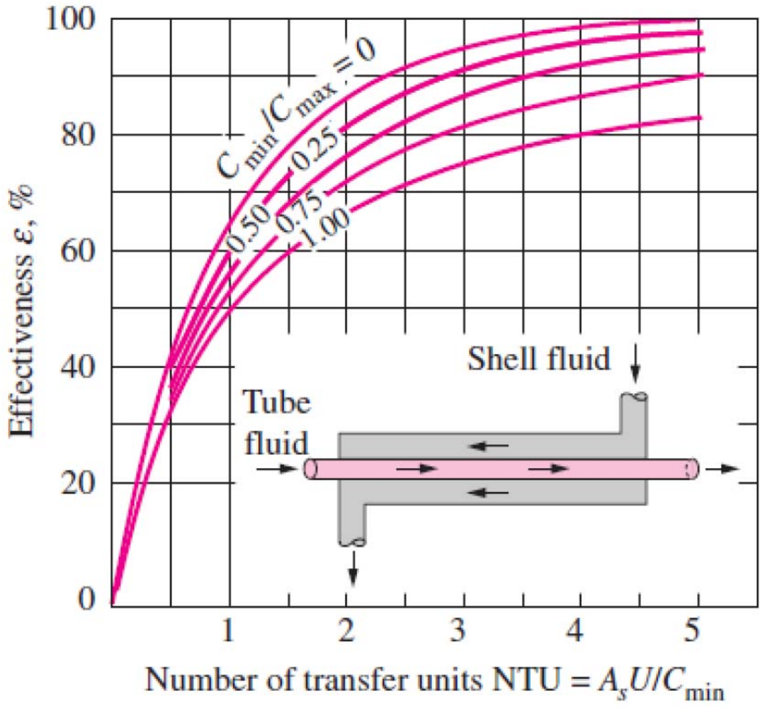

Figure 26: Counter – Flow Heat Exchanger

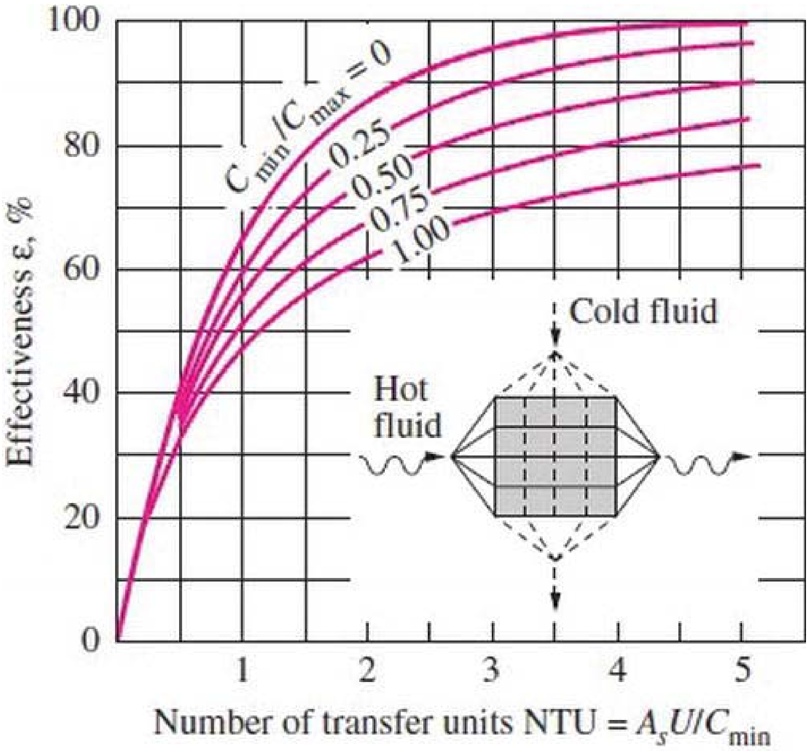

Figure 27: Single – Pass Cross – Flow Heat Exchanger unmixed fluids

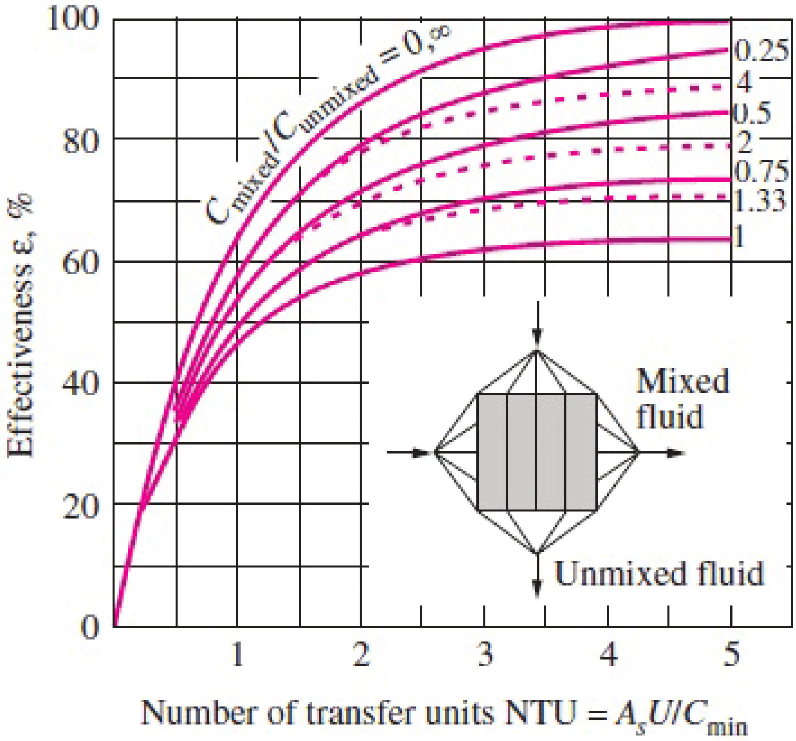

Figure 28: Single – Pass Cross – Flow Heat Exchanger with one fluid mixed and the other unmixed

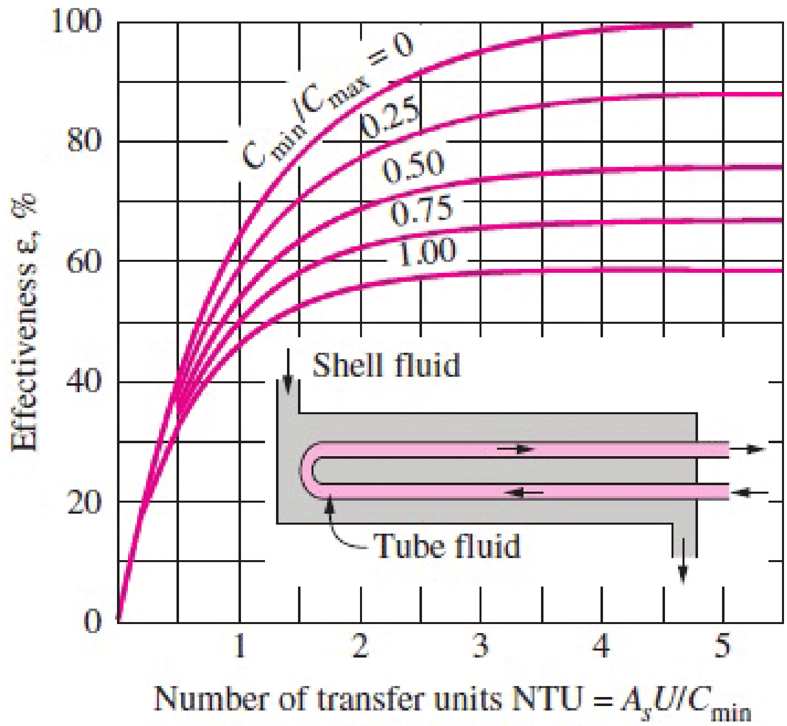

Figure 29: One – Shell Pass and 2,4,6, etc. (any multiple of 2), tube passes Heat Exchanger

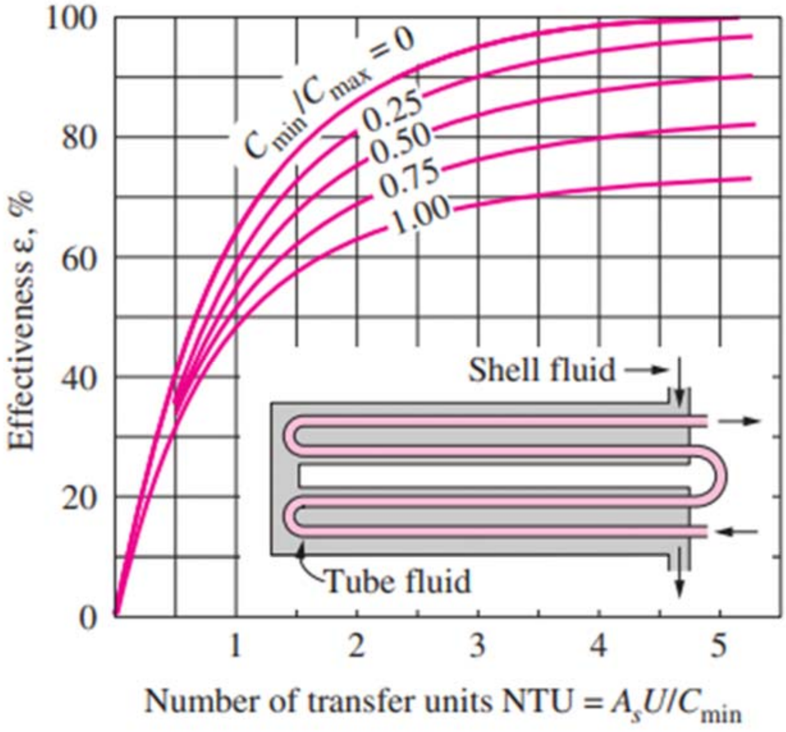

Figure 30: Two – Shell Passes and 4,8,12, etc. (any multiple of 4), tube passes Heat Exchanger

Chapter 3: Experimental Set – Up

3.1 Analysis of Experimental Set – Up

3.1.1 Introduction

The experimental configuration is designed to analyze heat exchangers with the aim of evaluating their efficiency by using the aforementioned methods of calculation described in *chapter 3*. This involves the use of various components, which will be analyzed in detail to understand their respective functions. The main objective of the experimental set – up is to be able to simulate the overall operation of an Internal Combustion Engine (I.C.E), for example someone who wants to upgrade their heat exchanger in their car, for a racing application can attach different types and sizes of heat exchangers in the experimental set – up so that they can be tested.

3.1.2 Heat Exchanger – Radiator

The experimental set – up incorporates a heat exchanger, depicted in *figure 31*, featuring specific fin configurations elucidated in *figure 32*. These visual representations offer comprehensive insights into the fluid and air pathways, crucial for understanding the heat dissipation processes facilitated by the heat exchanger. Comprising tubular cells with 400 x 400 mm blades and three columns of tubes are arranged heterogeneously, the heat exchanger is designed to optimize thermal transfer. Special spouts at the radiator inlets and outlets facilitates seamless rubber connections. Integrated sensors provide real time data on the inlet and outlet temperatures of the water, as well as the air outlet temperature from the fan to the radiator core and the surrounding environment.

The upper section of the radiator incorporates an overflow plug, accommodating a specialized radiator cap, as exemplified in *figure 34*. From the specific position of the radiator cap the entire system is filled with water. Additionally, a spring valve within the pressure cap serves to regulate pressure within the system, releasing excess pressure into the environment.

Radiator Data:

- Pipe Diameter: 25 mm
- Surface Area of Core (A): 0.3792 m^2
- Dimensions: 400 x 360 x 60 mm
- Radiator Type: Downflow

Figure 31: Downflow Heat Exchanger

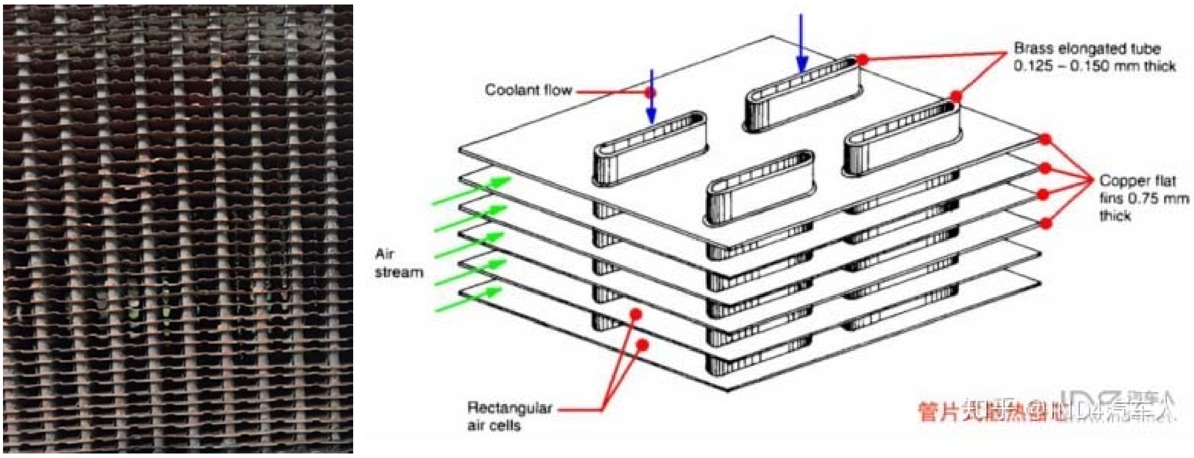

Figure 32: Type of Heat Exchanger Fins

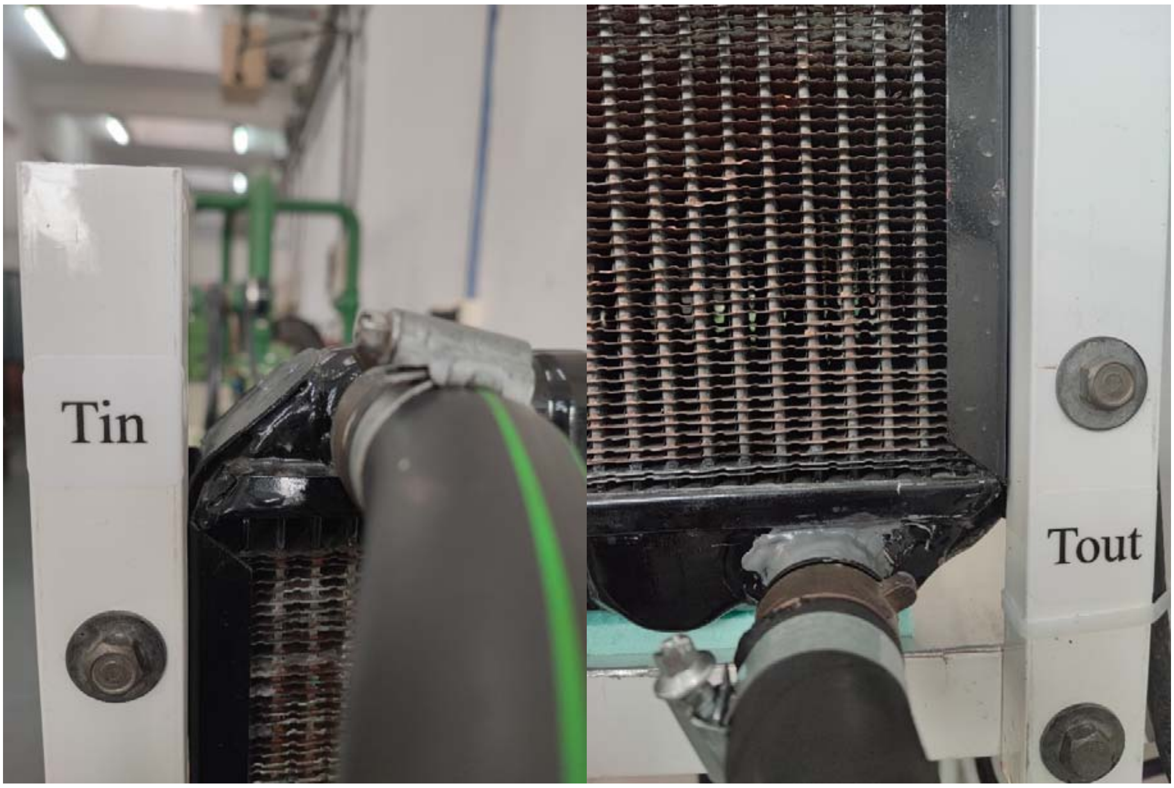

Figure 33: Stickers for Inlet & Outlet

Figure 34: Radiator Cap and Overflow Pipe

3.1.3 Water Heater – Boiler

The experimental set – up incorporates a boiler serving as a heat source, effectively emulating the functionality of an internal combustion engine. This process is facilitated through the utilization of the heating element illustrated in *figure 35*. Notably, the experimental boiler is equipped with the capability to adjust the desired temperature, providing a versatile feature for users to tailor the thermal conditions according to the specific requirements of their experiments. This adjustable temperature feature is elucidated in *figure 36*, enhancing the flexibility and adaptability of the experimental set – up for a diverse range of research endeavors.

Water Heater – Boiler Specifications:

- Brand: Romina
- Quantity: 40 L
- Power: 3000 W
- Voltage: 220 V
- Insulation: Polyurethane
- Weight: 15 kg
- Dimensions: 450 x 480 mm

Figure 35: Boiler – Water Heater (Romina)

Figure 36: Element Circuit & Temperature Set – Ups

Figure 37: Stickers of Inlet & Outlet

3.1.4 Water Pump

As mentioned previously, the experimental set – up is a simulation of an Internal Combustion Engine (I.C.E). Every Internal Combustion Engine (I.C.E) requires a water pump in its cooling system, as explained in *chapter 2.3*. To simulate the water pump in the Internal Combustion Engine (I.C.E) system in the experimental set – up, it is important to automate the experimental water pump in order to be able to control the flow in the system. Each Combustion Engine has a different type of water pump, where the maximum flow rate of each pump is different. By automating the flow rate in our system, we can achieve the maximum flow rate of each Internal Combustion Engine (I.C.E) water pump that is used in our experiment. A more predictive study will be provided for the particular engine, and it must be taken under consideration for selecting a heat exchanger.

Water Pump Specifications:

- Brand: Gianneschi & Ramacciotti
- Flow Rate: 40 – 100 L/min
- Max Height: 19/13 m
- Voltage: 230 V
- Max RPM’s: 2900 rpm
- Power: 0.55 kW

Figure 38: Gianneschi & Ramacciotti Water Pump

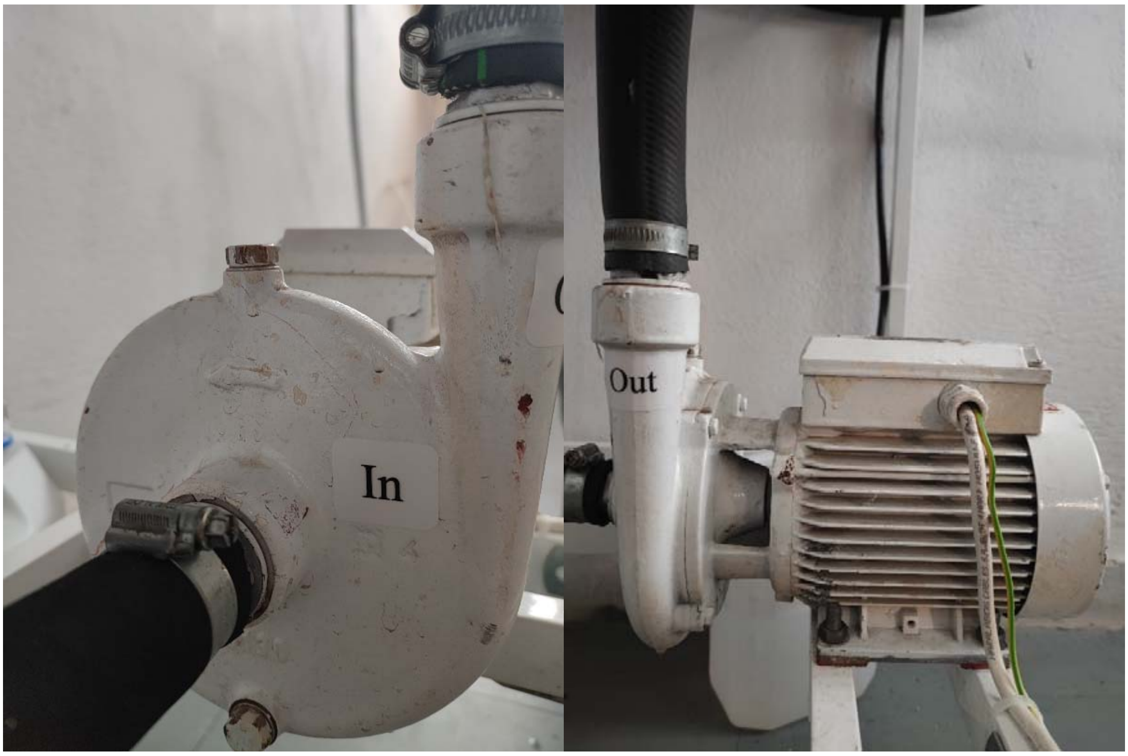

Figure 39: Stickers of Inlet & Outlet

3.1.5 Cooling Fan

The cooling fan plays a crucial role in the experimental set – up and also in car's cooling system for maintaining the optimal operating temperature of the engine. The primary purpose of the cooling fan is to dissipate the excess heat generated by the engine during combustion to the environment. The temperature of the air that is dissipated from the radiator core by the cooling fan is measured by a thermocouple, it is placed as shown in *figure 41* to allow a comparison between the air outlet temperature of the radiator core and the ambient temperature. Lastly, a potentiometer is provided to adjust the airflow of the cooling fan for testing purposes.

<u>Cooling Fan Specifications:</u>

- Brand: Aliberti M – 300
- Noise Level: 75 dB
- Power: 95 W
- Weight: 5 kg
- Air Flow: 1736 m^3/h
- Installation Hole: 310 mm
- Dimension: 402 ∅ mm

Figure 40: Aliberti M – 300 Cooling Fan

Figure 41: Tair Thermocouple Position

Figure 42: Stickers of Tair Flow Direction

3.1.6 Water Flow Sensor

The water flow sensor in the experimental set – up serves the purpose of measuring the flow rate in the system. The flow rate can be identified at any given moment to simulate the water pump that is used in any Internal Combustion Engine (I.C.E) according to the specifications of the experimental water pump, so that we can test the specific heat exchanger which is recommended to install this in the engine that is being studied.

Water Flow Sensor Specifications:

- Model: DN 32
- Working Range: 1 – 120 L/min
- Water Pressure: ≤ 2.0 MPa
- Operating Voltage: 3.5 – 24 VDC

Figure 43: Water Flow Sensor

Figure 44: Water Flow Sensor Position

3.1.7 Arduino – Microcontroller

Arduino is an open – source electronics platform based on easy – to – use hardware and software. It consists of a physical programmable circuit board and a development environment for writing and uploading code to the board. The programming is done by using a simplified version of C++ that is easy to learn for beginners. Moreover, Arduino's hardware designs and software's are open sources, meaning that their codes are freely available to the public. This encourages collaboration, innovation, and the creation of a diverse range of projects.

Within the experimental setup, the Arduino plays a pivotal role in acquiring data from the thermocouples and subsequently presenting it on the LCD screens. These LCD screens serve as the interface for reading temperature and monitoring the water flow rate within the system, facilitated by the integration of a water flow sensor. The Arduino functions as the central processing unit, arranges the data obtained from the process and provides real time information through the LCD displays, contributing to the comprehensive monitoring and control of the experimental set – up. The following *figure 45* presents an Arduino microcontroller.

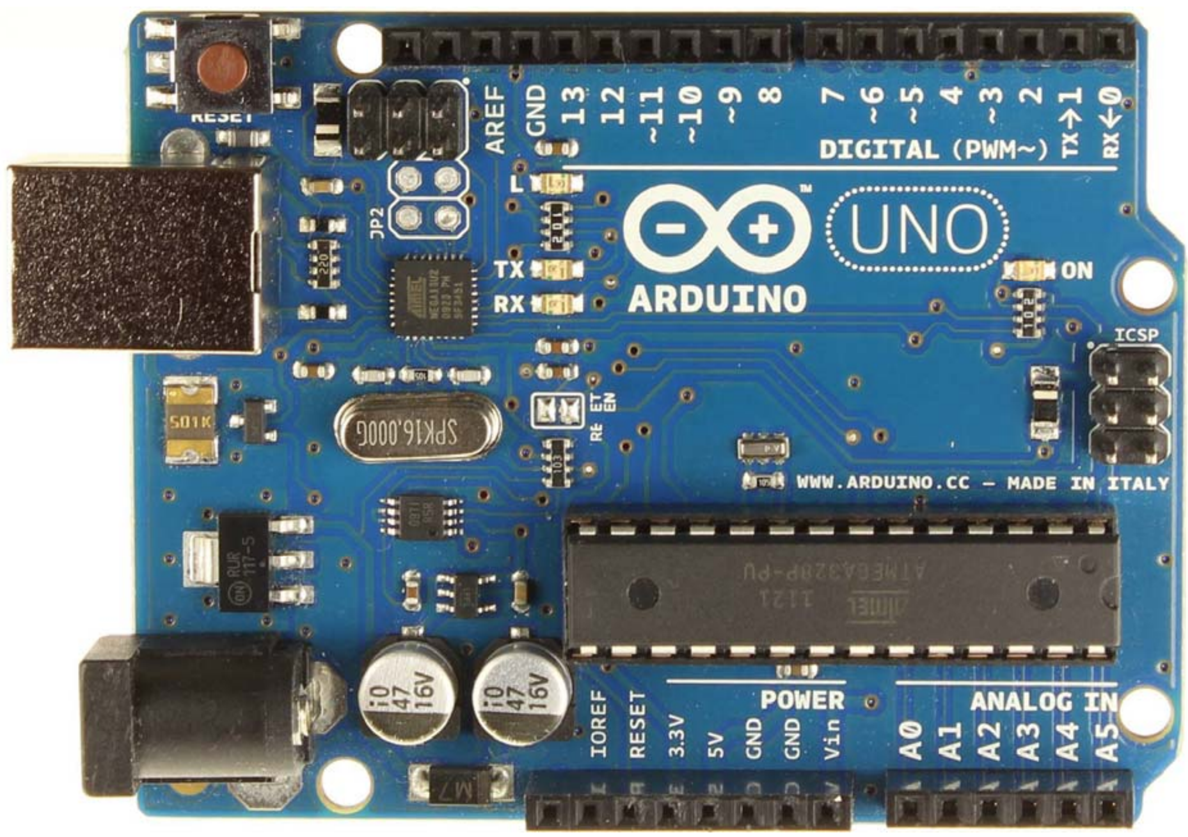

Figure 45: Arduino Uno Microcontroller Board

3.2 Methodology & Process of Experimental Set – Up

3.2.1 Work Bench

The Work Bench was designed using the SolidWorks program to obtain an accurate representation of the base, allowing us to determine the quantity and dimensions of the materials. For the construction of the base, aluminum profiles with dimensions of 20 x 35 x 1.5 mm were used. Once the materials arrived, we proceeded into cutting the aluminum to the dimensions specified in the design. Firstly, the positions of the joints were marked and the materials were drilled so that the rivets could be placed using steel brackets to hold the aluminum components in place. In the final stage, a sheet of aluminum was attached to the top of the base, marked and drilled for riveting to the aluminum profile. The Work Bench precision and structural integrity were ensured by this systematic construction process. The figures below demonstrate the materials used and the final design of the Work Bench.

Figure 46: Parts of Workbench Assembly

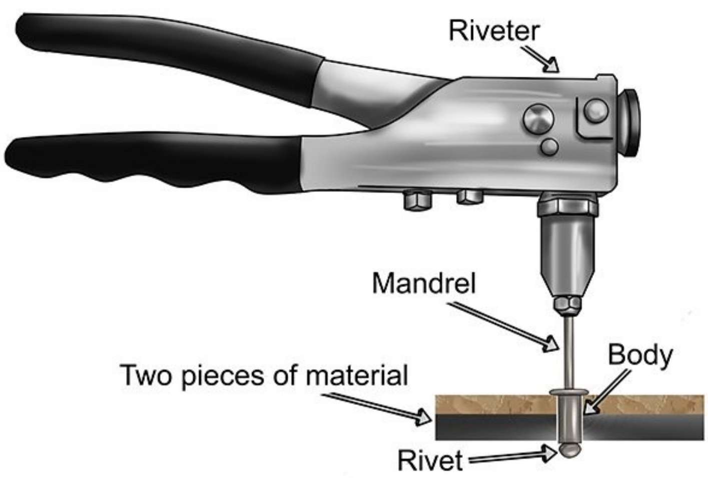

Figure 47: Process of Securing the Parts with Rivets

Figure 48: Workbench Part (Autodesk Inventor 2024)

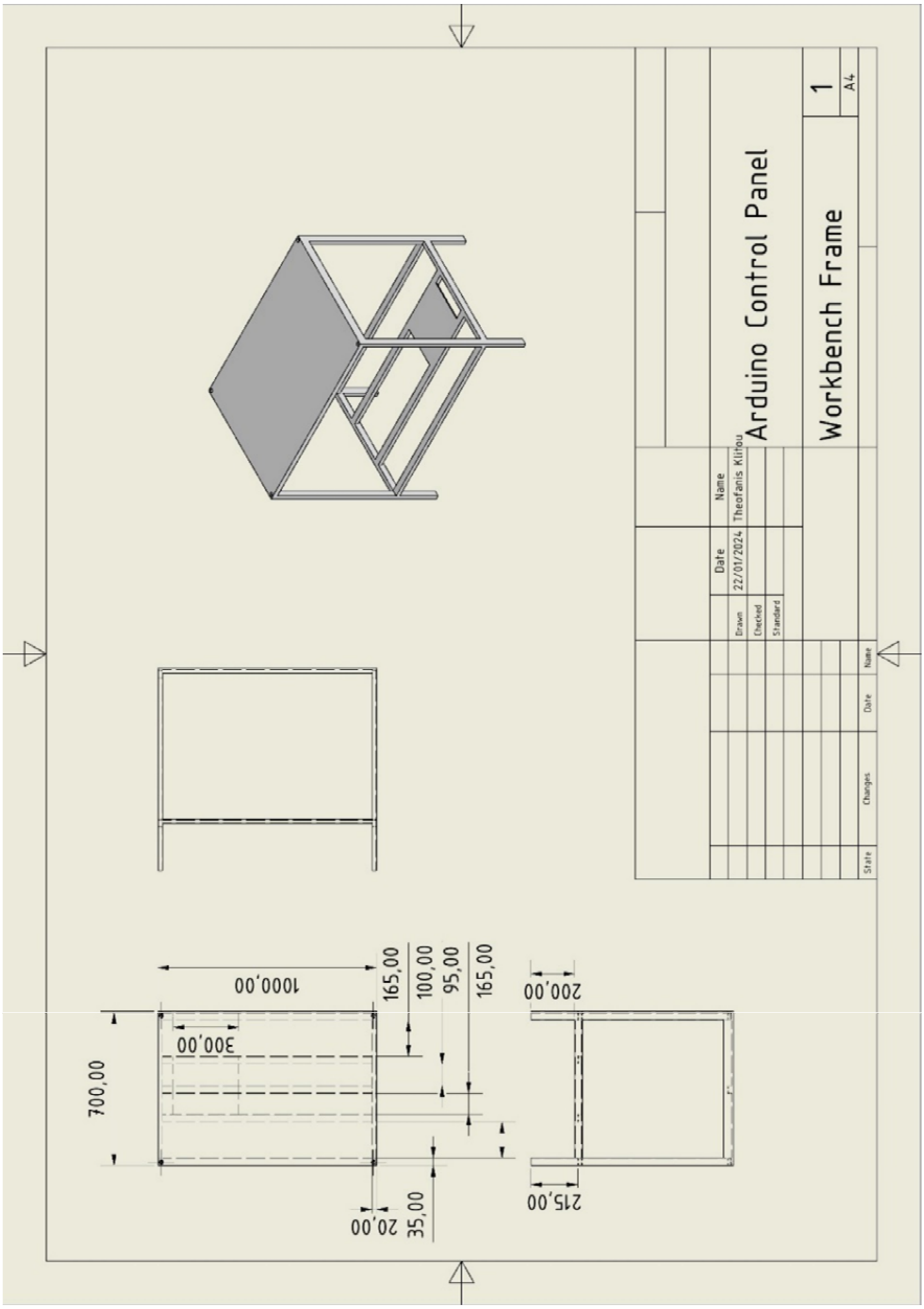

Figure 49: Workbench Drawing (Autodesk Inventor 2024)

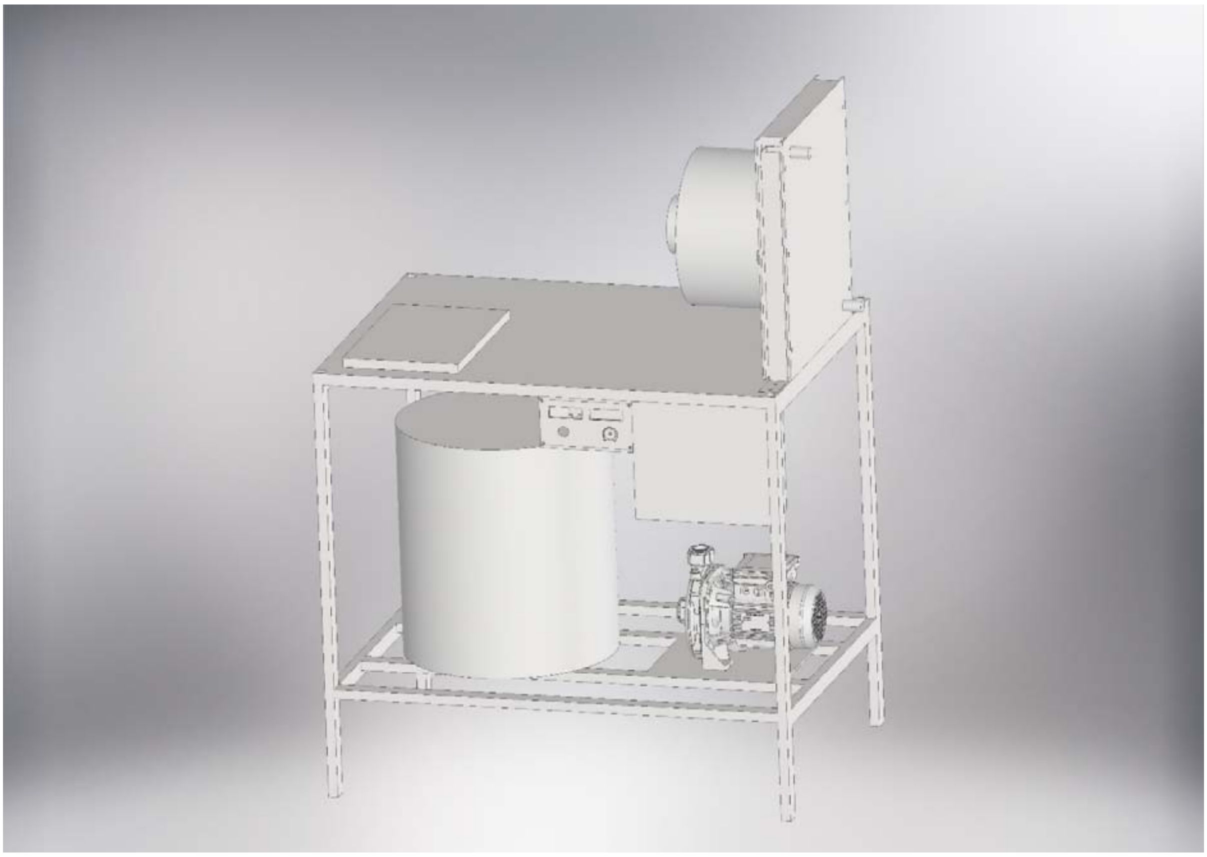

Figure 50: Workbench Assembly (Autodesk Inventor 2024)

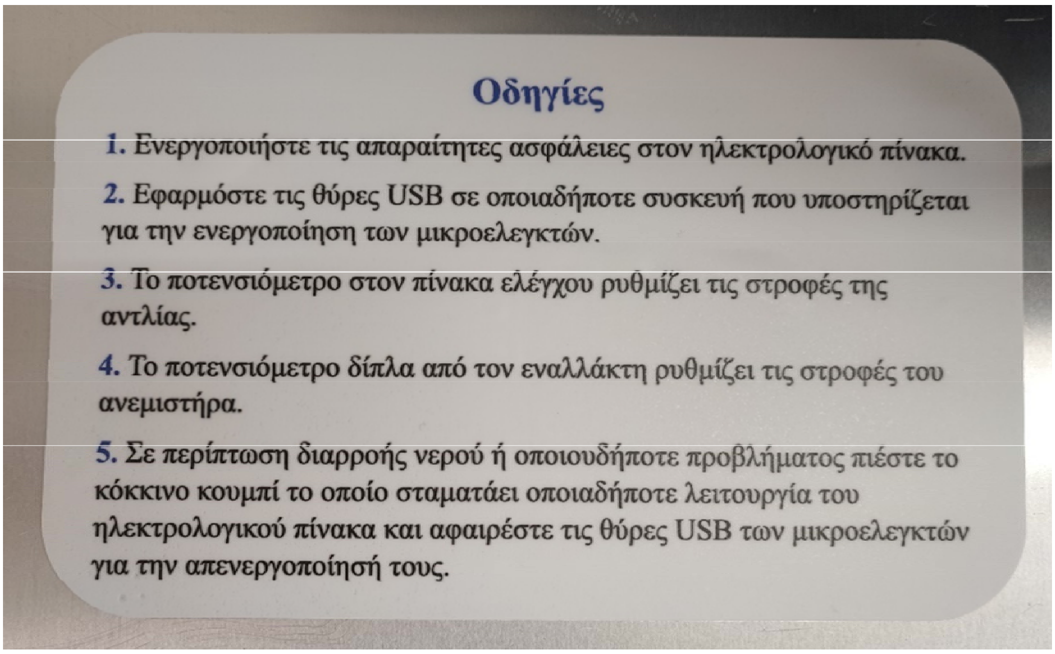

Figure 51: Sticker of Instructions for Experimental Set – Up

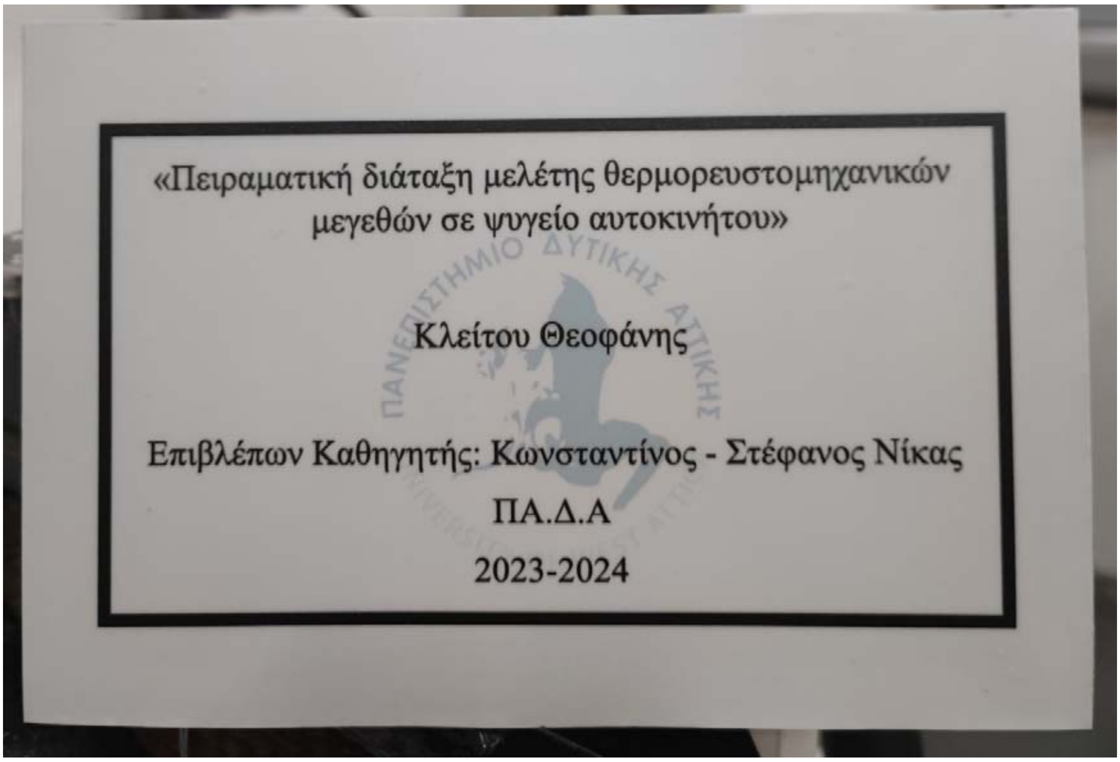

Figure 52: Sticker of Thesis Title, Author and Supervisor

3.2.2 Electrical Control Panel

The control panel, a creation of an electrical engineer, has been purposefully engineered to enhance the ease of manipulating the electrical components within the experimental setup. Its primary objective is to ensure the users safety throughout the operational phases. In the event of a potential leakage scenario, a failure – safe fuse is strategically incorporated, halting the operation of every single electrical element in the experimental set – up. Delving deeper into its functionalities, the control panel not only demonstrates its ability to safeguard against potential hazards but also provides a comprehensive interface for initiating and controlling various essential system components. The control panel permits the activation of the cooling fan, the boiler and the water pump of the system.

The electrical control panel has been integrated into the experimetal set – up by securing it with self – tapping screws onto the aluminum components.

Figure 53: Stickers of Electrical Control Panel Instructions

Figure 54: Electrical Control Panel Circuit

Emergency Button

An emergency button, also known as an emergency stop button, is a safety device designed to interrupt a process or operation in the event of an emergency. It is a physical button or switch that, when is pressed or activated, it triggers an immediate and complete cessation of a system's operation, shutting down immediately processes or equipment. The primary purpose of an emergency button is to ensure the safety of individuals and protect assets by rapidly bringing a system to a safe state in critical situations.

The emergency button in our experimental set – up is intricately linked to the electrical control panel. This safety feature is pivotal, providing a decisive and immediate means to bring the entire system to a controlled and secure state, thereby mitigating potential risks and ensuring the well – being of personnel and the integrity of equipment.

Figure 55: Emergency Button Schneider

Dimmer – Potentiometer

The integration of a dimmer with a water pump represents a unique and specialized control system designed to modulate the pump's operational speed and subsequently regulate water flow. These systems enable precise adjustments of the pump's speed, offering flexibility in managing water flow rates based on specific requirements. By providing an adjustable means to control the pump's performance, these dimmer devices contribute to the optimization of water circulation systems, fostering efficiency and adaptability in various applications.

In the experimental set – up, the dimmer has the capability to variably adjust the pump's rpm's, resulting in an adjustable flow within our system. This function is used for instrumental facilitating a comprehensive examination of heat exchange phenomenom. The ensuing figure illustrates the wiring configuration for the dimmer's operation and elucidates its connection within the experimental set – up.

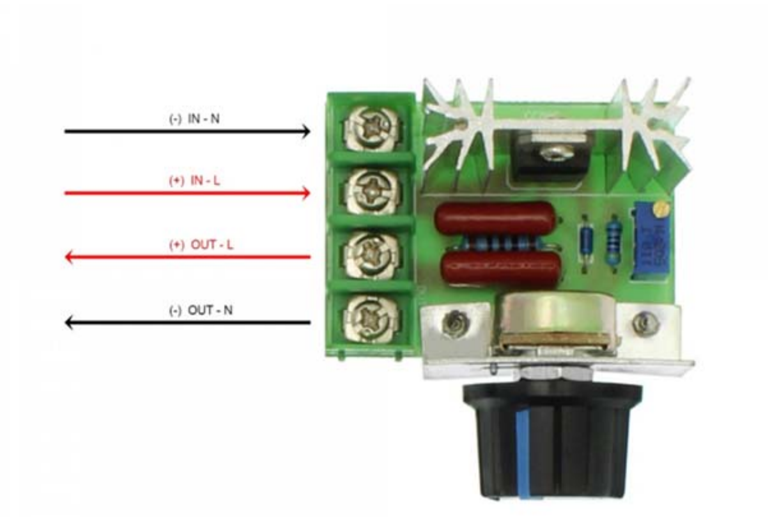

Figure 56: Water Pump Dimmer – Potentiometer

3.2.3 Arduino Control Panel

The design of the Arduino Control Panel was executed using the SolidWorks software, aimed at the comprehensive integration of essential components within a unified enclosure. This approach enhances both visual appeal and the ease of interconnecting the diverse elements. Subsequently, the casing was manufactured using a CR – 10S Pro 3D Printer, featuring strategically placed inserts to facilitate the assembly process and secure components in place using screws. Following up the meticulous arrangements of all components and the establishments of wiring connections, the Arduino microcontroller underwent programming, results in the successful activation of all programmed automations. The ensuing section will provide a detailed exposition of all the components meticulously utilizing the construction of the Arduino Control Panel. To enable the functionalities of the Arduino, a type – B cable is employed as shown in *figure 59*. This cable is compatible with various electrical devices equipped with a USB port and connected to a power source, such as a power bank, laptop, or phone charger. This versatile connectivity ensures that the Arduino can be powered by a range of commonly available devices. The Arduino Control Panel was securely affixed by constructing a dedicated base, firmly attaching it to the experimental set – up workbench using rivets.

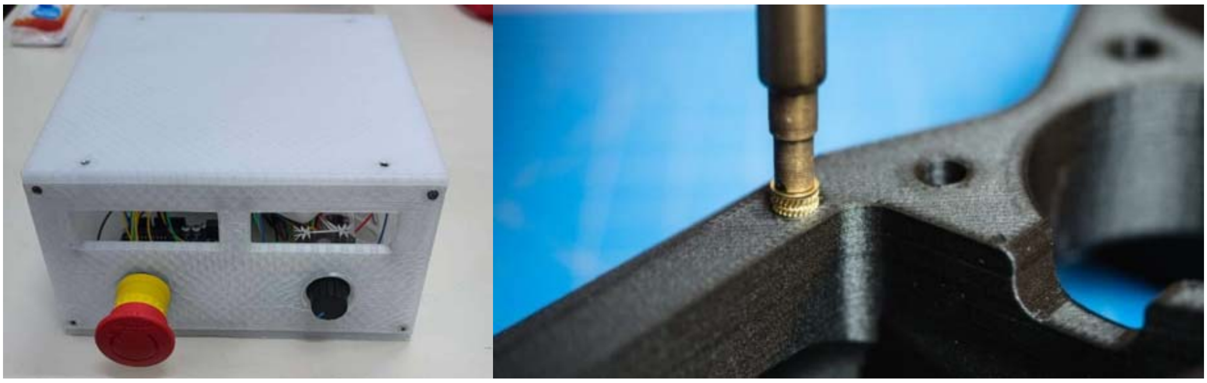

Figure 57: Arduino Control Panel Assembled & Example of Inserts in the 3D Printed Parts for Securing Fasteners

Figure 58: Arduino Control Panel in Operation & Sticker

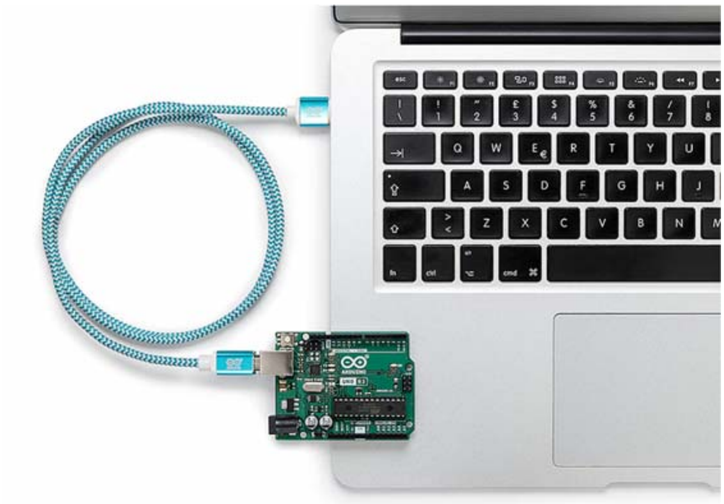

Figure 59: Example of Enabling the Arduino Uno Board

Figure 60: Arduino Control Panel Attached to Workbench

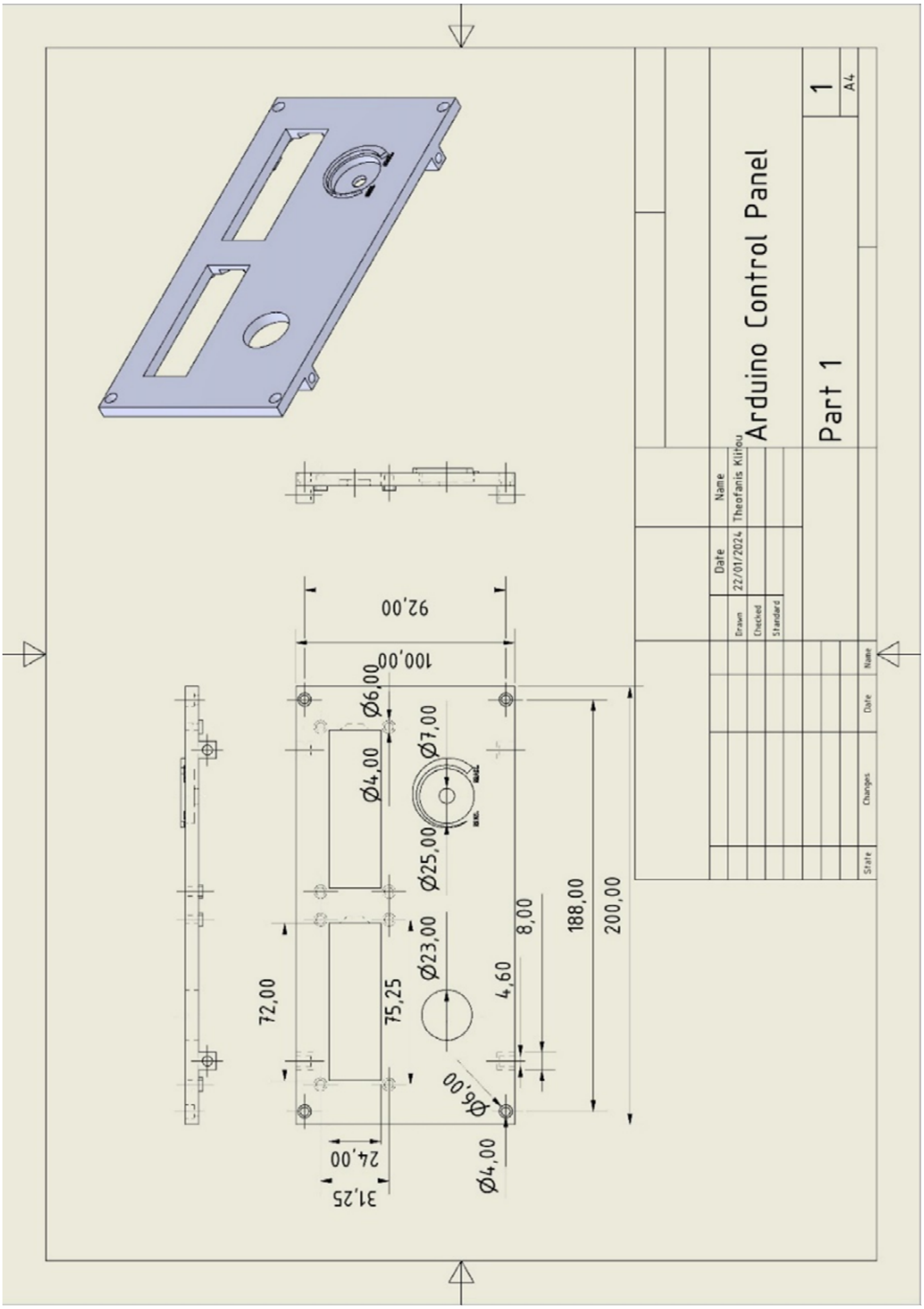

Figure 61: Arduino Control Panel Drawing Part 1 (Autodesk Inventor 2024)

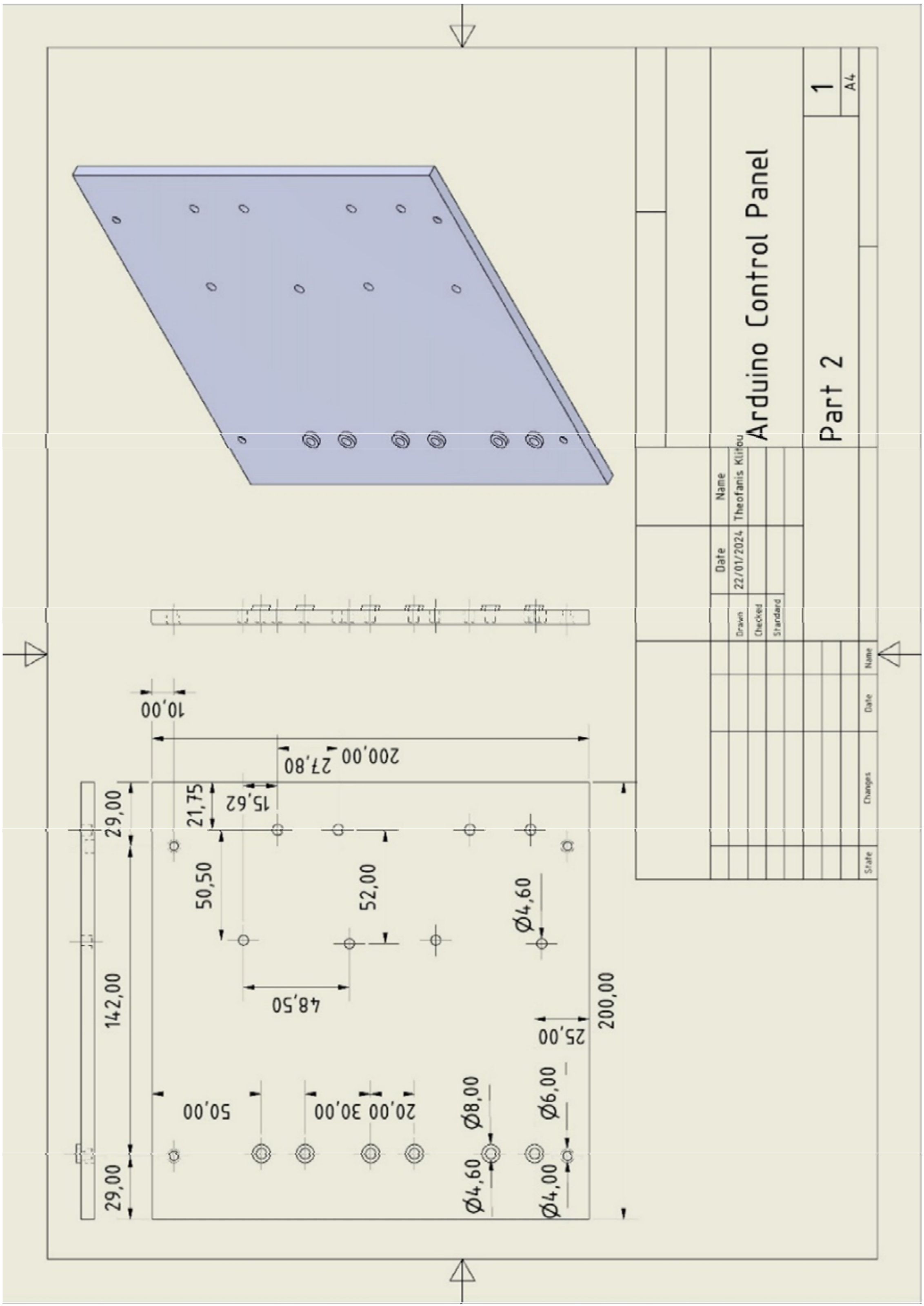

Figure 62: Arduino Control Panel Drawing Part 2 (Autodesk Inventor 2024)

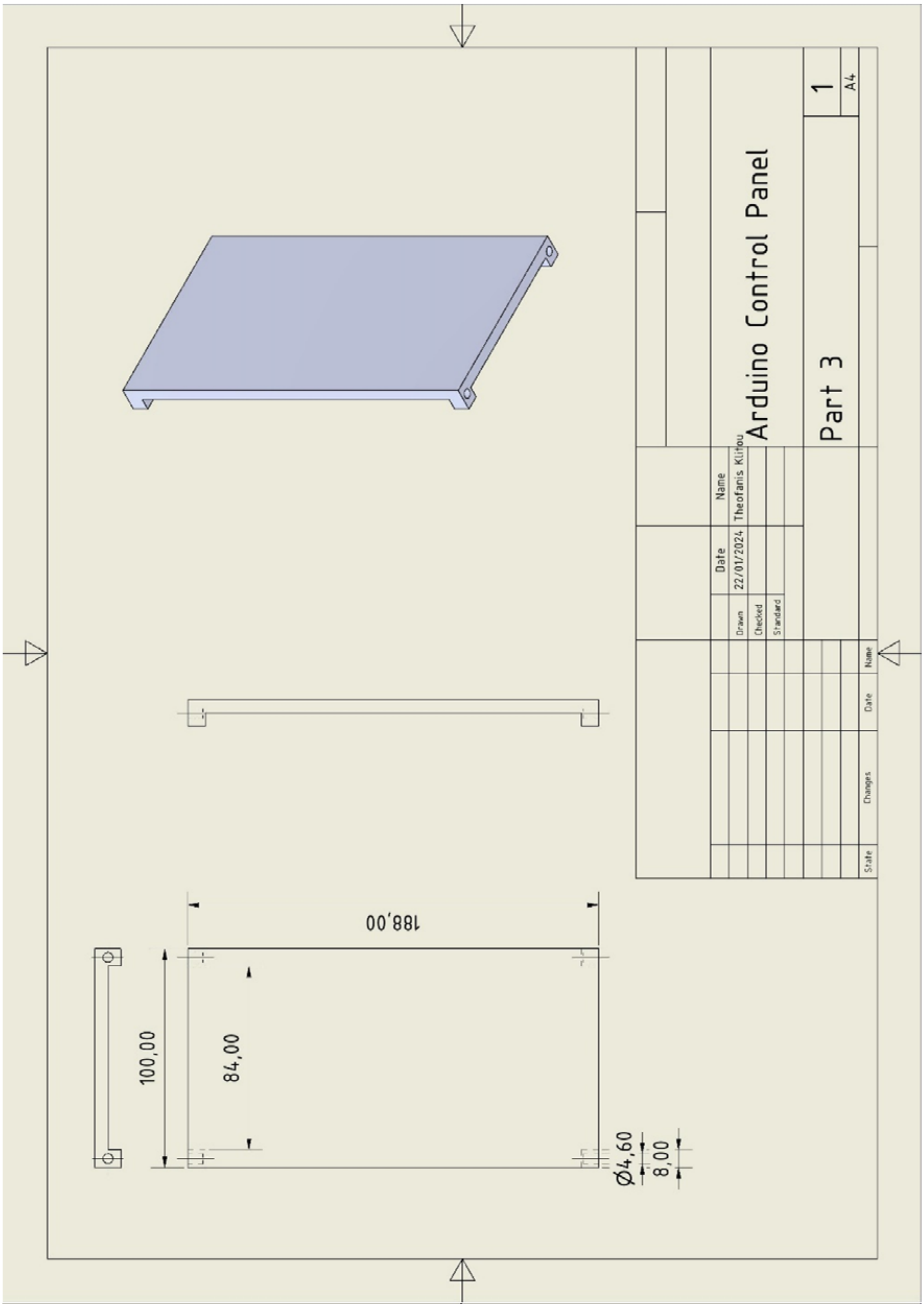

Figure 63: Arduino Control Panel Drawing Part 3 (Autodesk Inventor 2024)

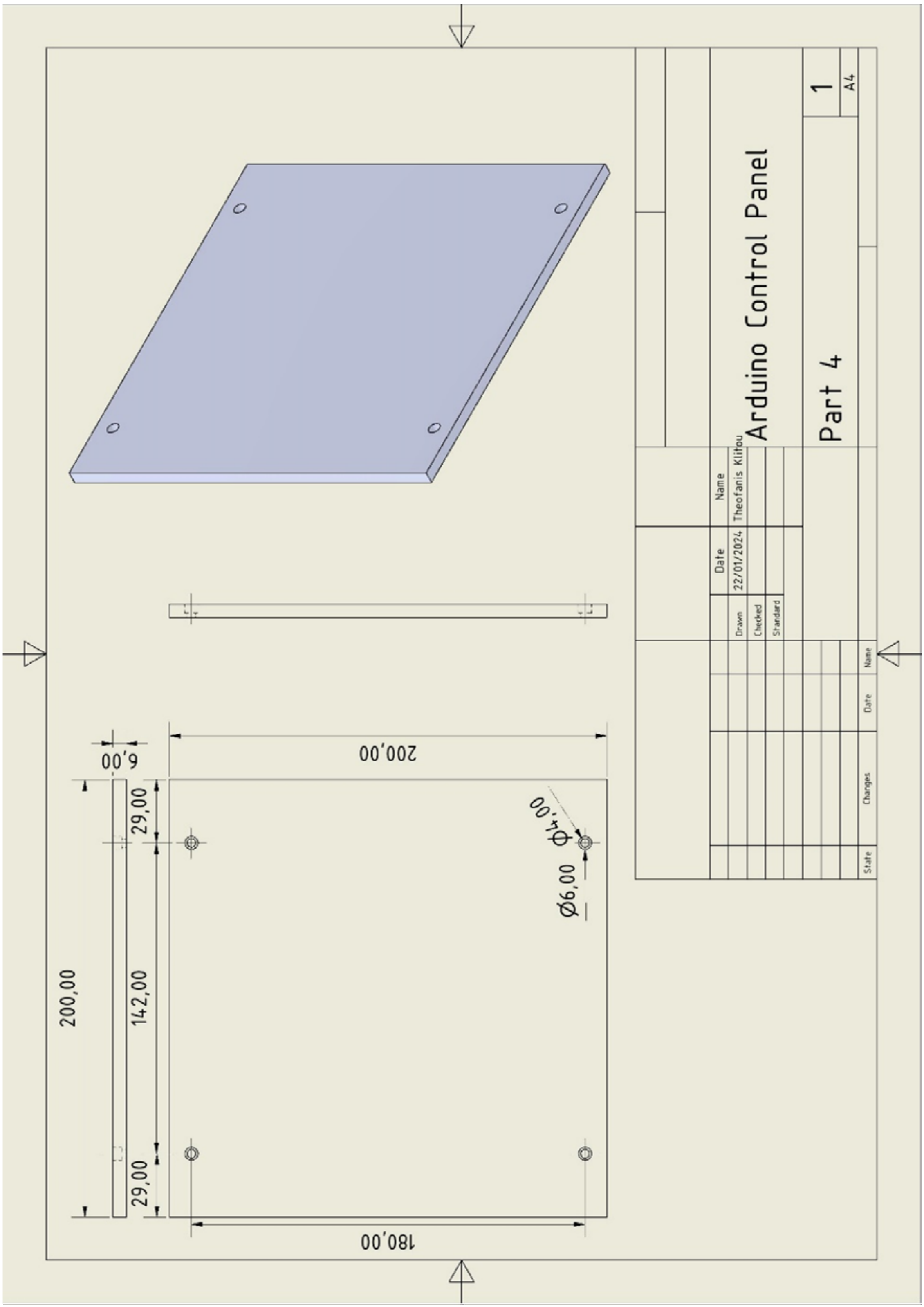

Figure 64: Arduino Control Panel Drawing Part 4 (Autodesk Inventor 2024)

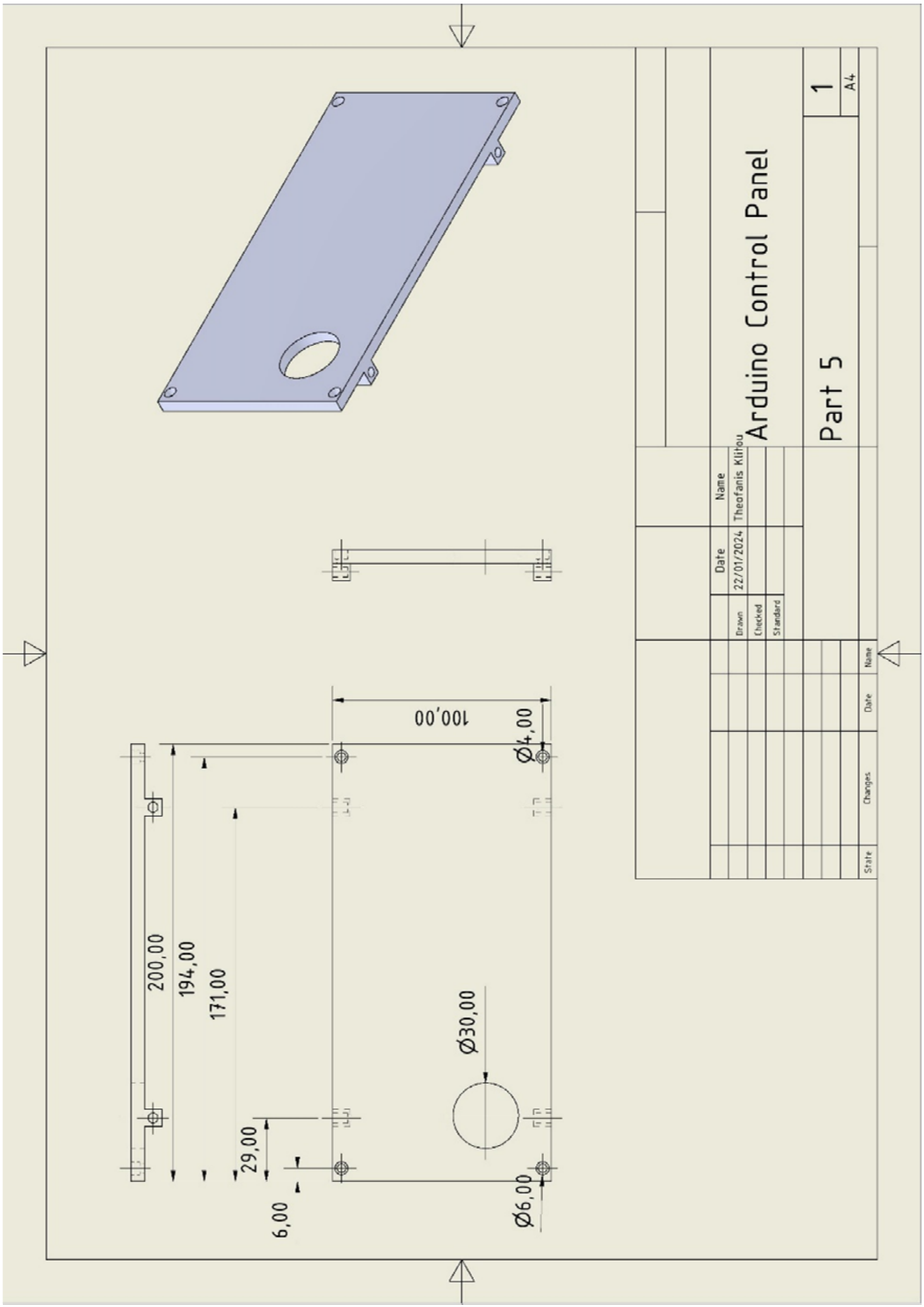

Figure 65: Arduino Control Panel Drawing Part 5 (Autodesk Inventor 2024)

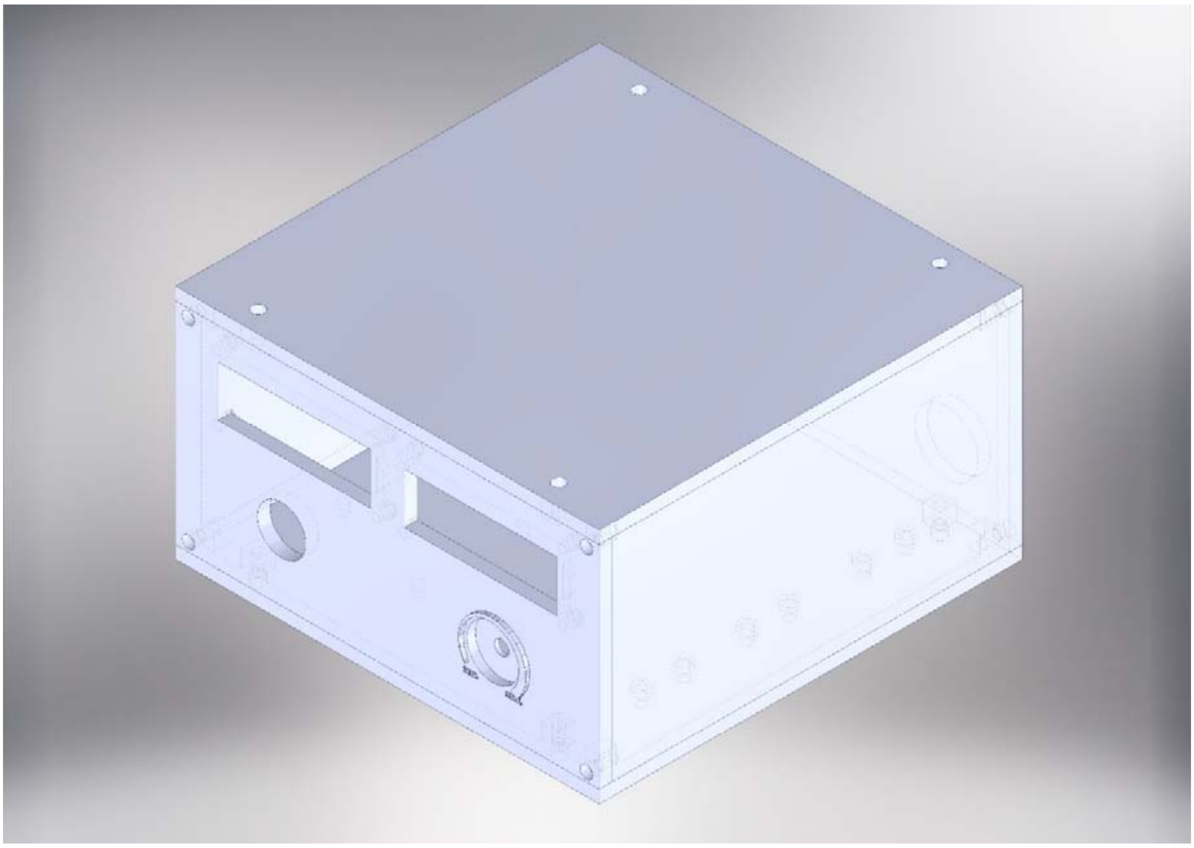

Figure 66: Arduino Control Panel Assembly (Autodesk Inventor 2024)

Liquid – Crystal – Display (LCD)

The LCD (Liquid Crystal Display) module is a display that uses liquid crystal technology to produce text or graphical content. In the context of Arduino, these modules are often characterized as LCDs, which display alphanumeric characters. Additionally, an Arduino LCD (Liquid Crystal Display) refers to the use of an LCD module in conjunction with an Arduino microcontroller. This combination allows to display information or create user interfaces in projects that involve Arduino – based electronics.

LCD illustration is shown in *figure 67*.

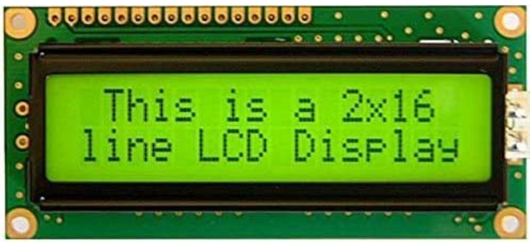

Figure 67: Liquid – Crystal – Display (LCD)

In the context of our control panel implementation, a pair of LCDs visually presents temperature readings for the inlet, outlet, and air parameters, as well as the water flow rate in liters per minute (L/min). *Figure 68* provides a visual depiction of the LCDs showcasing the real time temperature information. The use of LCD displays enhances the comprehensive data presentation capabilities of the control panel.

Figure 68: Liquid – Crystal – Display (LCD) in Operation

In *figure 69*, the schematic representation illustrates the LCD circuit interfaced with the Arduino microcontroller. Specifically, the grounding (GND) terminal of the LCD is intricately linked to the corresponding GND terminal on the Arduino. Furthermore, the voltage supply (VCC) terminal of the LCD is meticulously connected to the 5V output of the Arduino. In addition, the serial data line (SDA) if the LCD is adeptly linked to the A4 pin on the Arduino, while the serial clock line (SCL) of the LCD is judiciously connected to the A5 pin on the Arduino microcontroller. This configuration ensures the appropriate electrical connections between the LCD and the Arduino for seamless integration and functionality.

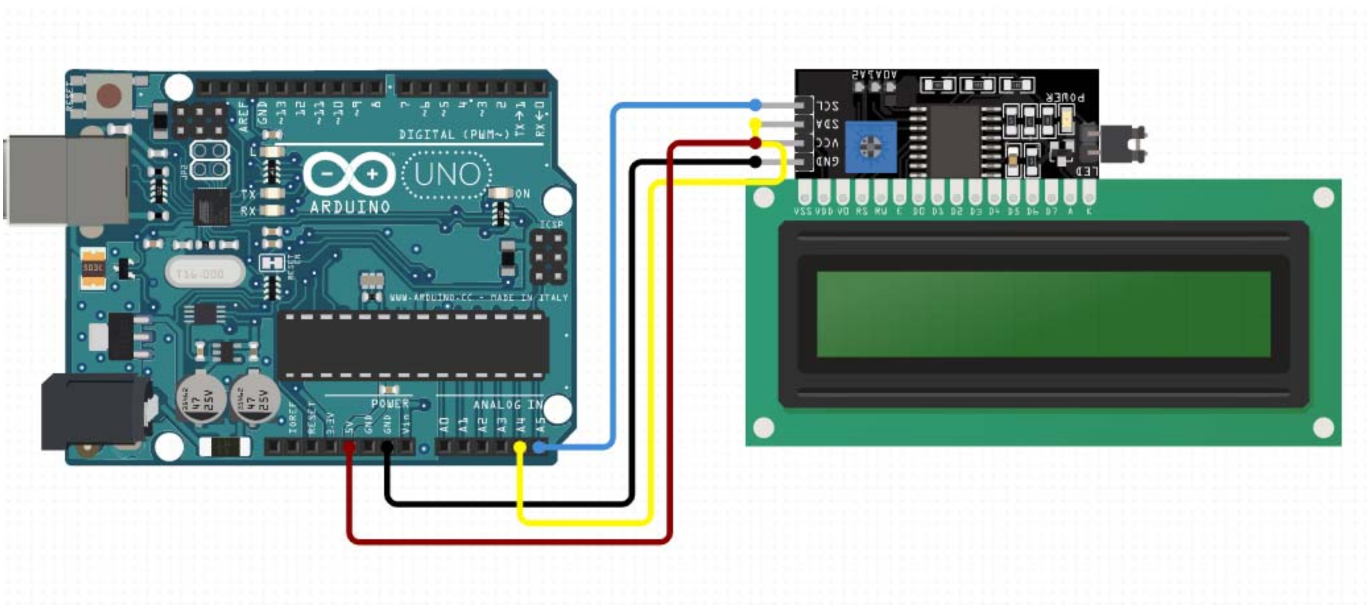

Figure 69: Schematic of Liquid – Crystal – Display (LCD) Interface

Jumpers

Jumpers utilized in Arduino applications, typically manifesting as jumper wires or cables, assume a pivotal role in establishing electrical connectivity within electronic circuits. These wires, featuring connectors at each terminus, are commonly deployed in tandem with breadboards for the purpose of prototyping and testing. Their principal function lies in facilitating the provisional interconnection of diverse electronic components, including sensors, LEDs, and resistors, on the breadboard. The incorporation of male and female connectors, couples with a color – coded system, enhances adaptability in generating organized and readily traceable connections. Jumpers play an instrumental role in the iterative and experimental phases of electronic projects, enabling flexible and expeditious modifications to circuit configurations without necessitating soldering. *Figure 70* provide visual examples.

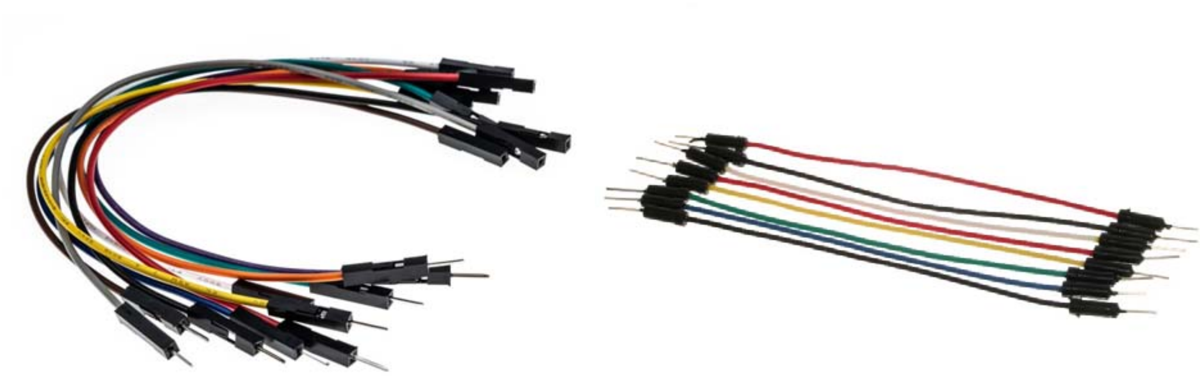

Figure 70: Arduino Cables for Connection (Jumpers)

Breadboard

The Arduino breadboard constitutes an integral component within electronic prototyping endeavors, providing a foundational platform for circuit development. Designed to facilitate experimentation without the need for soldering, the Arduino breadboard serves as a versatile testing ground for various electronic components. Its grid layout accommodates the insertion of jumper wires to establish temporary connection between components, promoting adaptability in circuit configurations. Employing a standardized grid pitch, often 2.54 mm, the breadboard aligns seamlessly with commonly used Arduino headers and components. As a fundamental tool in the iterative and experimental phase of electronics projects, the Arduino breadboard allows the systematic assembly and modification of circuits, fostering a streamlined and efficient prototyping process. For illustration, see *figure 71*.

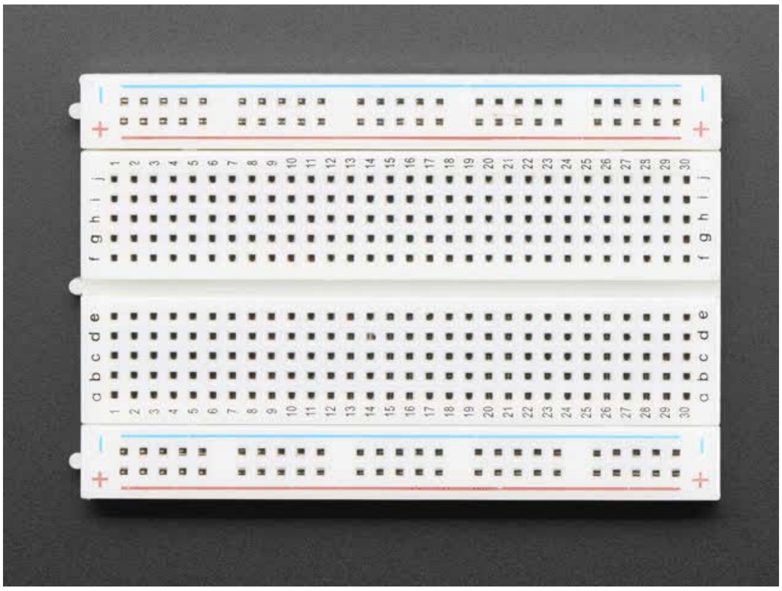

Figure 71: Breadboard Example

Water Flow Sensor

The Water Flow Sensor integrated into the Arduino circuit serves as a pivotal component designed for the precise measurement of water flow rates within a given system. Typically composed of a paddle wheel or turbine, the sensor registers rotational motion induced by the passage of water, translating such a movement into electrical pulses. These pulses are then transmitted to the Arduino microcontroller, where there are interpreted to derive accurate flow rate data. The integration process involves connecting the water flow sensor to specific digital or analog pins on the Arduino board, along with requisite power and ground connections. The resultant data, is often measured in units such as liters per minute (L/min), by enabling real time monitoring and facilitating automation in diverse applications, ranging from water consumption analysis to the management of irrigation systems and industrial processes requiring meticulous control of water flow dynamics.

The schematic representation below illustrates the integration of the water flow sensor with the Arduino circuit. Notably, the current supply of the sensor is meticulously linked to the 5V output of the Arduino, ensuring a stable power source. Furthermore, the ground (GND) terminal of the sensor is intricately connected to the corresponding ground terminal on the Arduino, establishing a common reference point. The signal output of the water flow sensor, is crucial for transmitting data to the Arduino, also is judiciously connected to the digital pin 2 of the Arduino board. This well – defined configuration ensures the seamless integration of the water flow sensor with the Arduino, facilitating accurate data acquisition and real time monitoring of water flow dynamics within the system.

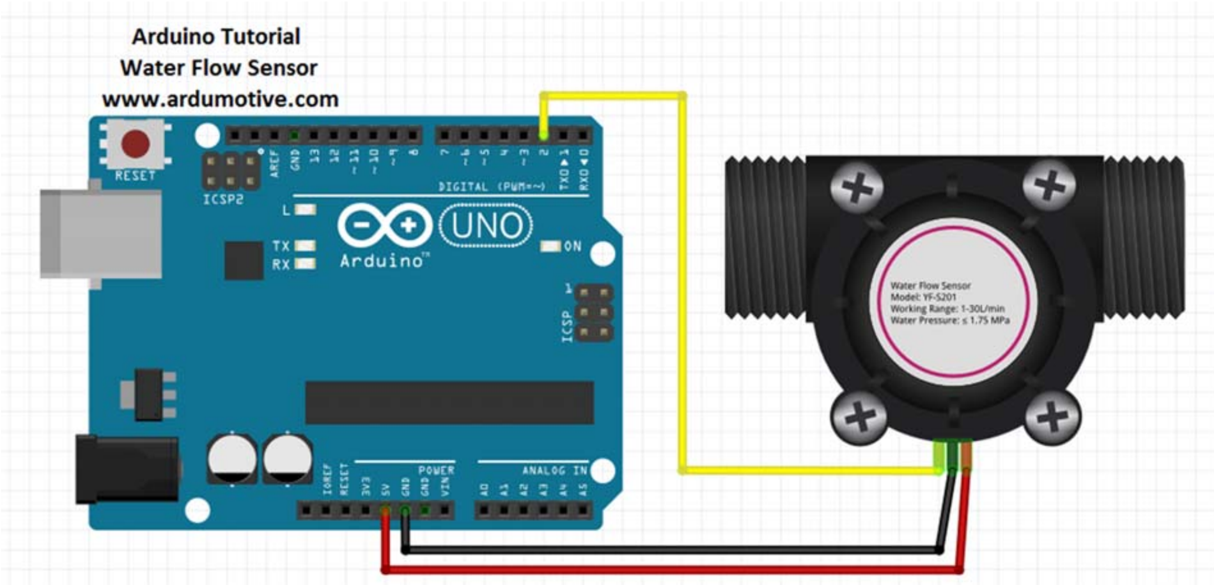

Figure 72: Schematic of Water Flow Sensor

During the programming phase of this circuit, a pre – existing code sourced from the internet was employed, which was tailored for a water flow sensor with a range of up to 30 liters per minute (L/min). Subsequently, the code was applied to the water flow sensor procured for this study, which possesses a measuring capability of up to 120 L/min. An observed discrepancy in sensor measurements prompted a meticulous examination. The experimental pump, with a maximum range of 100 L/min, yielded a reading of 7 L/min when operating at its peak capacity. To rectify this inconsistency, a mechanical flow meter available in the laboratory was utilized for comparative purposes. Adjustments were made to the code parameters, specifically modifying the pulse settings (from float calibration Factor = 4.5; to float calibration Factor = 0.47), until the reading was aligned with those of the mechanical flow meter. This iterative process ensured the calibration of the water flow sensor to accurately reflect the flow rates within the experimental set – up, fostering precision and reliability in data acquisition.

The water flow sensor was securely attached to the aluminum base of the radiator utilizing a tie wrap, as depicted in the following figure.

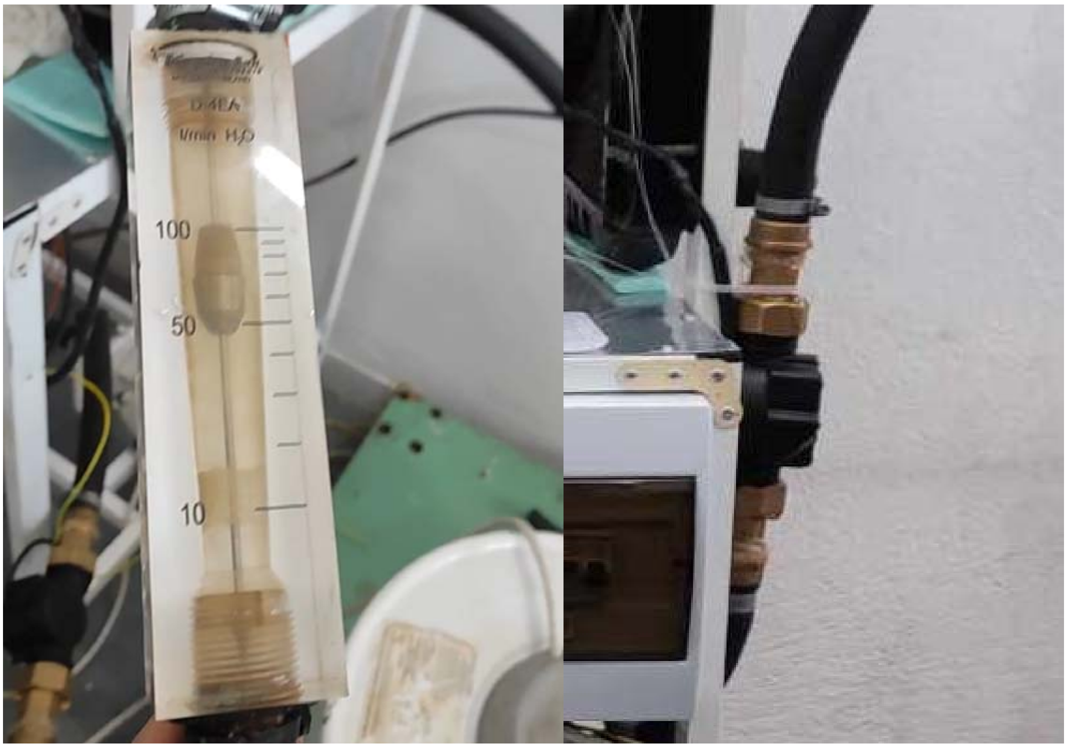

Figure 73: Mechanical & Electrical Water Flow Sensor

Resistance Temperature Detector (RTD Sensors – PT 100)

Resistance Temperature Detector Sensors, specifically PT 100, are a type of temperature sensors widely used for accurate and precise temperature measurement in a various industrial and scientific applications. PT 100 stands for Platinum 100 Ohms, indicating the nominal resistance of the sensor at 0 degrees Celsius. Their three – wire configuration, compensating for lead wire resistance, enhances accuracy, while their widespread applications encompass industries like HVAC, automotive, aerospace, and scientific research, where reliable and precise temperature monitoring is essential.

Within our experimental set – up, the PT100 sensor assumes the crucial role of real time temperature monitoring for both water inlet and outlet, as well as the air flow temperatures. This comprehensive monitoring not only facilitates an overall understanding of heat exchange processes but also ensures precise control and optimization of the experimental conditions.

Figure 74: Resistance Temperature Detector (RTD – PT 100)

Resistance Temperature Detector (RTD) to Digital Converter (MAX31865)

The MAX31865 serves a highly effective RTD – to – digital converter, facilitating the seamless integration of Resistance Temperature Detectors (RTDs) into digital systems. Employing a delta – sigma ADC, this converter accurately translates the analog voltage output from PT100 and PT1000 platinum RTDs into precise digital temperature readings. Compatible with both 2 – wire and 3 – wire RTD configurations, the MAX31865 ensures flexibility in diverse applications. Its high accuracy and reliability makes it a popular choice for systems requiring precise temperature monitoring, and its digital output simplifies interfacing with microcontrollers or other digital devices, contributing to the efficiency and accuracy of temperature sensing in various contexts.

Figure 75: MAX31865 Board

In the established circuit, three PT100 sensors with a 2 – wire configuration has been selectively implemented to monitor both inlet and outlet water temperature, and the ambient air temperature. The schematic representation illustrating the precise configuration necessary for optimal functionality is presented in the accompanying diagram. The cables of the temperature sensors are connected to the current and ground terminals of the MAX31865, securely attached to its circuit board. Subsequent to this, the jumpers are configured in accordance with the wiring specifications of the sensors, whether 2 or 3 wires. Following up a meticulous arrangement, the CS is attached to digital pin 10 of the Arduino, SD1 to digital pin 11, SD0 to digital pin 12, and CLK to digital pin 13. The grounding is established by linking GND to the corresponding ground pin on the Arduino, while the 3.3V is connected to the 3.3V supply on the Arduino, serving to power the MAX31865.

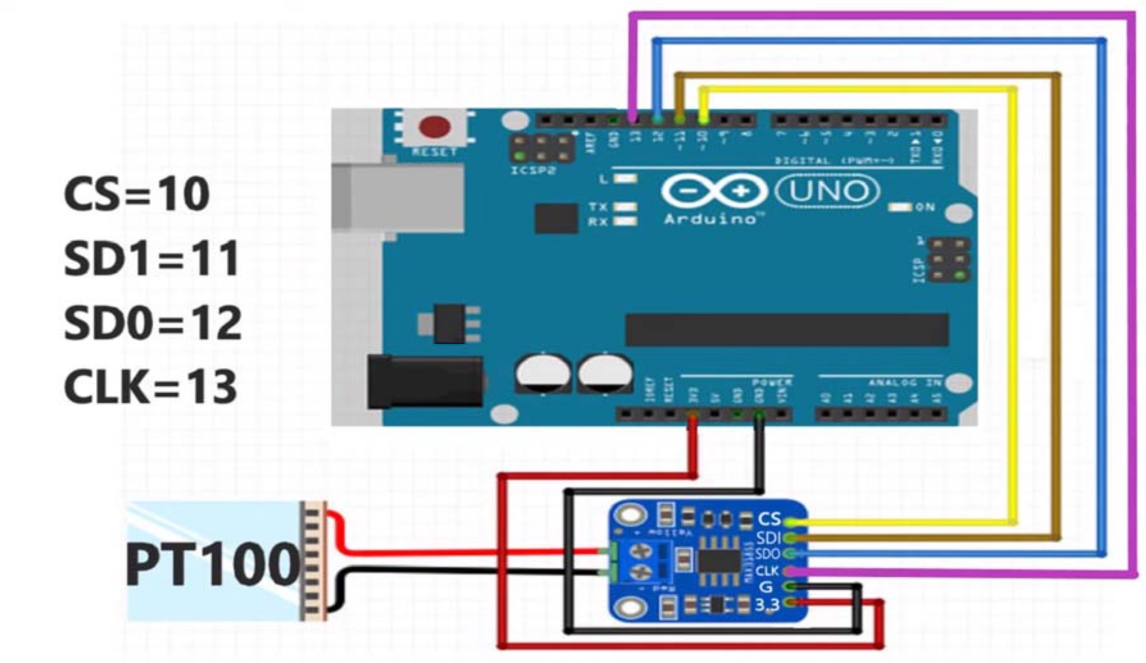

Figure 76: Schematic of MAX31865 & PT100 Sensor

3.2.4 Heat Exchanger – Radiator & Cooling Fan

Heat Exchanger – Radiator

To address the mounting and sealing requirements of the thermocouples within the heat exchanger, a specific adaptor was designed and subsequently produced using a 3D Printer. This custom adaptor was then attached to the thermocouples, and a specialized epoxy glue was applied, as illustrated in the figures below ensuring a secure seal within the system. Furthermore, to ensure structural integrity, custom – shaped aluminum supports have been strategically added to the sides of the radiator, providing robust support for both the fan and the radiator unit as a whole. These supports are attached using bolts, firmly connecting them to both the workbench and the radiator – cooling fan assembly.

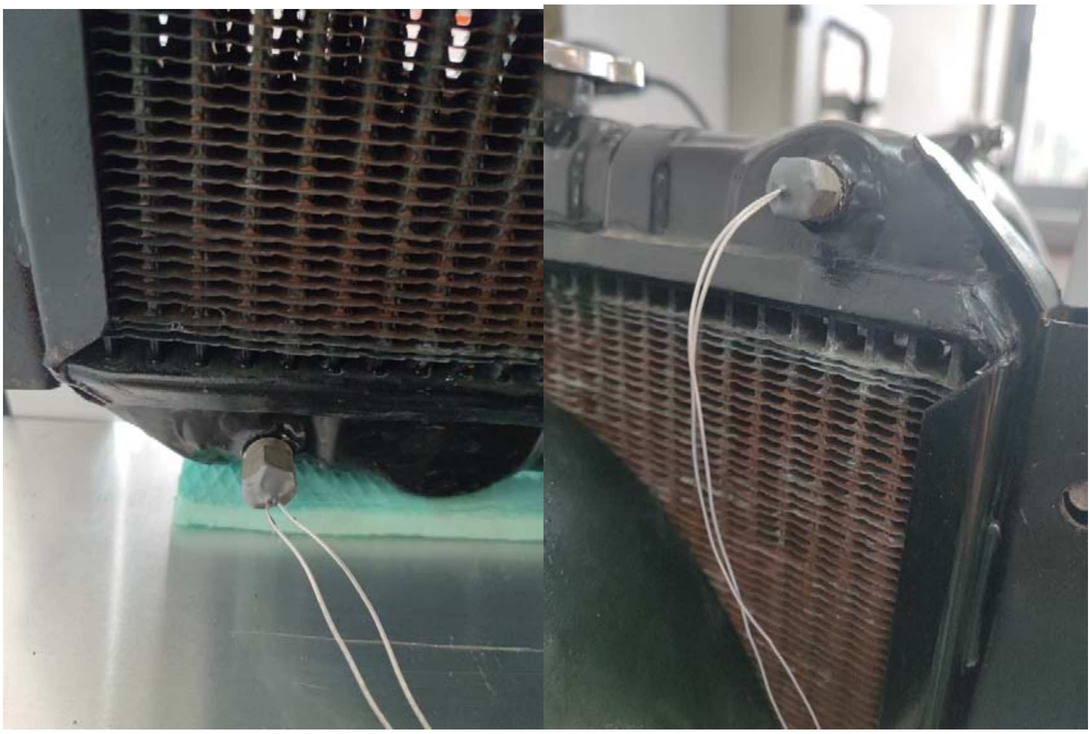

Figure 77: PT100 Sensors Sealed & Attached to Heat Exchanger Inlet & Outlet

Figure 78: Heat Exchanger Secured with brackets on Workbench

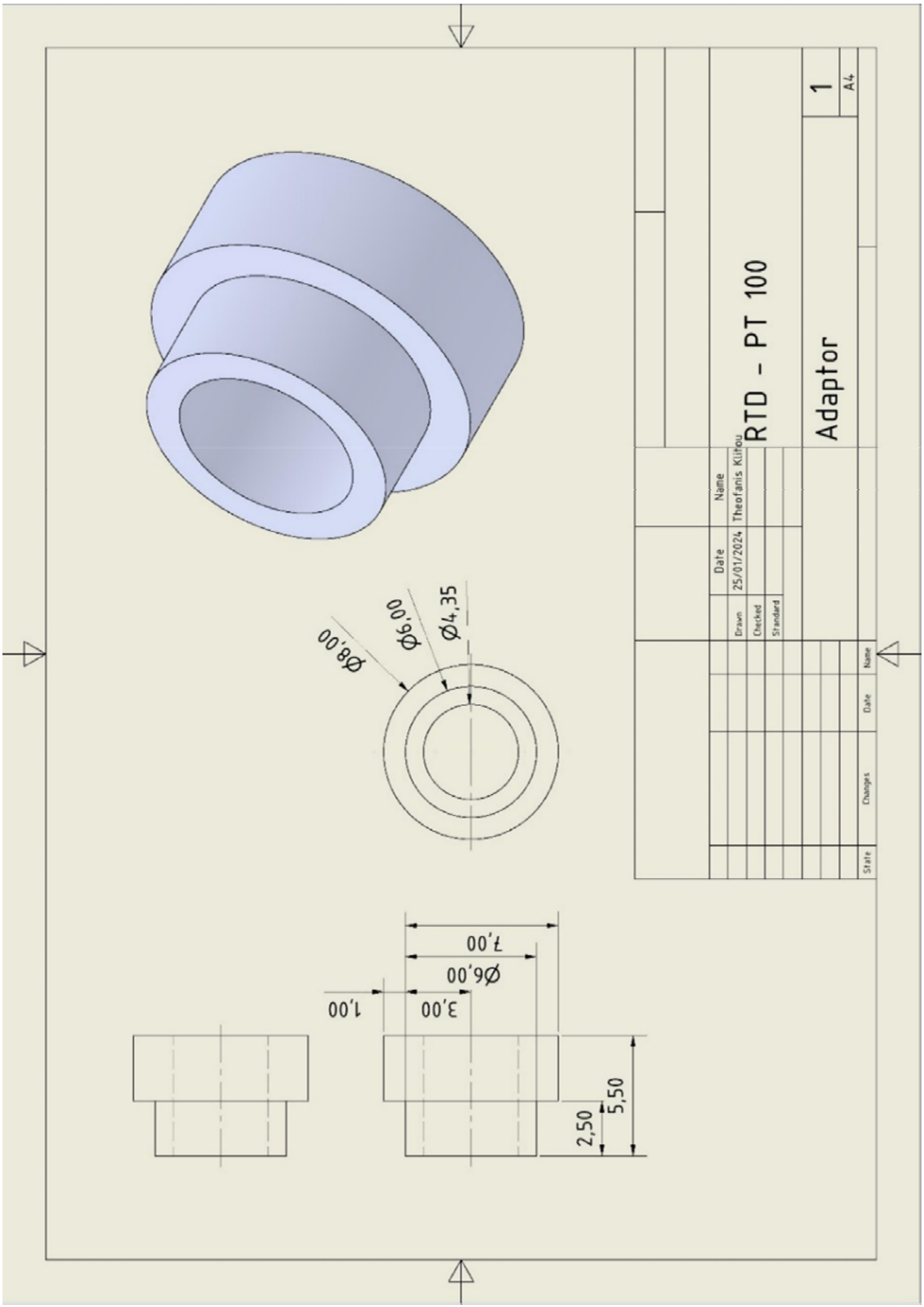

Figure 79: RTD – PT100 Adaptor Drawing (Autodesk Inventor 2024)

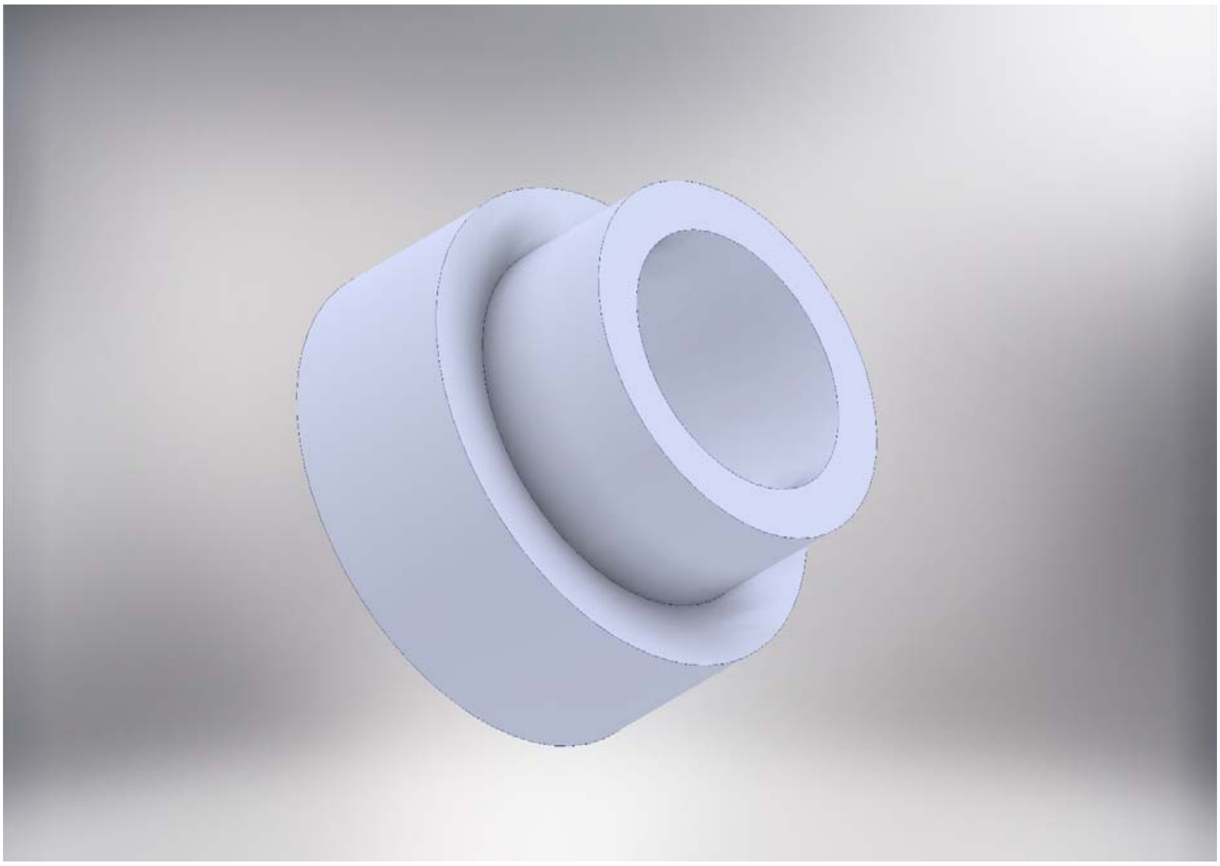

Figure 80: RTD – PT100 Part (Autodesk Inventor 2024)

Cooling Fan

In accordance with the details provided in the preceding paragraph, the cooling fan has been secured in conjunction with the custom radiator bases. Additionally, modifications were made to the potentiometer responsible of regulating the fan's speed, enabling secure fixation of the cable length at the designated point, as visually depicted in the following figure. The wires of the cooling fan have been routed and integrated into the electrical control panel, facilitating controlled activation and ensuring the safe and proper operation of the cooling fan. In order to measure the air outlet temperature from emanating from the radiator core, a thermocouple has been strategically installed, as illustrated in the accompanying figure. This placement of the thermocouple allows for accurate temperature monitoring at a crucial point within the system, contributing to a comprehensive understanding of the thermal dynamics associated with the radiator's core performance.

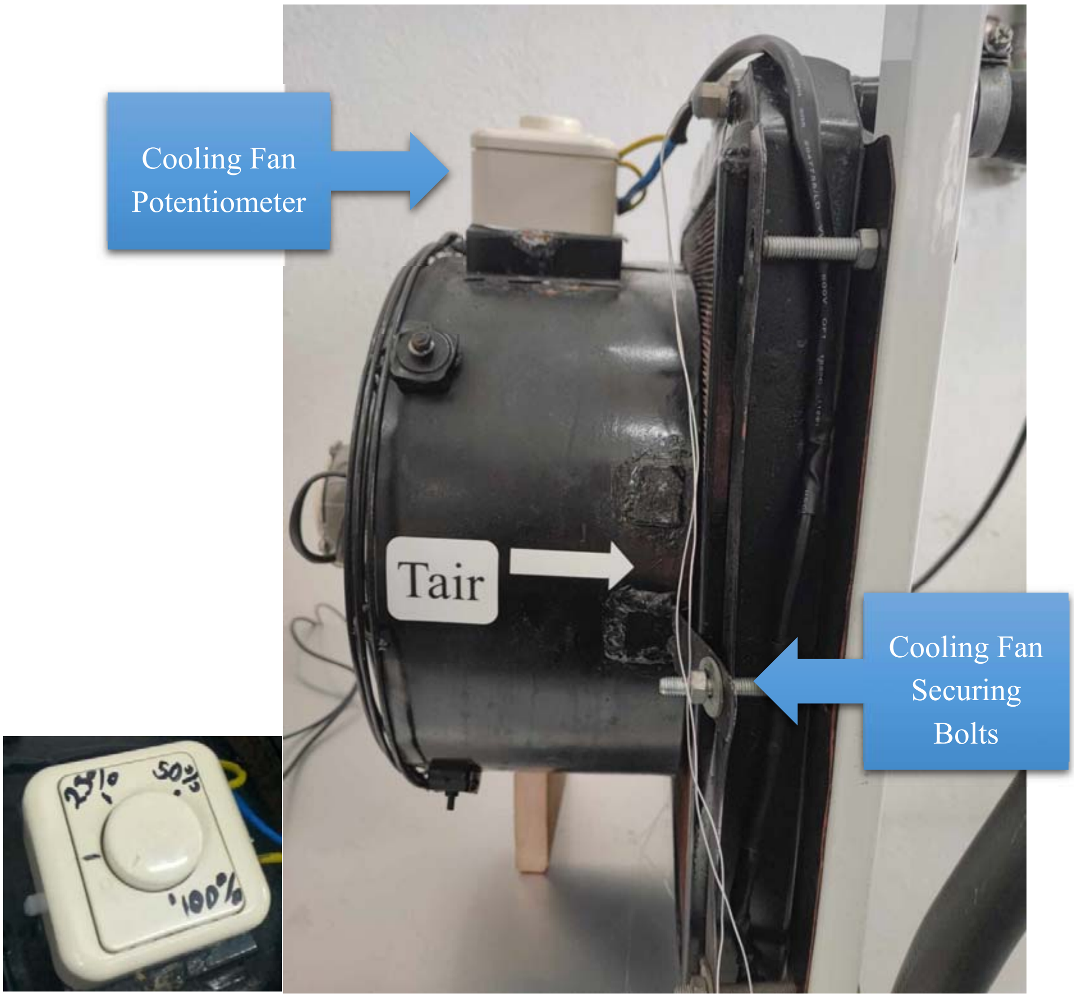

Figure 81: Cooling Fan Secure with bolts on the Workbench Brackets & Flow Positions

3.2.5 Water Pump

The water pump was been securely positioned on the workbench using an aluminum base. This base was been attached to the workbench using steel brackets and rivets, ensuring a robust attachment. Subsequently, the water pump was firmly bolted and attached to the experimental set – up. In order to facilitate its proper operation, the wires of the water pump were connected to the dimmer board and linked to the electrical control panel. Additionally, a crucial step in the process of filling the system with water invlolves the removal of a screw located on the water pump, as shown in *figure 82*.This step was undertaken to vent the water pump, ensuring the presence of water rather than air. Failing to verify the absence of air in the water pump before activation poses a potential risk of damage. By systematically addressing this consideration when filling the system with water, we mitigate the possibility of unintended consequences and uphold the operational integrity of water pump within the experimental set – up.

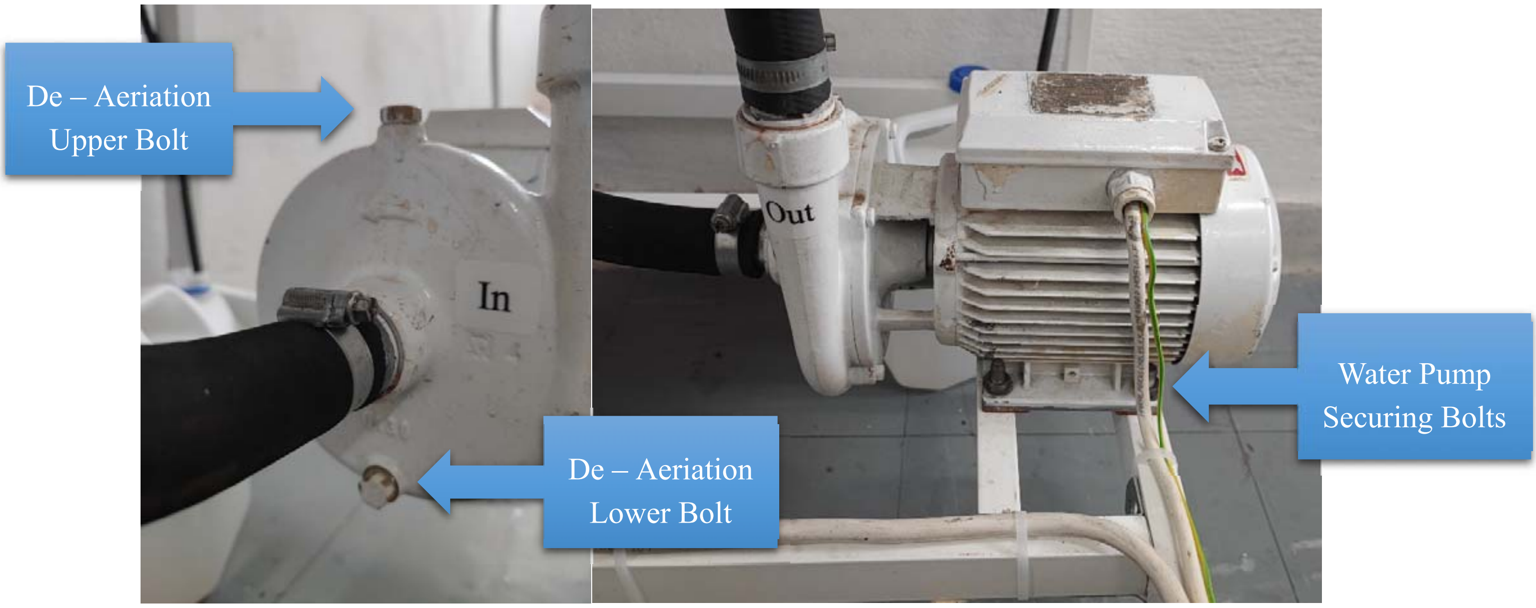

Figure 82: Water Pump Secured to Workbench & De – Aeration Bolts

3.2.6 Water Heater – Boiler

The boiler was intentionally oriented vertically, with the inlet and outlet positioned upwards, to facilitate an easy adjustment of the element's temperature. Due to water accumulation in the tank over several years, issues arose with the element. Consequently, a decision was made to disassemble the boiler for maintenance. After disassembly, the boiler underwent thorough cleaning, and the element was replaced. Following this maintenance procedure, a notable improvement was observed in both the water heating time and the overall performance of the element.

Figure 83: Boiler – Water Heater Placement

Figure 84: Old Element & Brand – New Element

3.2.7 Experimental Set – Up Circuit

Presented below is the circuit implemented in the experimental set – up, illustrating the interconnection of all components within the system.

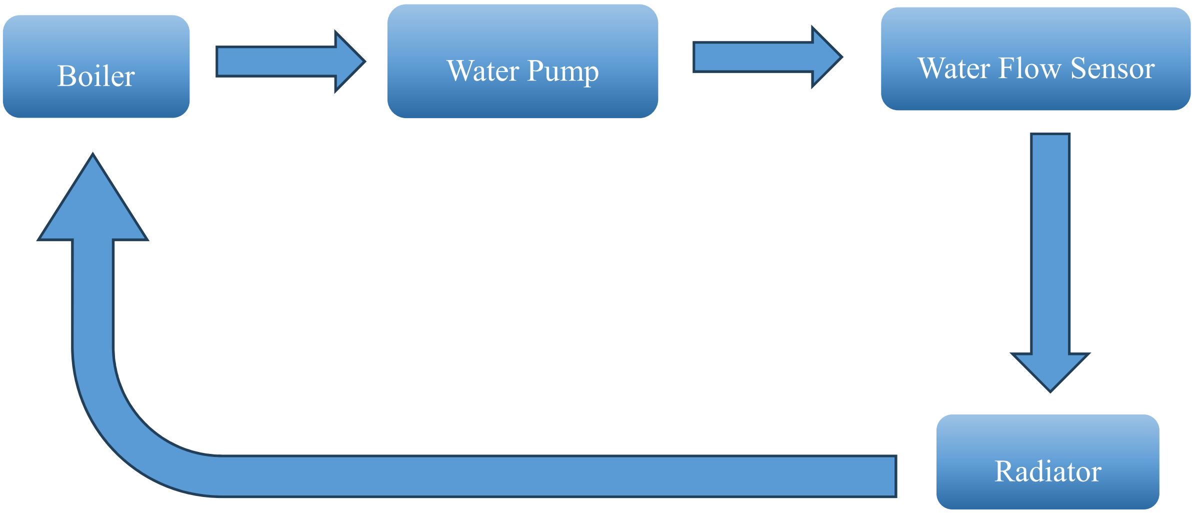

Figure 85: Final Assembly of Experimental Set – Up

3.2.8 Experimental Measurements

In the conducted experiments, variations of the water pump and cooling fan configurations were explored, as shown in the following tables. Throughout the experiments, the boiler temperature remained consistently set at 80 degrees Celsius. Following each experimental set – up, a waiting period ensued for the boiler to attain the predetermined temperature. In total, 12 distinct experimental scenarios were examined.

Table 1: Water Pump Alternatives 1st Attempt 25 L/min & 50% Cooling Fan Position

No.	*Time* [sec]	T_{in} [℃]	T_{out} [℃]	T_{air} [℃]	Ambient Temperature [℃]
1	0	70.7	65.6	59.7	21
2	30	70.6	65.4	59.7	21
3	60	70.5	65.4	59.7	21
4	90	70.5	65.3	59.6	21
5	120	70.4	65.3	59.6	21

Data	
Q [l/min]	25
Q [m³/sec]	0.00042
Fan Position [%]	50
Air Flow [m³/sec]	0.241
Water Density [kg/m³] (80℃)	971.76
Air Density [kg/m³] (25℃)	1.184
Radiator Core Area [m²]	0.3792
Cp_h (water) [kJ/kg*K] (80℃)	4.2
Cp_c (air) [kJ/kg*K] (25°C)	1.006
m_h (water) [kg/s]	0.405
m_c (air) [kg/s]	0.285

Table 2: Water Pump Alternatives 1st Attempt 50 L/min & 50% Cooling Fan Position

No.	Time [sec]	Tin [˚C]	Tout [˚C]	Tair [˚C]	Ambient Temperature [˚C]
1	0	70.1	66.3	60.4	21
2	30	70	66.2	60.4	21
3	60	69.9	66.1	60.4	21
4	90	69.8	66	60.3	21
5	120	69.8	65.9	60.2	21
Data					
Q [l/min]	50				
Q [m^3/sec]	0.00083				
Fan Position [%]	50				
Air Flow [m^3/sec]	0.241				
Water Density [kg/m^3] (80˚C)	971.76				
Air Density [kg/m^3] (25˚C)	1.184				
Radiator Core Area [m^2]	0.3792				
Cph (water) [kJ/kg*K] (80C)	4.2				
Cpc (air) [kJ/kg*K] (25C)	1.006				
mh (water) [kg/s]	0.810				
mc (air) [kg/s]	0.285				

Table 3: Water Pump Alternatives 1st Attempt 75 L/min & 50% Cooling Fan Position

No.	Time [sec]	Tin [˚C]	Tout [˚C]	Tair [˚C]	Ambient Temperature [˚C]
1	0	69.2	66.2	59.9	21
2	30	69.1	66.1	59.9	21
3	60	69.1	66.1	59.9	21
4	90	69	66.1	59.9	21
5	120	69	66	59.9	21
Data					
Q [l/min]	75				
Q [m^3/sec]	0.00125				
Fan Position [%]	50				
Air Flow [m^3/sec]	0.241				
Water Density [kg/m^3] (80˚C)	971.76				
Air Density [kg/m^3] (25˚C)	1.184				
Radiator Core Area [m^2]	0.3792				
Cph (water) [kJ/kg*K] (80˚C)	4.2				
Cpc (air) [kJ/kg*K] (25˚C)	1.006				
mh (water) [kg/s]	1.215				
mc (air) [kg/s]	0.285				

Table 4: Water Pump Alternatives 2nd Attempt 25 L/min & 100% Cooling Fan Position

No.	Time [sec]	Tin [˚C]	Tout [˚C]	Tair [˚C]	Ambient Temperature [˚C]
1	0	69.4	63.8	55.6	21
2	30	69	63.3	55.4	21
3	60	68.7	63.1	55.2	21
4	90	68.2	62.7	54.9	21
5	120	68	62.5	54.8	21

Data	
Q [l/min]	25
Q [m^3/sec]	0.00042
Fan Position [%]	100
Air Flow [m^3/sec]	0.482
Water Density [kg/m^3] (80˚C)	971.76
Air Density [kg/m^3] (25˚C)	1.184
Radiator Core Area [m^2]	0.3792
Cph (water) [kJ/kg*K] (80˚C)	4.2
Cpc (air) [kJ/kg*K] (25˚C)	1.006
mh (water) [kg/s]	0.405
mc (air) [kg/s]	0.571

Table 5: Water Pump Alternatives 2nd Attempt 50 L/min & 100% Cooling Fan Position

No.	Time [sec]	Tin [˚C]	Tout [˚C]	Tair [˚C]	Ambient Temperature [˚C]
1	0	69.2	65.2	56.9	21
2	30	68.8	64.7	56.8	21
3	60	68.5	64.4	56.6	21
4	90	68.1	64	56.3	21
5	120	67.7	63.7	56	21

Data	
Q [l/min]	50
Q [m^3/sec]	0.00083
Fan Position [%]	100
Air Flow [m^3/sec]	0.482
Water Density [kg/m^3] (80˚C)	971.76
Air Density [kg/m^3] (25˚C)	1.184
Radiator Core Area [m^2]	0.3792
Cph (water) [kJ/kg*K] (80˚C)	4.2
Cpc (air) [kJ/kg*K] (25˚C)	1.006
mh (water) [kg/s]	0.810
mc (air) [kg/s]	0.571

Table 6: Water Pump Alternatives 2nd Attempt 75 L/min & 100% Cooling Fan Position

No.	Time [sec]	Tin [˚C]	Tout [˚C]	Tair [˚C]	Ambient Temperature [˚C]
1	0	69.2	65.7	57.6	21
2	30	68.9	65.5	57.5	21
3	60	68.5	65.2	57.2	21
4	90	68.2	64.8	57	21
5	120	67.8	64.5	56.7	21
Data					
Q [l/min]	75				
Q [m^3/sec]	0.00125				
Fan Position [%]	100				
Air Flow [m^3/sec]	0.482				
Water Density [kg/m^3] (80˚C)	971.76				
Air Density [kg/m^3] (25˚C)	1.184				
Radiator Core Area [m^2]	0.3792				
Cph (water) [kJ/kg*K] (80˚C)	4.2				
Cpc (air) [kJ/kg*K] (25˚C)	1.006				
mh (water) [kg/s]	1.215				
mc (air) [kg/s]	0.571				

Table 7: Cooling Fan Alternatives 1st Attempt 50% Position & 25 L/min Flow Rate

No.	Time [sec]	Tin [˚C]	Tout [˚C]	Tair [˚C]	Ambient Temperature [˚C]
1	0	70.3	65.1	58.9	21
2	30	70	64.9	58.8	21
3	60	69.9	64.7	58.7	21
4	90	69.7	64.6	58.7	21
5	120	69.6	64.6	58.6	21

Data	
Q [l/min]	25
Q [m^3/sec]	0.00042
Fan Position [%]	50
Air Flow [m^3/sec]	0.241
Water Density [kg/m^3] (80˚C)	971.76
Air Density [kg/m^3] (25˚C)	1.184
Radiator Core Area [m^2]	0.3792
Cph (water) [kJ/kg*K] (80̊C)	4.2
Cpc (air) [kJ/kg*K] (25̊C)	1.006
mh (water) [kg/s]	0.405
mc (air) [kg/s]	0.285

Table 8: Cooling Fan Alternatives 1st Attempt 100% Position & 25 L/min Flow Rate

No.	Time [sec]	Tin [˚C]	Tout [˚C]	Tair [˚C]	Ambient Temperature [˚C]
1	0	69.4	63.4	54.4	21
2	30	69	63	54.2	21
3	60	68.6	62.6	53.9	21
4	90	68.3	62.3	53.6	21
5	120	68	62	53.3	21
Data					
Q [l/min]	25				
Q [m^3/sec]	0.00042				
Fan Position [%]	100				
Air Flow [m^3/sec]	0.482				
Water Density [kg/m^3] (80˚C)	971.76				
Air Density [kg/m^3] (25˚C)	1.184				
Radiator Core Area [m^2]	0.3792				
Cph (water) [kJ/kg*K] (80̊C)	4.2				
Cpc (air) [kJ/kg*K] (25̊C)	1.006				
mh (water) [kg/s]	0.405				
mc (air) [kg/s]	0.571				

Table 9: Cooling Fan Alternatives 2nd Attempt 50% Position & 50 L/min Flow Rate

No.	Time [sec]	Tin [˚C]	Tout [˚C]	Tair [˚C]	Ambient Temperature [˚C]
1	0	70.4	66.5	59.6	21
2	30	69.6	65.8	59.3	21
3	60	68.7	65	58.9	21
4	90	68	64.2	58.3	21
5	120	67.2	63.5	57.6	21
Data					
Q [l/min]	50				
Q [m^3/sec]	0.00083				
Fan Position [%]	50				
Air Flow [m^3/sec]	0.241				
Water Density [kg/m^3] (80˚C)	971.76				
Air Density [kg/m^3] (25˚C)	1.184				
Radiator Core Area [m^2]	0.3792				
Cph (water) [kJ/kg*K] (80˚C)	4.2				
Cpc (air) [kJ/kg*K] (25˚C)	1.006				
mh (water) [kg/s]	0.810				
mc (air) [kg/s]	0.285				

Table 10: Cooling Fan Alternatives 2nd Attempt 100% Position & 50 L/min Flow Rate

No.	Time [sec]	Tin [°C]	Tout [°C]	Tair [°C]	Ambient Temperature [°C]
1	0	67.9	63.7	55.1	21
2	30	66.8	62.8	54.6	21
3	60	65.8	61.9	54.1	21
4	90	64.9	61.1	53.4	21
5	120	64	60.2	52.5	21

Data	
Q [l/min]	50
Q [m^3/sec]	0.00083
Fan Position [%]	100
Air Flow [m^3/sec]	0.482
Water Density [kg/m^3] (80°C)	971.76
Air Density [kg/m^3] (25°C)	1.184
Radiator Core Area [m^2]	0.3792
Cph (water) [kJ/kg*K] (80C)	4.2
Cpc (air) [kJ/kg*K] (25C)	1.006
mh (water) [kg/s]	0.810
mc (air) [kg/s]	0.571

Table 11: Cooling Fan Alternatives 3rd Attempt 50 % Position & 75 L/min Flow Rate

No.	Time [sec]	Tin [˚C]	Tout [˚C]	Tair [˚C]	Ambient Temperature [˚C]
1	0	69	65.7	59.5	21
2	30	68.3	65.1	59.1	21
3	60	67.4	64.3	58.5	21
4	90	66.8	63.7	57.8	21
5	120	66	63	57.3	21

Data	
Q [l/min]	75
Q [m^3/sec]	0.00125
Fan Position [%]	50
Air Flow [m^3/sec]	0.241
Water Density [kg/m^3] (80˚C)	971.76
Air Density [kg/m^3] (25˚C)	1.184
Radiator Core Area [m^2]	0.3792
Cph (water) [kJ/kg*K] (80C)	4.2
Cpc (air) [kJ/kg*K] (25C)	1.006
mh (water) [kg/s]	1.215
mc (air) [kg/s]	0.285

Table 12: Cooling Fan Alternatives 3rd Attempt 100% Position & 75 L/min Flow Rate

No.	Time [sec]	Tin [˚C]	Tout [˚C]	Tair [˚C]	Ambient Temperature [˚C]
1	0	68	64.5	55.7	21
2	30	67.1	63.5	55.2	21
3	60	66	62.6	54.7	21
4	90	65.1	61.8	54	21
5	120	64.2	60.8	53.2	21

Data	
Q [l/min]	75
Q [m^3/sec]	0.00125
Fan Position [%]	100
Air Flow [m^3/sec]	0.482
Water Density [kg/m^3] (80˚C)	971.76
Air Density [kg/m^3] (25˚C)	1.184
Radiator Core Area [m^2]	0.3792
Cph (water) [kJ/kg*K] (80C)	4.2
Cpc (air) [kJ/kg*K] (25C)	1.006
mh (water) [kg/s]	1.215
mc (air) [kg/s]	0.571

The methodology employed to obtain the experimental measurements involved activating all components of the experimental set – up pertaining to the targeted data. Subsequently, a waiting period was observed until the values reached a stable state. The experiment commenced thereafter, with measurements taken at 30 second intervals for T_{in}, T_{out} and T_{air} data.

3.2.9 ε – NTU Calculations Example

An example of the procedure for resolving the ε – NTU method, derived from the aforementioned table results ensues.

$$C_h = \dot{m}_h Cp_h = 0.4049 \frac{kg}{sec} \cdot 4.2 \frac{kJ}{kg \cdot K} \tag{23}$$

$$C_h = 1.7 \frac{kW}{K}$$

$$C_c = \dot{m}_c Cp_c = 0.1427 \frac{kg}{sec} \cdot 1.006 \frac{kJ}{kg \cdot K} \tag{24}$$

$$C_c = 0.14 \frac{kW}{K}$$

$$C_r = \frac{C_{min}}{C_{max}} = \frac{C_c}{C_h} = \frac{0.14}{1.7} \tag{25}$$

$$C_r = 0.0844$$

$$\dot{Q}_{max} = C_{min} \Delta T_{max} = C_{min}\left(T_{h_{in}} - T_{c_{in}}\right) = 0.14 \frac{kW}{K} \cdot (71.3 - 21) \tag{26}$$

$$\dot{Q}_{max} = 7.2\ kW$$

$$\dot{Q}_h = \dot{m}_h Cp_h \Delta T_h = 0.4049 \frac{kg}{sec} \cdot 4.2 \frac{kJ}{kg \cdot K} \cdot (71.3 - 67.9) \tag{27}$$

$$\dot{Q}_h = 5.8\ kW$$

$$\dot{Q}_c = \dot{m}_c Cp_c \Delta T_c = 0.1427 \frac{kg}{sec} \cdot 1.006 \frac{kJ}{kg \cdot K} \cdot (65.8 - 21) \tag{28}$$

$$\dot{Q}_c = 6.4\ kW$$

$$\bar{Q} = \frac{\dot{Q}_h + \dot{Q}_c}{2} = \frac{5.8 + 6.43}{2} \tag{29}$$

$$\bar{Q} = 6.1\ kW$$

$$\varepsilon = \frac{\bar{Q}}{\dot{Q}_{max}} = \frac{6.1}{7.2} \tag{30}$$

$$\varepsilon = 0.85$$

Equation 31 is employed in single – pass crossflow heat exchangers.

$$NTU = -\left(\frac{1}{C_r}\right)\ln(C_r \ln(1-\varepsilon)+1) = -\left(\frac{1}{0.0844}\right)\cdot \ln(0.0844 \cdot \ln(1-0.85)+1) \tag{31}$$

$$NTU = 2.1$$

$$NTU = \frac{UA}{C_{min}} \tag{32}$$

$$U = \frac{NTU\ C_{min}}{A} = \frac{2.1 \cdot 0.1435 \cdot \frac{kW}{K}}{0.3792\ m^2}$$

$$U = 0.79\ kW/K \cdot m^2$$

Chapter 4: Results and Discussions

4.1 Results

4.1.1 Tables of Experimental Measurements and ε – NTU Results

Upon completing the computation of all formulas within the ε – NTU method, the next step entails reviewing the obtained results, diagrams and engaging in discussions regarding the entire process of the experimental set – up.

Table 13: Water Pump Alternatives 1st Attempt Results

50% Cooling Fan Position	ΔT_h (water) [˚C]	Q_h (water) [kW]	ΔT_c (air) [˚C]	Q_c (air) [kW]	ΔT_{max} [˚C]
25 L/min	5.2	8.8	38.7	11.1	49.7
50 L/min	3.9	13.3	39.2	11.3	49.1
75 L/min	3.0	15.3	38.9	11.2	48.2

ε – NTU Results

50% Cooling Fan Position	C_c (C_{min}) [kW/K]	C_h (C_{max}) [kW/K]	C_r	Q_{max} [kW]	Q [kW]	ε	NTU	U [kW/K*m²]
25 L/min	0.287	1.701	0.169	14.3	10.0	0.7	1.3	1.0
50 L/min	0.287	3.401	0.084	14.1	12.3	0.9	2.2	1.7
75 L/min	0.287	5.102	0.056	13.8	13.2	1.0	3.5	2.6

Table 14: Water Pump Alternatives 2nd Attempt Results

Experimental Measurements Results

100% Cooling Fan Position	ΔTh (water) [˚C]	Qh (water) [kW]	ΔTc (air) [˚C]	Qc (air) [kW]	ΔT max [˚C]
25 L/min	5.7	9.7	34.4	19.7	48.4
50 L/min	4.0	13.6	35.9	20.6	48.2
75 L/min	3.5	17.9	36.6	21.0	48.2

ε – NTU Results

100% Cooling Fan Position	Cc (Cmin) [kW/K]	Ch (Cmax) [kW/K]	Cr	Q max [kW]	Q [kW]	ε	NTU	U [kW/K*m²]
25 L/min	0.574	1.701	0.338	27.8	14.7	0.5	0.9	1.3
50 L/min	0.574	3.401	0.169	27.7	17.2	0.6	1.1	1.6
75 L/min	0.574	5.102	0.113	27.7	19.4	0.7	1.3	2.0

Table 15: Cooling Fan Alternatives 1st Attempt Results

Experimental Measurements Results					
25 L/min W.P Flow Rate	ΔTh (water) [˚C]	Qh (water) [kW]	ΔTc (air) [˚C]	Qc (air) [kW]	ΔT max [˚C]
50% Cooling Fan Position	5.2	8.8	37.9	10.9	49.3
100% Cooling Fan Position	6.0	10.2	33.4	19.2	48.4

ε – NTU Results							
25 L/min W.P Flow Rate	Cc (Cmin) [kW/K]	Ch (Cmax) [kW/K]	*Cr*	Q max [kW]	*Q [kW]*	*ε*	NTU	U [kW/K*m²]
50% Cooling Fan Position	0.287	1.701	0.169	14.2	9.9	0.7	1.3	1.0
100% Cooling Fan Position	0.574	1.701	0.338	27.8	14.7	0.5	0.9	1.3

Table 16: Cooling Fan Alternatives 2nd Attempt Results

Experimental Measurements Results					
50 L/min W.P Flow Rate	ΔTh (water) [˚C]	Qh (water) [kW]	ΔTc (air) [˚C]	Qc (air) [kW]	ΔT max [˚C]
50% Cooling Fan Position	3.9	13.3	38.6	11.1	49.4
100% Cooling Fan Position	4.2	14.3	34.1	19.6	46.9

ε – NTU Results								
50 L/min W.P Flow Rate	Cc (Cmin) [kW/K]	Ch (Cmax) [kW/K]	*Cr*	Q max [kW]	*Q [kW]*	*ε*	NTU	U [kW/K*m²]
50% Cooling Fan Position	0.287	3.401	0.084	14.2	12.2	0.9	2.1	1.6
100% Cooling Fan Position	0.574	3.401	0.169	26.9	16.9	0.6	1.1	1.6

Table 17: Cooling Fan Alternatives 3rd Attempt Results

Experimental Measurements Results					
75 L/min W.P Flow Rate	**ΔTh (water) [˚C]**	**Qh (water) [kW]**	**ΔTc (air) [˚C]**	**Qc (air) [kW]**	**ΔT max [˚C]**
50% Cooling Fan Position	3.3	16.8	38.5	11.1	48
100% Cooling Fan Position	3.6	18.4	34.2	19.6	47

ε – NTU Results								
75 L/min W.P Flow Rate	**Cc (Cmin) [kW/K]**	**Ch (Cmax) [kW/K]**	***Cr***	**Q max [kW]**	***Q [kW]***	***ε***	**NTU**	**U [kW/K*m^2]**
50% Cooling Fan Position	0.287	5.102	0.056	13.8	13.6	1.0	5.2	4.0
100% Cooling Fan Position	0.574	5.102	0.113	27.0	19.0	0.7	1.3	2.0

4.1.2 Diagrams of ε – NTU Results

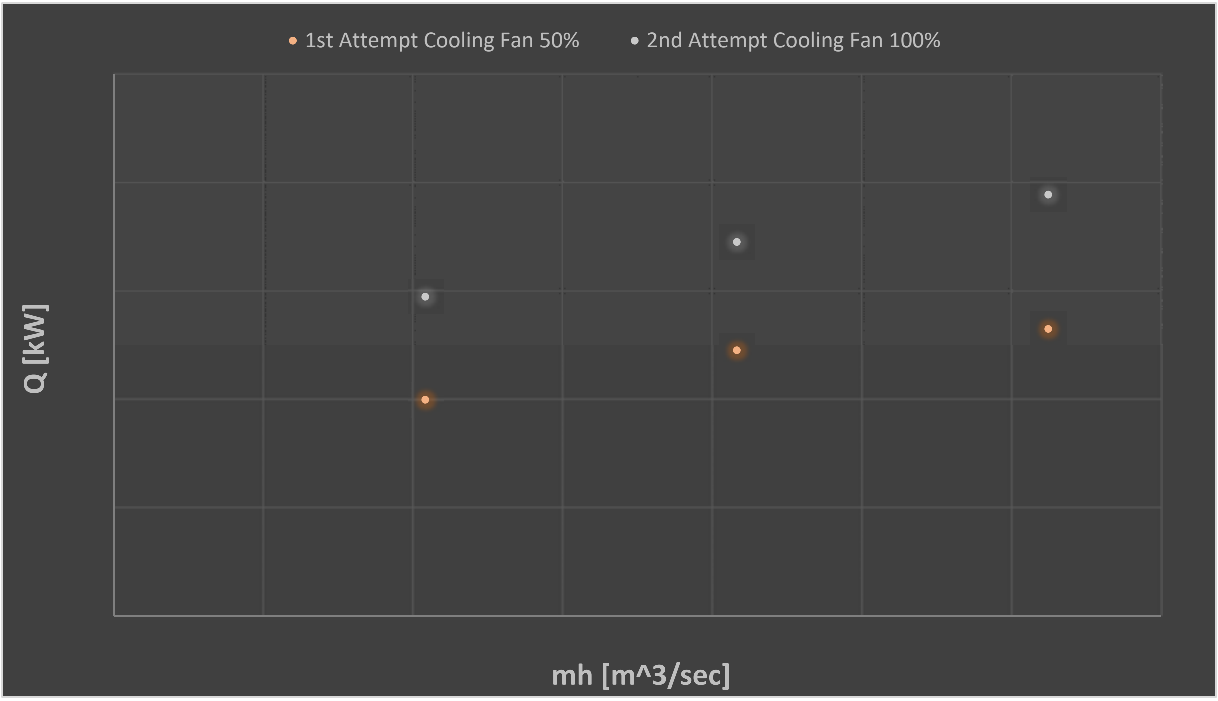

Figure 86: Water Pump Alternatives Heat Transfer Rate Q Diagram

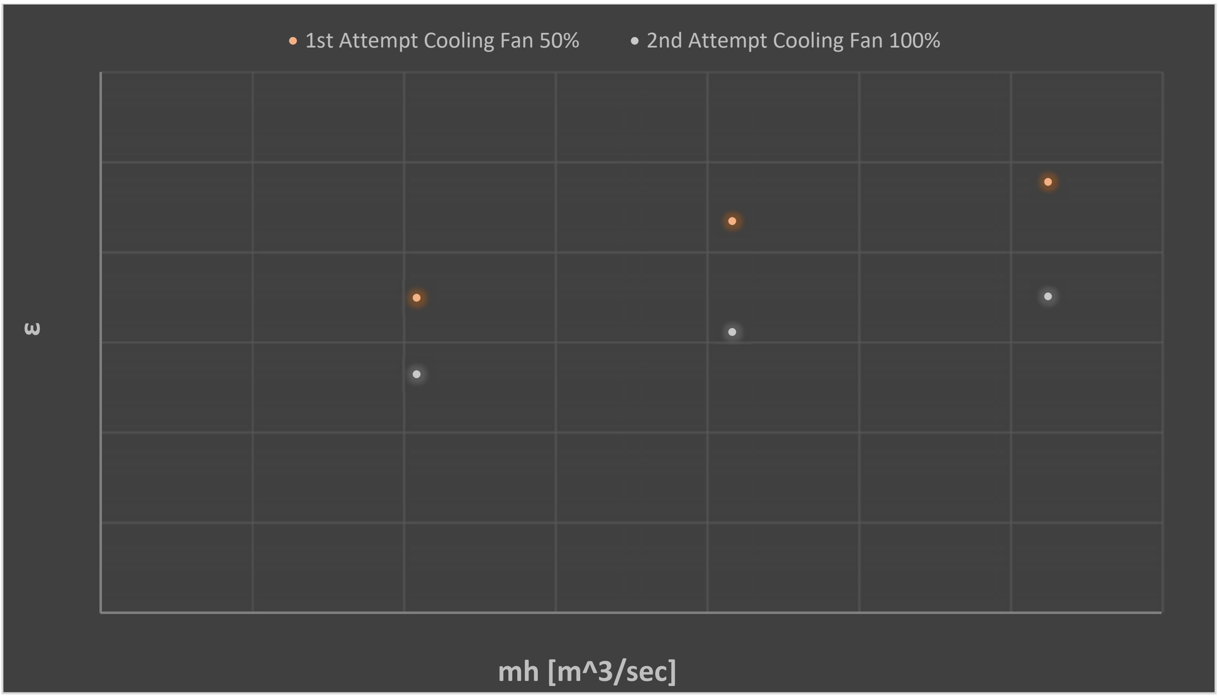

Figure 87: Water Pump Alternatives effectiveness Diagram

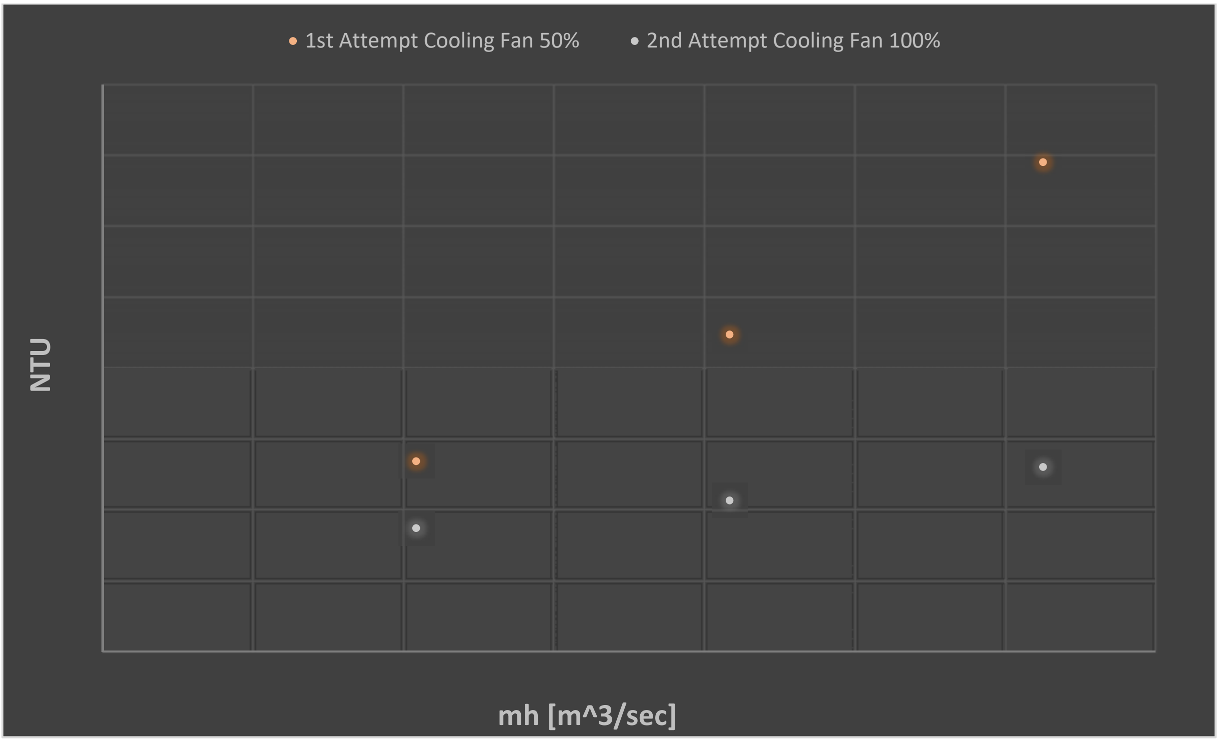

Figure 88: Water Pump Alternatives NTU (Number Transfer of Units) Diagram

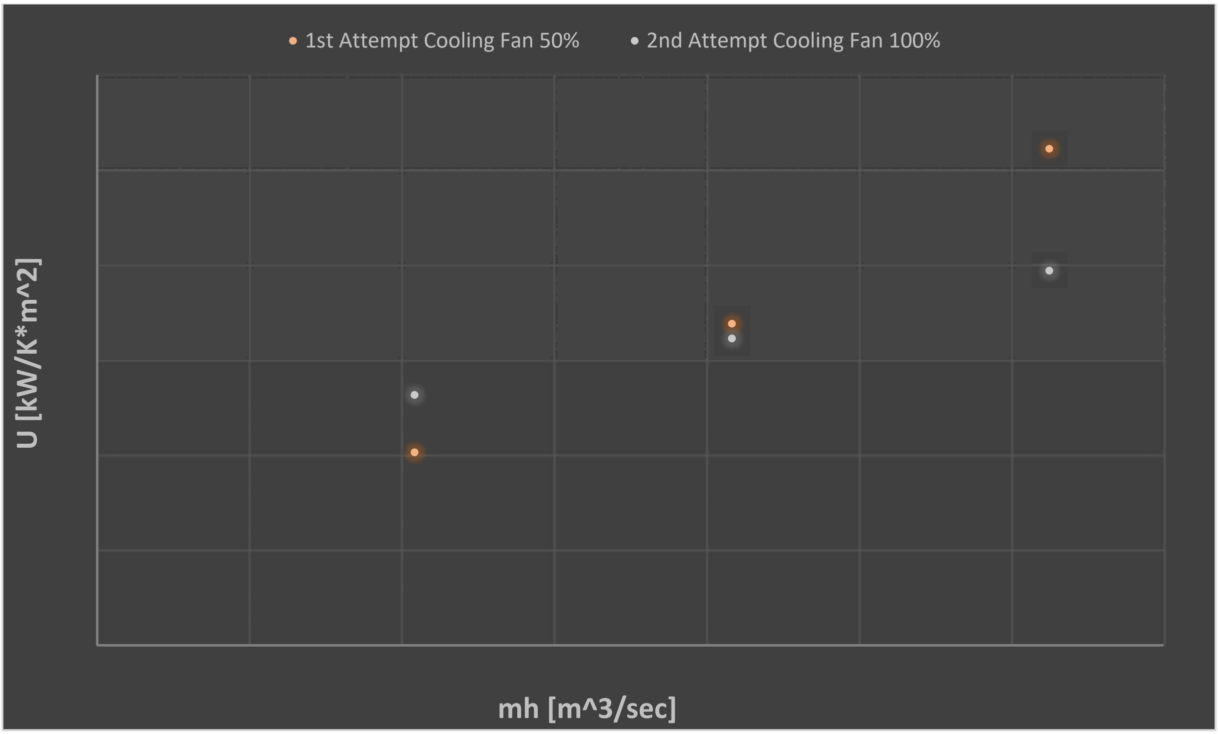

Figure 89: Water Pump Alternatives U (Heat Transfer Coefficient) Diagram

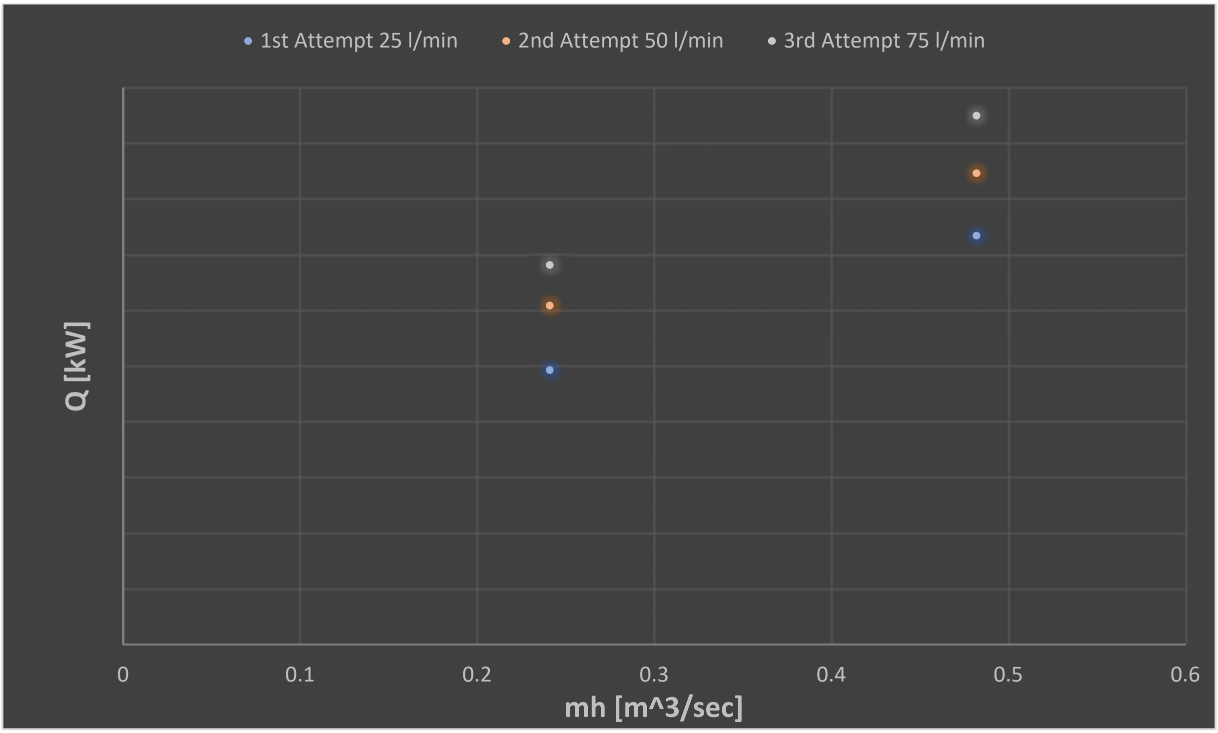

Figure 90: Cooling Fan Alternatives Heat Transfer Rate Q Diagram

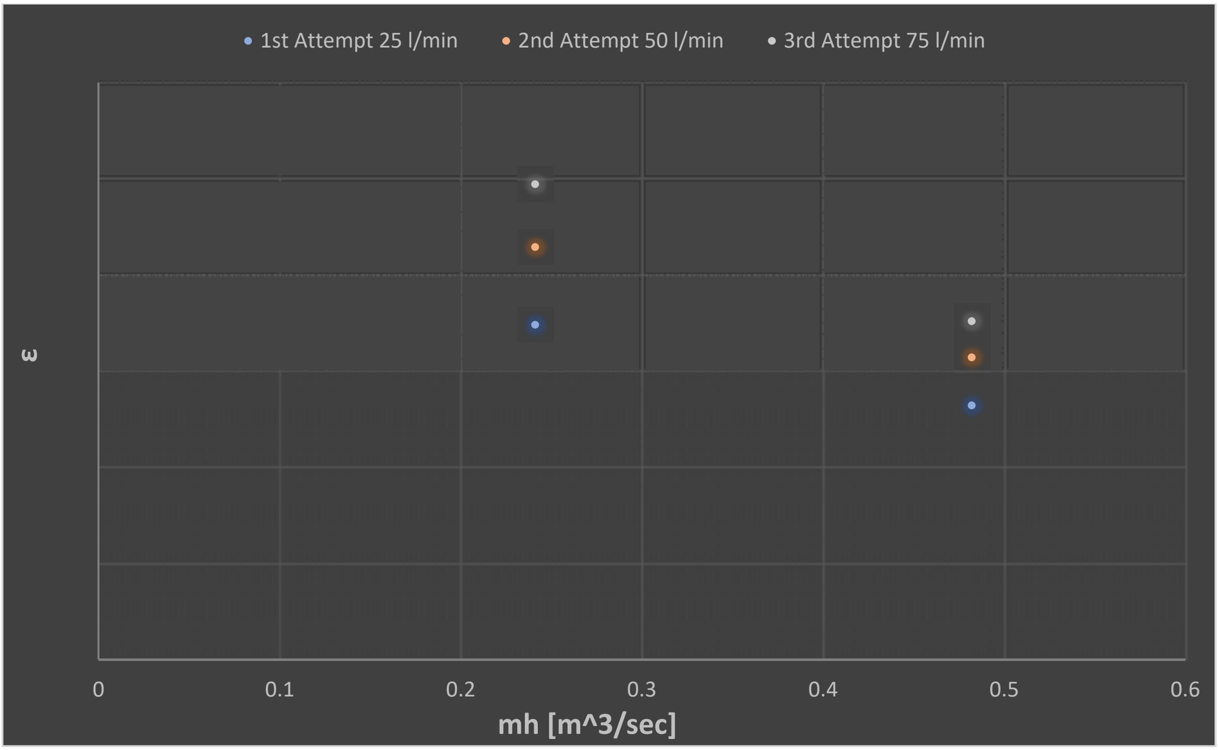

Figure 91: Cooling Fan Alternatives effectiveness Diagram

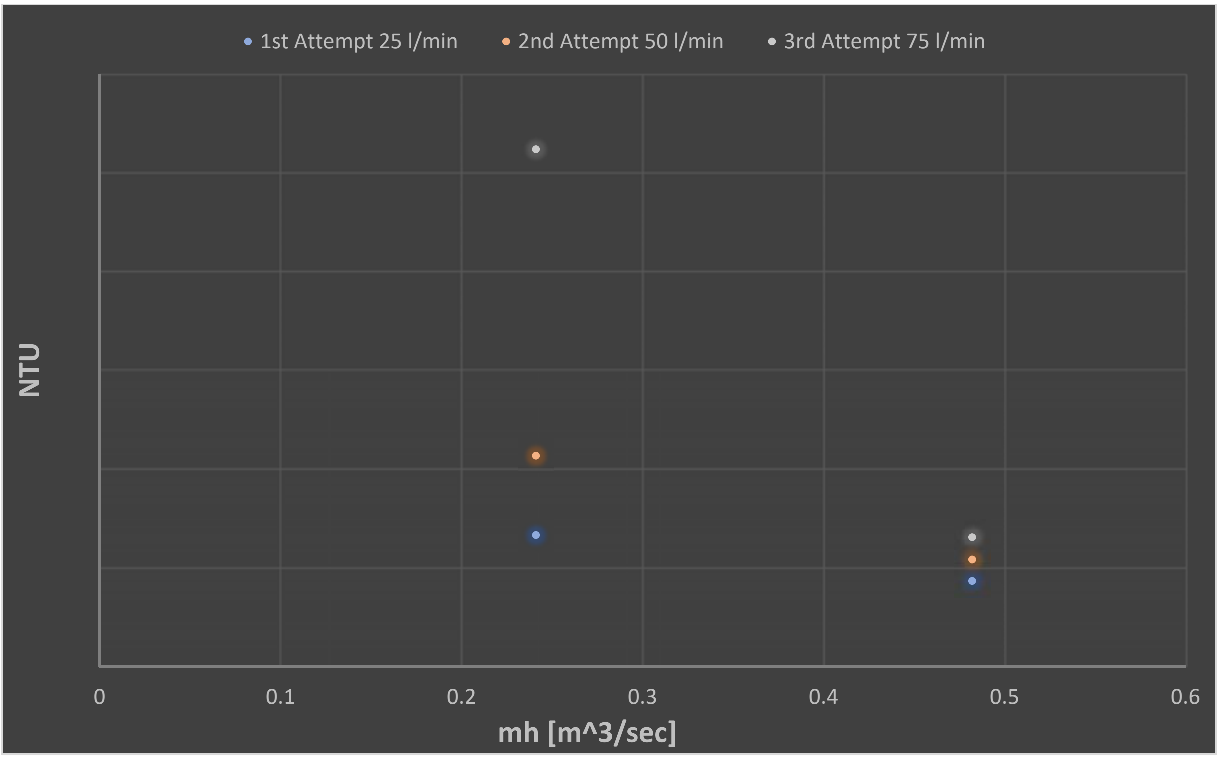

Figure 92: Cooling Fan Alternatives NTU (Number Transfer of Units) Diagram

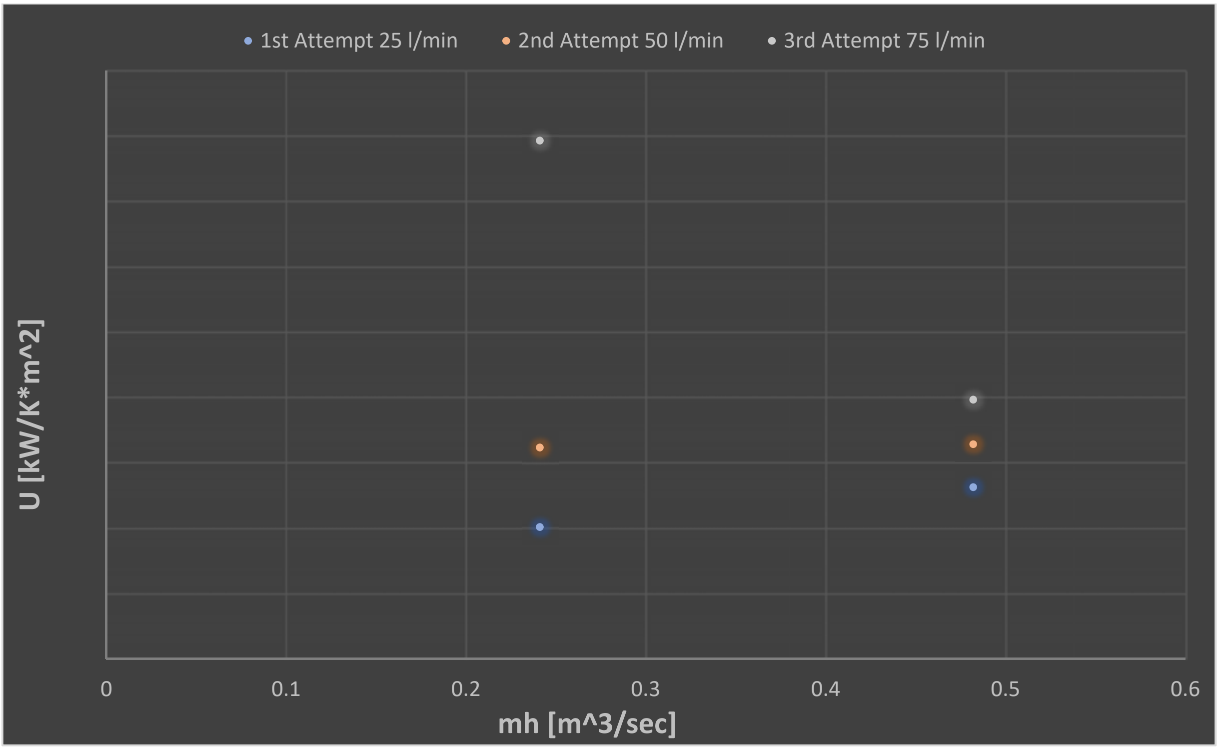

Figure 93: Cooling Fan Alternatives U (Heat Transfer Coefficient) Diagram

4.2 Discussion

4.2.1 Experimental Measurements & Results

All in all, the data from the results and charts allows for insightful commentary on the results. Initially, a notable observation is that maximum heat transfer occurs when the water pump operates at is maximum flow rate, in conjunction with maximum airflow facilitating heat dissipation from the radiator core. This finding is substantiated by the data presented in the tables and charts above. For instance, in *chapter 5.1*, the tables demonstrate that varying the mass flow rates of each fluid and influencing factors such as the water pump or cooling fan result in corresponding changes in heat dissipation. Notably, when adjusting the water pump flow rate while maintaining a low airflow rate, the heat transfer from water ($\dot{Q}_h$) surpasses that from air ($\dot{Q}_c$), and this relationship holds proportionally, as previously discussed.

4.2.2 Problems & Methodology of Calculations

In our calculations, if $\dot{Q}_{max}$ is less than $\bar{Q}$, it results in an effectiveness value greater than the unity, causing an error in *equations 31* and *32*, rendering these data unusable in our experimental measurements. This discrepancy arises from our use of the average heat transfer rates of the two fluids, where significant differences between the heat transfer effects in water and air may occur, depending on the factors influencing the operation of the water pump and cooling fan. Specifically, when the heat transfer rate exceeds $\dot{Q}_{max}$, as determined by *equation 26*, and using C_{min} calculated by *equation 24*, which is relied on the air mass flow rate for example at position 25%, errors might appear. Particularly, instances of low air mass flow and high – water mass flow. The methodology used for applying the data analysis involves the ε – NTU method. The decision to use the ε – NTU method over the LMTD approach was prompted by the availability of a heat exchanger in the faculty laboratory, which provided all the necessary data to complete the ε – NTU method. With this method, we can determine the effectiveness of the heat exchanger, which aligns with the objective of the experimental set – up. Conversely, the LMTD method allows us to ascertain the size of the heat exchanger that would be suitable for our calculations, depending on the specific case.

4.2.3 Problems of Experimental Set – Up

This section addresses the challenges that were encountered during the construction and utilization of the experimental set – up and measurements. One notable issue pertains to the utilization of outdated components such as the boiler, heat exchanger, cooling fan and water pump. These outdated components contribute to system losses, pose challenges in achieving a complete seal, and in increasing the possibility of component failure. Another issue involves local losses induced by various compounds and components, hindering the smooth flow of water. This limitation restricts the water pump from operating at its maximum flow rate, consequently diminishing the variability of experimental measurements. Lastly, a significant issue observed relates to the geometry of the boiler, particularly a peculiar slope at the top that traps air into the system. This configuration poses difficulties for the water pump to function optimally, impeding its abilities.

Chapter 5: Conclusions – Recommendations for further work

5.1 Conclusions

5.1.1 Experimental Set – Up Key Points & Target

Summarizing, the crucial points of the experimental set – up include its capability to test and analyze heat exchangers with the aid of all components presented into the experimental set – up. Additionally, the automated data provided allows users to perform calculations using the ε – NTU method for analyzing the effectiveness of any heat exchanger under study.

5.1.2 Closing

In conclusion, the thesis has successfully achieved its aim and targets. Moving forward, several improvements can be implemented, as outlined below.

5.2 Recommendations for further work

For future improvements of the experimental set – up, several important changes can be proposed. Firstly, replacing outdated components with new ones is essential to enhance the reliability and efficiency of the set – up. Secondly, constructing a variable base capable of accommodating heat exchangers of different sizes would be beneficial. This would involve integrating thermocouples into the tubes for variable monitoring of inlet and outlet temperatures. Thirdly, implementing dedicated cooling systems for the heat exchangers, including cooling fans and shrouds to optimize air flow across the radiator core, it is necessary to ensure experimental set – up that can accommodate various types of electrical connections for different types of cooling fans could be advantageous.

Bibliography

1. Arduino. (2021, September 15). Retrieved from Arduino.cc: https://www.arduino.cc
2. Chaware, P. (2016, August). Retrieved from Word Press: https://paragchaware.files.wordpress.com/2016/08/presentation_ntu.pdf
3. codevender_cc. (n.d.). Retrieved from Instructables: https://www.instructables.com/How-to-Use-Water-Flow-Sensor-Arduino-Tutorial/
4. Integrated, M. (2015, July). Retrieved from Analog Devices: https://www.analog.com/media/en/technical-documentation/data-sheets/MAX31865.pdf
5. Lubken, J. (2021, August 19). Retrieved from Speed Way Motors: https://www.speedwaymotors.com/the-toolbox/single-pass-double-pass-triple-pass-radiators-what-s-the-difference/28862
6. Nikas, K. -S. (2010). *Principles of Heat Exchangers for engineers 1st edition.* Athens.
7. Riyaz, J. (n.d.). Retrieved from Instructables: https://www.instructables.com/How-to-Connect-I2C-Lcd-Display-to-Arduino-Uno/
8. Shah, N. (2014, April 16). Retrieved from Sistemas EEL: https://sistemas.eel.usp.br/docentes/arquivos/5817712/LOQ4086/lmtd.correction.factor.pdf
9. Team, G. A. (2021, May 24). Retrieved from German Auto: https://germanauto.co.uk/how-a-vehicle-cooling-system-works/
10. Team, S. T. (2016, September 14). Retrieved from Speed Way Motors: https://www.speedwaymotors.com/the-toolbox/differences-between-downflow-and-crossflow-radiators/28799

Appendix

Programming Code of Arduino Uno

Water Flow Sensor Code:

```
/*
Liquid flow rate sensor -DIYhacking.com Arvind Sanjeev

Measure the liquid/water flow rate using this code.
Connect Vcc and Gnd of sensor to arduino, and the
signal line to arduino digital pin 2.

 */

 // Include the required Wire library for I2C<br>
 #include <Arduino.h>
 #include <IoAbstractionWire.h>
 #include <LiquidCrystalIO.h>
 #include <Adafruit_MAX31865.h>

//Max_31865

// Use software SPI: CS, DI, DO, CLK
Adafruit_MAX31865 thermo_3 = Adafruit_MAX31865(9, 10, 11, 12);

// The value of the Rref resistor. Use 430.0 for PT100 and 4300.0 for PT1000
#define RREF      430.0
// The 'nominal' 0-degrees-C resistance of the sensor
// 100.0 for PT100, 1000.0 for PT1000
```

```
#define RNOMINAL  100.0

 LiquidCrystalI2C_RS_EN(lcd, 0x27, false)

int LED = 13;
int x = 0;

byte statusLed    = 13;

byte sensorInterrupt = 0;  // 0 = digital pin 2
byte sensorPin       = 2;

// The hall-effect flow sensor outputs approximately 4.5 pulses per second per
// litre/minute of flow.
float calibrationFactor = 0.47;

volatile byte pulseCount;

float flowRate;
unsigned int flowMilliLitres;
unsigned long totalMilliLitres;

unsigned long oldTime;

void setup()
{
```

```
//Max_31865
thermo_3.begin(MAX31865_2WIRE); // set to 2WIRE or 4WIRE as necessary

  //LCD
  Serial.begin(9600);
    Serial.println("Starting LCD example");
    Serial.println("Configure LCD");

    // set up the LCD's number of columns and rows, must be called.
    lcd.begin(16, 2);

    // most backpacks have the backlight on pin 3.
    lcd.configureBacklightPin(3);
    lcd.backlight();

  // Initialize a serial connection for reporting values to the host
  Serial.begin(9600);

  // Set up the status LED line as an output
  pinMode(statusLed, OUTPUT);
  digitalWrite(statusLed, HIGH);  // We have an active-low LED attached

  pinMode(sensorPin, INPUT);
  digitalWrite(sensorPin, HIGH);

  pulseCount        = 0;
  flowRate          = 0.0;
```

```
  flowMilliLitres   = 0;

  totalMilliLitres  = 0;

  oldTime           = 0;


  // The Hall-effect sensor is connected to pin 2 which uses interrupt 0.

  // Configured to trigger on a FALLING state change (transition from HIGH

  // state to LOW state)

  attachInterrupt(sensorInterrupt, pulseCounter, FALLING);

}


void loop()

{


  //MAX_31865


  float f = (thermo_3.temperature(RNOMINAL, RREF));


  lcd.setCursor(0,1);

  lcd.print("Tair:");

  lcd.print(f, 1);

  lcd.print(char(223));

  lcd.print("C");


  //thermo_3 MAX31865


  uint16_t rtd2 = thermo_3.readRTD();
```

```
Serial.print("Tair: "); Serial.println(thermo_3.temperature(RNOMINAL, RREF));


 // Check and print any faults
 uint8_t fault = thermo_3.readFault();
 if (fault) {
   Serial.print("Fault 0x"); Serial.println(fault, HEX);
   if (fault & MAX31865_FAULT_HIGHTHRESH) {
     Serial.println("RTD High Threshold");
   }
   if (fault & MAX31865_FAULT_LOWTHRESH) {
     Serial.println("RTD Low Threshold");
   }
   if (fault & MAX31865_FAULT_REFINLOW) {
     Serial.println("REFIN- > 0.85 x Bias");
   //}
   if (fault & MAX31865_FAULT_REFINHIGH) {
     Serial.println("REFIN- < 0.85 x Bias - FORCE- open");
   }
   if (fault & MAX31865_FAULT_RTDINLOW) {
     Serial.println("RTDIN- < 0.85 x Bias - FORCE- open");
   }
   if (fault & MAX31865_FAULT_OVUV) {
     Serial.println("Under/Over voltage");
   }
   thermo_3.clearFault();
 }
```

```
  Serial.println();
  delay(2000);
}


  //LCD


  lcd.setCursor(0,0);
  lcd.print("L/min:");
  lcd.print(flowRate);  // Print the integer part of the variable
  //lcd.print("\t");      // Print tab space


   if((millis() - oldTime) > 1000)    // Only process counters once per second
  {
    // Disable the interrupt while calculating flow rate and sending the value to
    // the host
    detachInterrupt(sensorInterrupt);


    // Because this loop may not complete in exactly 1 second intervals we calculate
    // the number of milliseconds that have passed since the last execution and
use
    // that to scale the output. We also apply the calibrationFactor to scale the
output
    // based on the number of pulses per second per units of measure (litres/minute
in
    // this case) coming from the sensor.
    flowRate = ((1000.0 / (millis() - oldTime)) * pulseCount) / calibrationFactor;


    // Note the time this processing pass was executed. Note that because we've
```

```
    // disabled interrupts the millis() function won't actually be incrementing right
    // at this point, but it will still return the value it was set to just before
    // interrupts went away.
    oldTime = millis();

    // Divide the flow rate in litres/minute by 60 to determine how many litres have
    // passed through the sensor in this 1 second interval, then multiply by 1000 to
    // convert to millilitres.
    flowMilliLitres = (flowRate / 60) * 1000;

    // Add the millilitres passed in this second to the cumulative total
    totalMilliLitres += flowMilliLitres;

    unsigned int frac;

    // Print the flow rate for this second in litres / minute
    Serial.print("L/min:");
    Serial.print(int(flowRate));  // Print the integer part of the variable
    Serial.print("\t");       // Print tab space

    // Reset the pulse counter so we can start incrementing again
    pulseCount = 0;

    // Enable the interrupt again now that we've finished sending output
    attachInterrupt(sensorInterrupt, pulseCounter, FALLING);
```

```
  }


}


/*
Insterrupt Service Routine
 */
void pulseCounter()
{
  // Increment the pulse counter
  pulseCount++;
}
```

MAX – 31865 RTD – PT 100 Code:

```
/***************************************************
  This is a library for the Adafruit PT100/P1000 RTD Sensor w/MAX31865


  Designed specifically to work with the Adafruit RTD Sensor
  ----> https://www.adafruit.com/products/3328


  This sensor uses SPI to communicate, 4 pins are required to
  interface
  Adafruit invests time and resources providing this open source code,
  please support Adafruit and open-source hardware by purchasing
  products from Adafruit!


  Written by Limor Fried/Ladyada for Adafruit Industries.
```

```
 BSD license, all text above must be included in any redistribution
 ****************************************************/
//LCD
// include the library code:
#include <Arduino.h>
#include <LiquidCrystalIO.h>
#include <IoAbstractionWire.h>
#include <Adafruit_MAX31865.h>

// For most standard I2C backpacks one of the two helper functions below will create you a liquid crystal instance
// that's ready configured for I2C. Important Note: this method assumes a PCF8574 running at 100Khz. If otherwise
// use a custom configuration as you see in many other examples.

// If your backpack is wired RS,RW,EN then use this version
LiquidCrystalI2C_RS_EN(lcd, 0x27, false)

// Use software SPI: CS, DI, DO, CLK
Adafruit_MAX31865 thermo_1 = Adafruit_MAX31865(10, 11, 12, 13);
Adafruit_MAX31865 thermo_2 = Adafruit_MAX31865(6, 7, 8, 9);

// The value of the Rref resistor. Use 430.0 for PT100 and 4300.0 for PT1000
#define RREF      430.0
// The 'nominal' 0-degrees-C resistance of the sensor
// 100.0 for PT100, 1000.0 for PT1000
#define RNOMINAL  100.0
```

```
void setup() {


  Serial.begin(9600);
  Serial.println("Adafruit MAX31865 PT100 Sensor Test!");


  thermo_1.begin(MAX31865_2WIRE);  // set to 2WIRE or 4WIRE as necessary
  thermo_2.begin(MAX31865_2WIRE);


  //LCD
  Serial.begin(9600);
    Serial.println("Starting LCD example");
    Serial.println("Configure LCD");


    // set up the LCD's number of columns and rows, must be called.
    lcd.begin(16, 2);


    // most backpacks have the backlight on pin 3.
    lcd.configureBacklightPin(3);
    lcd.backlight();
}


void loop() {


 float h = (thermo_1.temperature(RNOMINAL, RREF));


 float t = (thermo_2.temperature(RNOMINAL, RREF));

```

```
//LCD
taskManager.runLoop();

lcd.setCursor(0,0);
lcd.print("Tin:");
lcd.print(h, 1);
lcd.print(char( 223));
lcd.print("C");

lcd.setCursor(0,1);
lcd.print("Tout:");
lcd.print(t, 1);
lcd.print(char( 223));
lcd.print("C");

uint16_t rtd = thermo_1.readRTD();

Serial.print("Tin: "); Serial.println(thermo_1.temperature(RNOMINAL, RREF));

// Check and print any faults
uint8_t fault = thermo_1.readFault();
if (fault) {
  Serial.print("Fault 0x"); Serial.println(fault, HEX);
  if (fault & MAX31865_FAULT_HIGHTHRESH) {
    Serial.println("RTD High Threshold");
  }
  if (fault & MAX31865_FAULT_LOWTHRESH) {
```

```
      Serial.println("RTD Low Threshold");
    }
    if (fault & MAX31865_FAULT_REFINLOW) {
      Serial.println("REFIN- > 0.85 x Bias");
    }
    if (fault & MAX31865_FAULT_REFINHIGH) {
      Serial.println("REFIN- < 0.85 x Bias - FORCE- open");
    }
    if (fault & MAX31865_FAULT_RTDINLOW) {
      Serial.println("RTDIN- < 0.85 x Bias - FORCE- open");
    }
    if (fault & MAX31865_FAULT_OVUV) {
      Serial.println("Under/Over voltage");
    }
    thermo_1.clearFault();
  }

  Serial.println();
  delay(2000);

//thermo_2 MAX31865

uint16_t rtd1 = thermo_2.readRTD();

  Serial.print("Tout: "); Serial.println(thermo_2.temperature(RNOMINAL, RREF));

  // Check and print any faults
```

```
  uint8_t fault1 = thermo_2.readFault();
  if (fault) {
    Serial.print("Fault 0x"); Serial.println(fault, HEX);
    if (fault & MAX31865_FAULT_HIGHTHRESH) {
      Serial.println("RTD High Threshold");
    }
    if (fault & MAX31865_FAULT_LOWTHRESH) {
      Serial.println("RTD Low Threshold");
    }
    if (fault & MAX31865_FAULT_REFINLOW) {
      Serial.println("REFIN- > 0.85 x Bias");
    }
    if (fault & MAX31865_FAULT_REFINHIGH) {
      Serial.println("REFIN- < 0.85 x Bias - FORCE- open");
    }
    if (fault & MAX31865_FAULT_RTDINLOW) {
      Serial.println("RTDIN- < 0.85 x Bias - FORCE- open");
    }
    if (fault & MAX31865_FAULT_OVUV) {
      Serial.println("Under/Over voltage");
    }
    thermo_2.clearFault();
  }

  Serial.println();
  delay(2000);
}
```